# Molecular characterisation of human adenoviruses from environmental samples in Tshwane, Gauteng

**Michaela Davids**

**2020**

# MOLECULAR CHARACTERISATION OF HUMAN ADENOVIRUSES FROM ENVIRONMENTAL SAMPLES IN TSHWANE, GAUTENG

BY

**MICHAELA DAVIDS**

**Submitted in partial fulfilment of the requirements for the degree**

**Magister Scientiae**

**MSc (Medical Virology)**

**Department of Medical Virology**

**Faculty of Health Sciences**

**University of Pretoria**

**Pretoria**

**December 2020**

# DECLARATION OF ORIGINALITY

---

I, Michaela Davids, declare that the dissertation hereby submitted to the University of Pretoria for the degree MSc (Medical Virology) and the contained herein is my own original work. I have not copied, repeated or plagiarised this work from any national or international publications. All work was completed in accordance with the ethical rules prescribed by the Faculty of Health Sciences Research Ethics Committee, University of Pretoria.

Signature: ----------

Date: ----------

## ACKNOWLEDGEMENTS

***I would like to thank:***

First and foremost, God, the Almighty, for his amazing grace and presence throughout my MSc. Through Him, anything is possible.

To my supervisor, Dr WB van Zyl and co-supervisor, Prof J Mans, for their continuous support, guidance and assistance in improving my knowledge throughout my research project.

The Department of Medical Virology, with special reference and uttermost appreciation to Mr VV Mabasa (PhD Student), for his unfailing assistance with learning new laboratory techniques and prudent advice and patience.

The Enteric Virus and Environmental Research Group, for their support throughout my MSc.

To all the research funding bodies, Poliomyelitis Research Foundation (PRF) and National Research Foundation (NRF), for the post-graduate bursaries. Without these funding bodies, my MSc would not have been possible.

Lastly, and most importantly, to my phenomenal Mother. Words cannot describe her unconditional love and endless support and encouragement. For all her sacrifices and prayers, I am profoundly grateful and in awe.

## ETHICAL CONSIDERATION

Ethical approval was obtained from the Faculty of Health Sciences, Research Ethics Committee of the University of Pretoria for the human adenovirus testing of environmental samples from two wastewater treatment plants in the Tshwane region. The Research Committee granted umbrella ethical approval for an on-going study, reference number 75/2018. This master's study is a continuation of the umbrella study. The City of Tshwane has provided permission for the detection and characterisation of enteric viruses from the wastewater samples in Tshwane. Specific ethical approval for this master's project for the characterisation of HAdVs was approved by the Faculty of Health Sciences, Research Ethics Committee of the University of Pretoria, reference number 249/2020.

## PRESENTATIONS

---

**Davids M**. Mabasa VV. Mans J. Van Zyl WB. VIROLOGY AFRICA 2020. Molecular characterisation of human adenovirus from environmental samples in Tshwane, Gauteng [Oral Presentation]. Virology Africa 2020. 10-15 February 2020, Radisson Blu Waterfront hotel, Cape Town, South Africa.

**Davids M**. Mabasa VV. Mans J. Van Zyl WB. Molecular detection and characterization of human adenoviruses from South African clinical and environmental samples [Poster Presentation]. University of Pretoria Health Sciences Faculty Day. 20-21 August 2019, Medical Campus, Prinshof, Pretoria, South Africa

**Molecular characterisation of human adenoviruses from environmental samples in Tshwane, Gauteng**

by

**Michaela Davids**

**SUPERVISOR: Dr WB van Zyl**

**CO-SUPERVISOR: Prof J Mans**

**DEPARTMENT: Medical Virology, Faculty of Health Sciences**

**DEGREE: MSc (Medical Virology)**

## ABSTRACT

Human adenoviruses (HAdV) are non-enveloped viruses with an icosahedral capsid and a linear double-stranded DNA genome. These viruses belong to the family *Adenoviridae* and genus *Mastadenovirus.* An important property of the HAdV is that it is non-enveloped making it highly resistant to detergents and harsh environmental conditions. This virus is grouped in seven species (A-G) with more than 88 genotypes. These seven species are associated with several diseases, such as, respiratory infections, keratoconjunctivitis, urinary infections, hepatitis and gastrointestinal infections. The HAdV is one of the etiological causes of acute gastroenteritis, mainly caused by HAdV-F40 and HAdV-F41. The virus can be transmitted *via* the faecal-oral route, inhalation of respiratory droplets and direct contact with contaminated environments. The virus is known to be ubiquitous in environments where human contamination is likely to occur such as wastewater treatment plants. These human contaminations could occur through contaminated secretion and excretions within aqueous environments. There is currently a limited amount of information on the HAdV in water

environments, particularly in Tshwane, Gauteng. Therefore, the aim of the study was to investigate the presence and genotypes of human adenovirus in environmental samples namely raw sewage and treated effluent, using molecular methods. For genotypic characterisation, Sanger sequencing was used on amplicons from 12 HAdV positive samples and next generation sequencing were used on all the amplicons from HAdV positive samples.

A total of 150 environmental samples (75 raw sewage and 75 effluent) were collected from two wastewater treatment plants in Tshwane over the study period of 18 months. These environmental samples comprised of 1 L raw sewage and 10 L treated effluent samples. The primary viral recovery for the 1 L raw sewage and 10 L treated effluent samples were performed using skimmed milk flocculation procedure and glass wool adsorption elution technique, respectively. For secondary viral recovery, both environmental samples were subjected to polyethylene glycol/sodium chloride precipitation. Manual extraction was used to extract the nucleic acids from the virus concentrate with mengovirus (MV) used as an extraction control. For the quantification of HAdV, standard curves prepared from known dilutions of HAdV and MV were used.

Human adenovirus was detected in 140/150 (93%) of the environmental samples comprising of 69/75 (92%) being raw sewage and 71/75 (95%) being effluent samples. The HAdV concentrations detected in wastewater treatment plant 1 (WWTP 1) ranged from $1.38x10^5$ gc/L to $4.50 \times 10^9$ gc/L for raw sewage and $5.08x10^3$ gc/l to $4.30x10^8$ gc/L for effluent. The HAdV concentrations detected in WWTP 2 ranged from $6.84x10^4$ gc/L to $1.69x10^{12}$ gc/L for raw sewage and $5.27x10^3$ gc/L to $1.16x10^8$ gc/L for effluent. The HAdV hexon amplification success rate from the nucleic acids was 43/140 (31%).

Eighteen HAdV genotypes were successfully characterised using Sanger sequencing. The HAdV-D was the most predominant species in both WWTPs, follow by HAdV-B and HAdV-F. The HAdV-A and HAdV-E species were the least identified. Next generation sequencing identified four times as many genotypes as Sanger sequencing (77 different genotypes). The HAdV-D (types 8, 9, 13, 17, 19, 20, 23, 24, 28, 29, 32, 33, 36, 42, 44, 47, 49, 51, 56, 60, 62, 64, 67 and 81) and HAdV-B (types 2, 3, 7, 11 and 66) were the most predominant species followed by HAdV-F (types 40 and 41), HAdV-A (types 12 and 76), HAdV-E ( type 4) and HAdV-C (type 1).

Testing wastewater treatment plants is advantageous as it allows for the detection and identification of HAdV types circulating in the surrounding communities. Due to the large

number of species identified using NGS, it is the superior typing method and should be used for future studies. These include strains causing symptomatic and asymptomatic infections. Human adenovirus was detected at comparable frequencies in raw sewage and treated effluent wastewater, with slightly higher detection in effluent samples. However, the viability of these viruses is unknown and should be investigated in further studies. The detection of viruses in wastewater treatment plants are a public health concern as the treated effluent is discharged into rivers, which may be used by communities for domestic and recreational purposes.

.

# TABLE OF CONTENTS

# LIST OF TABLES

# LIST OF FIGURES

# ABBREVIATIONS AND SYMBOLS

| | |
|---|---|
| **A** | Adenosine |
| **AD** | Adenoid degeneration |
| **AdV-2** | Adenovirus type 2 |
| **Ad Pol** | Adenovirus polymerase |
| **AIDS** | Acquired immunodeficiency syndrome |
| ***α*** | Alpha |
| **β** | Beta |
| **BLAST** | Basic local alignment search tool |
| **BMT** | Bone marrow transplant |
| **bp** | Base pairs |
| **CA** | California |
| **CAR** | Coxsackie adenovirus receptor |
| **CF** | Complement fixation |
| **©** | Copyright |
| **ct** | Cycle threshold |
| **CPE** | Cytopathic effect |
| **C** | Cytosine |
| **CPE** | Cytopathic effect |
| **bp** | Base pairs |
| **DBP** | DNA binding protein |
| **dCMP** | Deoxyribo-cytosine monophosphate |
| **°C** | Degree Celsius |
| **DNA** | Deoxyribose nucleic acid |
| **Dr** | Doctor |
| **DRC** | Democratic Republic of Congo |
| **dH2O** | Distilled water |
| **E. coli** | *Escherichia coli* |
| **ELISA** | Enzyme-linked immunosorbent assay |
| **ER** | Early region |
| **ER** | Endoplasmic reticulum |
| **E** | Effluent |
| **E** | Early region |
| **EIA** | Enzyme immunoassay |
| ***et al*** | Et alia |
| **EV** | Enteric viruses |
| **F** | Forward |
| **Feb** | February |
| **FAM** | 6-carboxy fluorescein |
| **g** | Gram |
| **G** | Guanine |
| **GBEB** | Glycine beef extract buffer |
| **gc** | Genome copies |
| **GON** | Group of nine hexons |
| **H** | Hexon |
| **h** | Hour |

| | |
|---|---|
| **HAdV** | Human adenovirus |
| **HAdV E4p** | Human adenovirus E4 prototype |
| **HAdV pol** | Human adenovirus polymerase |
| **HAdV WG** | Human Adenovirus Working Group |
| **HCl** | Hydrochloric acid |
| **HEK** | Human embryonic kidney cells |
| ∞ | Infinity |
| **IF** | Immunofluorescence |
| **IFN** | Interferon |
| **IC** | Internal control |
| **ITR** | Internal terminal repeats |
| **Kbp** | Kilobase pairs |
| **L** | Litre |
| **L** | Late region |
| **M** | Molar |
| **MHC** | Major histocompatibility complex |
| **µL** | Microlitre |
| **mL** | Millilitre |
| **MLP** | Major late promoter |
| **mg** | Milligram |
| **MEGA** | Molecular Evolutionary Genetics Analysis |
| **mm** | Millimetre |
| **$mm^2$** | Millimetre squared |
| **MOI** | Multiplicity of infection |
| **mRNA** | Messenger ribonucleic acid |
| **n** | number |
| **NaCl** | Sodium chloride |
| **NaOH** | Sodium hydroxide |
| **ng/µL** | Nanograms per microliter |
| **NEB** | New England Biolabs |
| **NGS** | Next generation sequencing |
| **NICD** | National Institute of Communicable Diseases |
| **nm** | Nanometre |
| **Ψ** | Package sequence |
| **PBS** | Phosphate buffer saline |
| **PCR** | Polymerase chain reaction |
| **$PEG_{8000}$** | Polyethyleneglycol 8000 |
| **%** | Percentage |
| **pH** | Potential of hydrogen |
| **PK** | Porcine kidney cell |
| **PSM** | Preflocculated skimmed milk solution |
| **pTP** | Precursor terminal protein |
| **pTP-CAT** | Precursor terminal protein-trinucleotide intermediate |
| **pmol** | Picomole |
| **qPCR** | Quantitative PCR |
| ***rt*-PCR** | Reverse transcriptase PCR |
| **RNA** | Ribonucleic acid |
| **Sec** | Seconds |
| **SA** | South Africa |
| **SMF** | Skimmed milk flocculation |

| | |
|---|---|
| **TAE** | Tris acetate-ethylenediamineletra acetic acid |
| **TB** | Terrific broth |
| **T** | Thymine |
| **$TCID_{50}$** | Medium tissue culture infectious dose |
| **™** | Trademark |
| **TAMRA** | 5-Carboxytetramethylehidamine |
| **TP** | Terminal Protein |
| **®** | Registered Trademark |
| **UTI** | Urinary Tract Infection |
| **UV** | Ultraviolet |
| **VFF** | Vortex flow filtration |
| **WWTP** | Wastewater treatment plant |

# CHAPTER 1

# LITERATURE REVIEW

## 1.1 INTRODUCTION

Human adenoviruses (HAdVs) are one of the most important etiological causes of acute gastroenteritis worldwide. Approximately 1%-8% of acute gastronenteritis cases are attributed to HAdV F-40 and HAdV F-41 occurring in high income countries and 2%-31% in middle to low-income countries (GBD Diarrhoeal Disease Collaboration., 2017). The HAdV disease varies from sporadic to epidemic based on the viral serotype and age (children or adults) in a particular population (Berk, 2013). Human adenoviruses are predominantly spread *via* the faecal-oral route and are associated with long lasting diarrhoea, infant dehydration and malnutrition (Dashti *et al*., 2016). Worldwide, the virus is detected all year round but is most prevalent during spring, early summer and midwinter in temperate climates (Vergatat, 2007). The virus is also known to be waterborne and it is frequently found within environmental samples, such as raw sewage and treated effluent water as well as rivers and lakes (Pina *et al*., 1998).

The HAdV was first isolated in 1953 by Rowe and colleagues while analysing adenoid tissue for the presence of poliovirus (Rowe *et al*., 1953). Rowe and colleagues discovered a transmissible agent capable of cytopathic effects causing changes in the adenoid tissue, which was isolated and named the adenovirus (Ghebremedhin, 2014). The HAdV belongs to the family *Adenoviridae*, genus *Mastadenovirus*, with more than 103 genotypes which are divided into seven species namely: A, B, C, D, E, F and G (HADVWG, http://hadvwg.gmu.edu/). Originally, the identification of the different HAdV types was done using serum neutralisation and hemagglutination. Currently, genotyping is done using molecular techniques to analyse the partial or complete sequences of the hexon, penton base or fibre genes (Singh *et al*., 2013). The different HAdV types have variable tissue tropism, which result in a wide range of human diseases (Kenmoe *et al*., 2018). In particular, HAdV A is involved with urinary and respiratory tract infections, HAdV B, C and E cause upper and lower acute respiratory tract infections, HAdV B and D are associated with conjunctivitis and HAdV F and G with gastroenteritis (Ghebremedhin, 2014). The HAdV is a non-enveloped virus, with an icosahedral capsid and a double stranded linear DNA genome (Cook and Radke, 2017).

Human adenoviruses are associated with several diseases, such as those within the respiratory tract (species HAdV-B3, HAdV-B7, HAdV-C1, HAdV-C2, HAdV-C5, HAdV-C6 and HAdV-E4) which are spread *via* respiratory droplets (Tabain *et al*., 2012). The gastrointestinal tract infections (species HAdV-F40, HAdV-F41 and HAdV-G52) are spread *via* faecal-oral transmission. This includes person-to-person contact, fomites, foodborne and waterborne transmission (Jones *et al*., 2007). Infections occurring in the conjunctiva (species HAdV-A31 HAdV-B16, HAdV-B35, HAdV-D8, HAdV-D37, HAdV-D53, HAdV-D54, HAdV-D56 and HAdV-E4) are spread *via* direct contact (Ismail *et al*., 2019). Species HAdV-C1, HAdV-C2, HAdV-C5, HAdV-B3, HAdV-B7, HAdV-B21, HAdV-E4, HAdV-F40 and HAdV-F41 are globally distributed and cause periodic outbreaks. The HAdV-F40 and HAdV-F41 predominantly cause gastroenteritis and are frequently present within sewage water. There are other types found in stool, which have also been associated with gastroenteritis, such as HAdV-A31, HAdV-C1, HAdV-C2, HAdV-C5, HAdV-D32 and HAdV-G52 (Cook and Radke, 2017). In addition, species HAdV-F40 and HAdV-F41 as well as HAdV-A31 and HAdV-A12 were detected in stool specimens from children with gastroenteritis in South Africa (Rossouw, 2004).

Gastroenteritis is one of the main causes of the increase in infant and child morbidity and mortality (Abdoli and Maspi, 2018). Adenovirus-related diarrhoeal diseases occur worldwide but mostly in lower- to middle-income countries situated in Africa, South-East Asia and the Eastern Mediterranean. These countries have several overpopulated rural and semi-urban communities, which lack clean drinking water, insufficient sanitation, and poor hygiene conditions. These types of communities are at high risk of contracting infections, which may lead to outbreaks (Walker *et al.*, 2012).

The HAdV is frequently detected in sewage at high concentrations. The virus is excreted from infected patients in concentrations as high as $10^{11}$ viral particles per gram of faeces (Fong *et al*., 2010). A study done in the Eastern Cape, South Africa reported the presence of HAdV in final effluents of all five wastewater treatment plants, tested and emphasised the potential adverse effects on public health from these contaminated water samples (Osuolale and Okoh, 2015).

Globally, WWTPs are crucial resources in areas where water is scarce as treated wastewater can be used as a reliable source of water throughout the year. Although these wastewaters undergo sewage treatment, not all of the viral pathogens are removed.

Therefore, these water sources may become a potential health hazard to the public (Gonzales-Gustavson *et al*., 2019). The HAdV is found to be highly resistant to these treatments due to the virus being able to survive a range of pH values, adverse temperatures as well as chemical and physical agents used during tertiary treatments and is therefore prevalent in treated wastewater (Hamza *et al*., 2011).

## 1.2 VIROLOGICAL CHARACTERISTICS

### 1.2.1 History

The adenoviruses were first discovered in 1953 by Wallace Rowe and colleagues, whereby the virus was identified during the study of the growth of human adenoid tissue while evaluating poliovirus (Rowe *et al*., 1953). The virus was recognised as a transmissible agent causing the degeneration of the epithelial-like adenoid cells. This led to adenoviruses being cultured and reported as distinct viral agents (Berk, 2013). These distinct viral agents were then later isolated from throat swabs of patients with acute respiratory disease by Hilleman and colleague (Hilleman and Werner, 1954). The HAdV was found to be oncogenic in 1962, by Trentin and colleagues, when human adenovirus induced malignant tumours in newborn hamsters (Wadell, 1999). In 1973, it was discovered that enteric adenoviruses were associated with infantile diarrhoea and differed from other HAdVes by being fastidious (Wadell, 1999). For this reason, the enteric adenoviruses were difficult to culture and therefore were identified using electron microscopy (De Jong *et al.*, 1999).

### 1.2.2 Classification and nomenclature

Human adenoviruses were originally classified with a family status *Adenoviridae* in 1976 anddivided into two genera: *Mastadenovirus* and *Aviadenovirus.* The *Mastadenovirus* consist of isolations from mammals including of all the HAdVes and the *Aviadenovirus* contains isolates of birds. The family status was further divided into two more genera, *Atadenovirus* and *Siadenovirus*. The *Atadenovirus* genus is named according to the high adenine (A) and thymine (T) base content and this genus contains isolates of adenoviruses associated with reptiles, birds, marsupials and mammals and the *Siadenovirus* are mainly isolates from reptiles and birds (Berk, 2013).

The evolution of adenoviruses was initially driven by sequence divergence and frequent recombination between different serotypes of the adenovirus members. These adenovirus members share common epitopes on the capsid protein known as the hexon region (Dhingra, 2019). Between the 1960s and 1970s the number of HAdV serotypes grew substantially resulting in 51 serotypes. These 51 serotypes were determined by serotype-specific neutralisation assays (Mahy and Van Regenmortel, 2010). Recently, studies have shown that the virus comprises of more than 103 types that are identified based on oncogenic, hemagglutinating, morphological and DNA sequence properties. These viruses are classified into seven species (A-G) ( HADVWG, http://hadvwg.gmu.edu/).

The virus was initially called adenoid degeneration (AD) and later renamed the "Adenovirus", by Enders *et al*, as it occurred in adenoid tissue. The adenovirus was further named into subdivisions with each subgroup representing different clinical diseases (Enders *et al*, 1956). Previously, the HAdV types were identified using serum neutralisation and hemagglutination (HI) (Lord *et al*. 2000). However, recent studies have shown that genomic and bioinformatics analyses of an entire genome have overcome the serological methods (Seto, 2009; Seto, 2011). The grouping into different species represents not only the high similarity at a nucleotide level but also reflects the general cell tropism of the viruses causing different diseases (Lion, 2014).

### 1.2.3 Morphology and structure

The HAdV has a non-enveloped, icosahedral capsid (Russell, 2009). The virus is encapsulated with large proteins leading to the virus structure of 90 nm in diameter (Berk, 2013). The outer shell comprises of seven protein types with three main proteins forming the core of the capsid faces, providing stability and forming the vertices. Another five core proteins (V, VII, Mu, IVa2 and terminal protein TP) are involved in genome packaging (Pérez-Berná *et al*., 2015). Figure 1.1 illustrates a schematic drawing of the HAdV structure (Russel., 2009). The three major structural proteins are components of the viral capsid, namely, the hexon, the penton bases and the extended fibres (Russell, 2009).

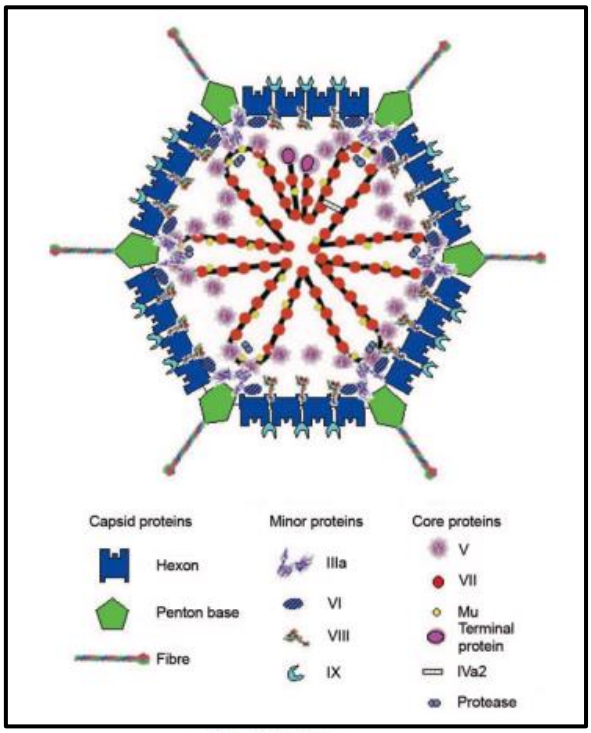


**Figure 1.1: A schematic representation of the human adenovirus structure** (Russel., 2009).

The basic structural units of the virus comprise of four different types of hexons, namely; H1, H2, H3 and H4 (Burnett, 1985). A total of 540 hexons are found in the capsid. Of the 540 hexons, 60 surround the penton proteins and are known as the peripentonal hexons. The remaining hexons are the group of nine (GON) hexons, which are situated on 20 facets of the icosahedron capsid forming pseudo-hexagonal trimers. These pseudo-hexagonal trimers allow for close alignment between the facet and the exterior tower regions. The base of the hexon proteins are made up of one loop and two eight-stranded 'jelly-rolls' which aid in the interaction with neighbouring capsomeres and flexibility (Russell, 2009). The hexon proteins are principal components in activating the immune responses such as the humoral, cellular and innate responses during infection. The stability of the whole virus structure during infection is dependent on the interaction of the hexon proteins between themselves and other structural components. Beneath the hexon proteins, are the minor capsid proteins with polypeptides VI, VIII and IX closer to the virion and these polypeptides differ based on their stabilising proteins (San Martín, 2012).

The penton capsomere proteins are covalent complexes consisting of two proteins, the homopentameric penton base and the homotrimer fibre protein as well as penton minor polypeptide III. The homopentameric penton bases and the polypeptide III form the capsid vertices. These capsid vertices are covalent complexes forming the backbone for the vertices spikes which are fibres (protein IV) (Cauet *et al*., 2005). The penton bases are spade-like shaped with a polygonal cross-section that sometimes forms a hole. The homotrimer fibre

proteins have three distinct regions: tail, flexible shaft and globular knob that connects to the Coxsackie adenovirus receptor (CAR) on the host surface (Feng *et al*., 2018). The structure of the fibre has a site for receptor-binding. Penton capsomere proteins play an important role in the viral cell entry as these proteins serve as attachment sites for cell surface integrin's during viral internalisation (Zubieta, 2005).

### 1.2.4 Genomics and replication

Human adenoviruses have a linear double-stranded DNA genome with a length varying between 26 and 46 kilo base pairs (Kbp), encoding over 40 proteins. Studies suggest that the HAdV genome is likely to be shaped in a loop (Newcomb *et al*., 1984; Kennedy and Parks, 2009). The HAdV-B2 genome was the first HAdV type to be fully sequenced, followed by the HAdV-B5. The genome encodes for three consecutive proteins (terminal protein, DNA polymerase and viral single-stranded DNA binding protein (SSBP). These three proteins form the central portion of the genome (Berk, 2013). The viral genome is divided into two regions, the early region, and the late region. The early-stage region contains the major transcriptional units (E1A, E1B, E2, E3 and E4), four intermediate transcriptional units (IX, IXa, L4 intermediate and E2 late) and one late (Major late) transcriptional unit (McConnell and Imperiale, 2004). The early region units are the first to be transcribed and are involved in transcription activation of the late viral region. This early region also promotes viral production through regulating cellular environments. The E1A region proteins induce mitogenic activity in the host cells and stimulate the expression of other genes and the E1B region proteins play a role the accumulation of the late region viral mRNA (Babiss, 1985; Seth, 1999). The E2 region proteins assist in the viral DNA replication, while the E3 and E4 region proteins alter the host cellular signalling and immune responses (Horwitz, 2004; Weitzman, 2005).

The late region contains transcriptional units (L1-L5) that mainly encode for structural proteins (McConnell and Imperiale, 2004). Once the major late promoter is activated, the late region unit is transcribed from alternatively spliced transcripts (Saha, 2014). During the intermediate region, when the early and late region proteins are transcribed, four small proteins are synthesised. The first two proteins are IX (pIX) and IVa2 which play a role in the packaging of the viral DNA into mature virions (Christensen, 2008). The remaining two proteins are viral associated RNA I and II, which inhibit the activation of interferon responses and block micro-RNA processing that could be expressed by the host gene (O'Malley, 1986; Aparicio, 2006). Figure 1.2 illustrates the map of the adenoviral genome and transcriptional units.

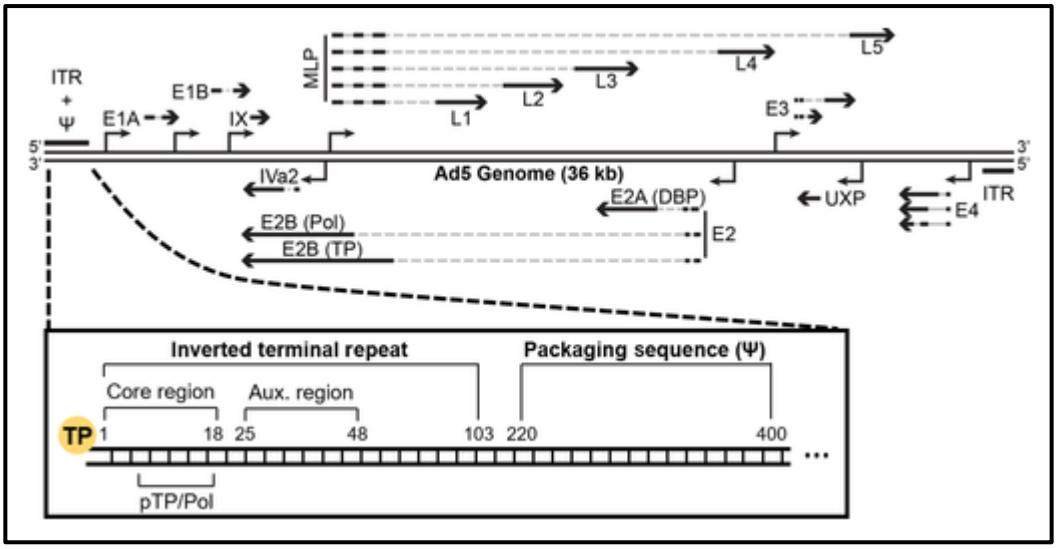


**Figure 1.2: Map of the adenoviral genome and transcription units** (Leen *et al.*, 2006). The central bold line represents the viral genome. The arrows indicate the direction of transcription. *Key:* ITR (internal terminal repeats*),* Ψ (packaging sequence), *E1-4* (early regions), *L1-5* (late regions) and *MLP* (major late promoter) (Charman et al.,2019).

Human adenovirus replication takes place through a strand displacement mechanism (Charman *et al*., 2019). Several protein-protein and protein-DNA interactions occur between the viral machinery, NF1, OCT-1 and the origin of replication. The new DNA duplex is generated and displaces the nontemplate strand. This single-stranded DNA is replicated to generate a new dsDNA genome (Charman *et al*., 2019). The origin of replication is located on both ends of the HAdV genome at the 100 bp inverted terminal repeats (ITR) (Gaggar *et al*. 2003), together with a 200 bp packaging sequence next to the left ITR (Saha, 2014). Each ITR is divided into two origins known as the minimal origin and auxiliary origin. The minimal origin consists of the first 18 bp and the auxiliary origin represents the remaining base pairs (Hoeben, 2013). The left ITR contains a 200 bp packaging sequencing to assist in the replication (Saha, 2014). For replication to take place, three proteins are encoded by the E2 region unit. These three viral proteins are precursor terminal protein (pTP), HAdV DNA polymerase (HAdV Pol) and the DNA-binding protein (DBP). The DNA synthesis begins with the addition of a deoxyribo-cytosine monophosphate (dCMP) residue that is added to the pTP. This forms the protein primer and two cellular transcription factors, NFI and Oct-1, which bind to the auxiliary origin (Hoeben, 2013). This interaction forms the pre-initiation complex causing the structure of the origin to alter by bending extensively. Initiation begins at position 4 of the template, followed by the formation of a pTP-trinucleotide intermediate (pTP-CAT). The pTP-CAT jumps back three bases causing the HAdV Pol to dissociate from the pTP. This increases the polymerisation and proofreading that occurs during the final stages of replication, resulting in the final DNA progeny (de Jong *et al*., 2003).

### 1.2.5 Viral Stability

The HAdV viral stability is comprised of two properties, namely, biological, and physical properties. The biological properties are based on the structure of the virus and the physical properties are based on the virus's ability to withstand different conditions.

#### *1.2.5.1 Biological properties*

The HAdVs non-enveloped and capsomeric lipophilic characteristics allows for chemical sensitivities (Sauerbrei *et al*., 2004a). Despite the viruses being sensitive to chemicals, it can remain infectious for almost three weeks on fomites and has a high potential to spread at room temperature (Lion, 2014). The genome of the virus is also known to show more chemical resistance than the complete viral particle (Sauerbrei *et al*., 2004b). These viruses are stable at a pH ranging from 3 to 8. This allows the virus to survive the gastric acidic conditions within the human stomach. It also permits replication within the gut achieving high viral loads (He *et al*., 2010). The HAdV is known to be the most environmentally stable amongst other non-enveloped viruses (Thurston-Enriquez *et al*., 2005).

#### *1.2.5.2 Physical properties*

Human adenoviruses are highly resistant to several common disinfectants, such as lipid-based disinfectants. The virus stays viable for prolonged periods on environmental surfaces, such as sinks, hand towels, medical equipment and instruments. During the wastewater treatment processing, the HAdV may not be completely removed. However, the virus can be inactivated by chlorine or formaldehyde (Flomenberg, 2009). Temperature is an important factor when analysing the persistance of HAdV within a certain environment. A study done in France by Prevost and colleagues showed that the HAdV encapsulated genomes persisted longer than 70 days in both drinking and surface waters, irrespective of the water temperature (Prevost *et al*., 2016). Heating at temperatures higher that 60ºC-65ºC for 30 minutes and autoclaving at 121 ºC for 30 minutes can also be a method of inactivation (Robinson and Echavarria, 2011). Other environments such as bathrooms, offices and homes should be disinfected with 10% bleach, followed by 70% ethanol. The HAdV is classified as the most UV-resistant pathogen and a dose of approximately 170 mJ/ $cm^2$ is needed to achieve an inactivation of HAdV (Thompson *et al*., 2003). Due to the virus being able to withstand harsh conditions, it is known to be an indicator of faecal contamination in water sources (Rames *et al*., 2016).

## 1.3 CLINICAL ASPECTS

The HAdV is associated with various clinical manifestations in humans. The HAdV is classified into different types and each type causes different diseases.

### 1.3.1 Human adenovirus species classification

Historically, the HAdV strains were type-specifically identified by complement fixation and for the majority, hemaggultination-inhibition (Pereira, 1956; Binn *et al*., 1958; Rosen, 1960). Furthermore, identification based on the genomic structure by cross-hybridisation and restriction mapping was also used (Hall *et al*., 2006). More recent studies have shown that HAdV species can also be identified based on the genetic make-up, which is determined by bioinformatic analysis of whole genome sequencing (WGS) (Hashimoto *et al*., 2018). The designation of each type occurs in chronological order of virus decription ranging from A to G, together with numbers (HAdV-1, HAdV-2, HAdV-3, etc.) as illustrated in Table 1.1.

**Table 1.1:** Genotypic characterisation of the human adenovirus species ( HADVWG, http://hadvwg.gmu.edu/)

| Human adenovirus species | Genotype |
|---|---|
| A | 12, 18, 31, 61, |
| B1 | 3, 7, 16, 21, 50, 55, 66, 68, 76 - 79, |
| B2 | 11, 14, 34, 35 |
| C | 1, 2, 5, 6, 89, |
| D | 8 - 10, 13, 15, 17, 19, 20, 23 - 30, 32, 33, 36 - 39, 42 - 49, 51, 53, 54, 56, 58 - 60, 62 - 65, 67, 69 - 75, 80 - 88, 90 - 103 |
| E | 4 |
| F | 40, 41 |
| G | 52 |

All novel HAdV genotypes must be submitted to the Human Adenovirus Working Group (HADVWG, http://hadvwg.gmu.edu/), which was established in 2011 to coordinate and standardise the designation process of HAdV genotypes (Kajon *et al.*, 2019). The increase in knowledge of differences in virulence and tissue tropism amongst different serotypes have been of clinical value (Swenson *et al*., 1995). Subsequently, this led to the HAdV types being associated with a variety of clinical syndromes.

*1.3.1.1 Species A*

The HAdV-A species comprise of HAdV-A1, HAdV-A12, HAdV-A31 and HAdV-A61 which are present exclusively in the gastrointestinal tract causing enteric infections mainly in children (Mahy and van Regenmortel, 2010). These HAdV types have also shown to be highly oncogenic in rodents, especially HAdV-A12 and HAdV-A18 (Ip et al.,2020). The HAdV-A31 has been detected in stool and urine from immunosuppressed individuals and affect allogenic stem cell transplant patients (Hierholzer, 1992) .

*1.3.1.2 Species B*

Human adenovirus B is subdivided into subspecies B1 and B2 based on tropism and restriction cleavage patterns. The HAdV-B1 types are known to cause mild and self-limiting infections in immunocompromised individuals. Five genomes of the subgenus B1 have been detected from patients with acute respiratory disease (Dehghan *et al*., 2012). There are several types of HAdV-B1, namely HAdV-B3, HAdV-B7, HAdV-B16, HAdV-B21, HAdV-B50 (De Jong *et al*., 1999). The HAdV-B1 types HAdV-B3 and HAdV-B7 are more likely to be associated with morbidity and development of severe complications in children with long-term respiratory infections (Fu *et al*., 2019). The HAdV-B3 is also associated with keratoconjunctivitis (Ghebremedhin, 2014). The HAdV-B1 type HAdV-B50 was first isolated from a faecal specimen from a patient with human immunodeficiency virus (HIV) (De Jong *et al*., 1999). The HAdV-B2 types are known to infect the kidney and urinary tract. Types from this species also causes re-emerging infections leading to fatality in immunocompromised individuals (Kälin *et al*., 2010). The HAdV-B2 types are HAdV-B11, HAdV-B14, HAdV-B34 and HAdV-B35 (Ghebremedhin, 2014).

*1.3.1.3 Species C*

The HAdV-C species are the most well researched and understood adenovirus species. The HAdV types that have been extensively studied for many years are HAdV-C2 and HAdV-C5. These two types comprise of many homologous genes within their genome (Weaver *et al*., 2011). The HAdV-C2 was the first adenovirus genome to be completely sequenced (Roberts *et al*., 1984). This HAdV species causes symptomatic respiratory tract infections mainly in children younger than five years old (Garnett *et al*., 2002) as well as persistent infections that can be detected in faecal excretions (Fox *et al*., 1977). Other members of the HAdV-C species are HAdV-C1 and HAdV-C6, which are common causes of liver and muscle infections (Koren *et al*., 2016). The HAdV-C6 is the most potent cause of liver infections amongst the HAdV C species types, with HAdV-C1 and HAdV-C2 being the least implicated (Weaver *et al*., 2011).

*1.3.1.4 Species D*

Human adenovirus D species are the largest and rapidly growing species compared to all the other species (Ismail *et al.*, 2018). These species are known to mainly cause keratoconjunctivitis and to a lesser extent gastroenteritis. The HAdV-D8, HAdV-D19 and HAdV-D37 were the first HAdV-D types to be described with severe keratoconjunctivitis (Jernigan *et al*., 1993). The HAdV-D8 is the etiological agent known to cause the most epidemic keratoconjunctivitis (Jawetz *et al*., 1955; Espínola *et al*., 2017). The HAdV-D19 and HAdV-D37 were found to cause sporadic outbreaks of keratoconjunctivitis in dry and overcrowded settings (Lord *et al*., 2000). Studies have shown that most of the HAdV-D species causing acute gastroenteritis, usually occur in patients with acquired immunodeficiency syndrome (AIDS) (Li *et al*., 2004; Madisch *et al*.; 2006; Matsushima *et al*., 2013). However, the HAdV- D65 and HAdV-D67 are also associated with gastroenteritis in healthy children that do not have an immunodeficiency (Matsushima *et al*., 2013).

*1.3.1.5 Species E*

The HAdV-E species is comprised of only one type (HAdV-E4) and was identified in the early 1950s during a military outbreak of a well-recognised acute respiratory disease (ARD) (Hilleman and Werner, 1954). These respiratory outbreaks are more likely to occur in closed, overcrowding settings as well as in areas with environmental contamination, which facilitates the transmission of the virus (Kajon *et al*., 2018; Lynch *et al*., 2018). The respiratory infections caused specifically by HAdV-E4 and HAdV-B7 are preventable by vaccination with a live, oral non-attenuated strain, however it is mainly available for usage in the United States of America military (van der Veen *et al.*, 1968; Binder *et al*., 2017). This HAdV-E4 is also known to be the prevalent causative agent of ocular diseases causing pharyngoconjunctival fever (Chigbu and Labib, 2018). Li and Wadell showed that there are two genotypes of HAdV-E4, the HAdV-E4 prototype (HAdV-E4p) and HAdV-E4a (Li and Wadell, 1988). The HAdV-4p are closely related to the HAdV prototype strain RI-67. The HadV-4a exhibits distinct *Bam*HI restriction profiles, inverted terminal repeats and different genetic make-up in the E3 region (Dehghan *et al*., 2013).

*1.3.1.6 Species F*

Human adenovirus F species include two types, HAdV-F40 and HAdV-F41 (Reis *et al*., 2016). These types are known as the fastidious adenoviruses and are difficult to cultivate, requiring optimum conditions (Kidd and Madeley, 1981). The HAdV-F mainly cause acute

gastroenteritis in children less than 5 years old as well as immunocompromised individuals. This HAdV species accounts for approximately 1.5% to 5.4% of diarrhoea cases in children younger than 2 years (Abubakar., 2015; Platts-Mills *et al*., 2018). The virus occurs in high and low-income countries; causing sporadic and outbreak cases and sometimes leads to death (Verma *et al*., 2009; Troeger *et al*., 2017).

#### *1.3.1.7 Species G*

The HAdV-G species is a newly described species and has one type, HAdV-G52. This HAdV species was discovered in 2003, at the Los Angeles County Public Health Department, from diarrhoeal samples, causing gastroenteritis. Research showed that it was closely related to Simian adenovirus (SAdV-1) (Jones *et al*., 2007).

### 1.3.2 Clinical infections

The HAdV causes a wide variety of diseases. Therefore, it is important to understand how the HAdV infection occurs.

#### *1.3.2.1 Infectious cycle*

The HAdVs are lytic DNA viruses with infection occurring by receptor-mediated endocytosis (Leen *et al*., 2006). For viral entry, there is an interaction between the viral fibre protein on the viral capsid and the Coxsackie-adenovirus receptor (CAR). This applies to all HAdV species except to HAdV-B and HAdV-D18, HAdV-D19a and HAdV-D37. The HAdV-B fibre proteins interact with the target cells through CD46 and species HAdV-D18, HAdV-D19a and HAdV-D37 bind to sialic acid residues instead of CAR on the target cells (Arnberg *et al*., 2000; Gaggar *et al.*, 2003). Following the binding, the viral penton base mediates secondary interaction between the virus and specific integrins on the target cell surface. When the adenoviral particles are inside the target cell, they migrate to the nucleus *via* the cellular microtubule network (Greber *et al*., 1996). These viral particles then bind to the nuclear pore complexes and translocate their viral genomes to the nucleus for expression of viral genes (Greber *et al*., 1997). This viral trafficking route is determined by the fibre knob domain whereby the virion protein is able to gain access to the major histocompatibility complex (MHC) class I and II pathways, making the target cells sensitive to the adenovirus T-cell recognition (Shayakhmetov *et al*., 2003). The adenoviral replication has large amounts of adenoviral polypeptides which enable viral assembly in the target host. Figure 1.3 illustrates the adenovirus viral replication cycle and multistage infection process. The multistage infection involves adsorption, internalisation, viral uncoating and virion antigen presentation, trafficking into the nucleus, viral replication,

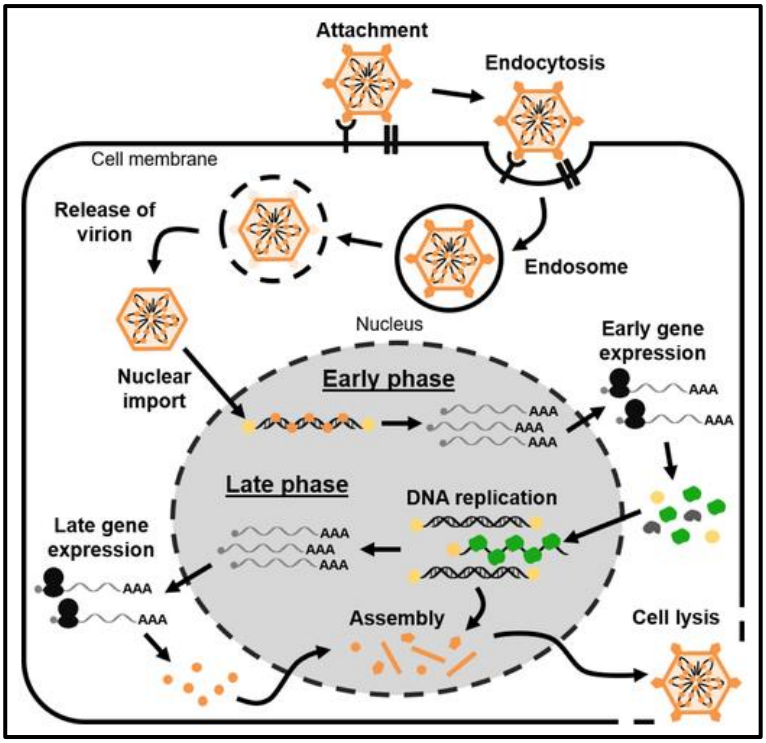


**Figure 1.3: The human adenovirus multistage infection cycle**. This image shows the virus uncoating and antigen presentation before the expression of the immune evasion genes. These steps occur in a temporary fashion after the viral entry into nucleus (Charman et al.,2019)

followed by assembly occurring the nucleus, host cell lysis and release (Charman et al.,2019). During early phase of infection, the viral replication compartments contain the ssDNA accumulating sites where the ssDNA replication intermediates bind to the viral DBP for replication to take place. During late phase of infection, the viral replication compartment undergoes morphological changes, whereby the DBPs which are initially spherical and crescent shaped transition into broken up ring-like assemblies. This transition is an indication of early to late infection progress (Charman at al., 2019).

*1.3.2.2 Pathogenesis*

The adenovirus pathogenicity differs according to species, types, tissue and organ specificity as well as disease patterns (Horwitz, 2001). The virus creates a robust activation of the immune response, affecting several cellular pathways (Hartman *et al*., 2007). During viral entry, the virus activates a strong proinflammatory response and induces an inflammasome and inflammatory responses (Barlan *et al*., 2011). During the infection cycle, prior to immune evasion, several pathogen-associated molecular outcomes, such as the activation of NF-κB and signal transduction, determining the type of immune response. The innate immune response is activated first, which represents the first line of defence, recognising intracellular and extracellular compartment receptors (Leen *et al*., 2006). Subsequently, adaptive immunity is then activated and is mediated by the T and B cells (Olive *et al*., 2001). The expression of the

E1A gene after infection, assists in the increase in efficiency of other genes in the cell cycle and represses the early inflammatory responses such as NF-κB and signal transduction pathways (Cook *et al*., 2002). The HAdV inhibits the cellular DNA, mRNA and protein synthesis causing cell degeneration. The E3 transcription encodes for proteins which alter the innate and adaptive immune responses (Burgert *et al*., 2002). Overall, there are three main types of infections in which the HAdV interacts with the host cell. Firstly, the lytic infection of epithelial cells whereby the virus completes the multiplication cycle, producing cellular death and releasing 5% of new infectious viruses. Secondly, the latent infections which occur in the lymphoid cells where only small amounts of virus particles are released and cellular death is not affected by the multiplication process. Thirdly, the oncogenic transformation in rodents, where the HAdV DNA is included in replication without producing new infectious viral particles (Ghebremedhin, 2014).

*1.3.2.3 Clinical syndromes*

The HAdV is known to be a worldwide causative agent of several diseases associated with sporadic and epidemic diseases. The virus is seldom associated with life-threatening diseases but there is evidence of latent infections that persist, particularly with HAdV-C (Garnett *et al*., 2002). When the HAdV becomes an opportunistic pathogen within immunosuppressed individuals, it causes prolonged, severe and potentially fatal infections (Leen and Rooney, 2005). Therefore, the clinical manifestations of the virus are based on age and immunocompetence as shown in Table 1.2 below, illustrating the adenoviral diseases according to age population.

**Table 1.2:** Adenoviral diseases most commonly caused by specific human adenovirus types according to patient population (Flomenberg *et al*., 2012; Arnold and MacMahon, 2017)

| **Patient Information** | **Clinical syndromes** | **Human adenovirus types** |
|---|---|---|
| Infants | Pharyngitis, coryza, otitis media | 1-7 |
| | Pneumonia | 1-3,7 |
| | Diarrhoea | 40, 41 |
| Children | Upper respiratory disease, pneumonia | 1-3, 7 |
| | Pharyngoconjunctival fever | 3, 4, 7 |
| | Diarrhoea | 40, 41 |
| | Haemorrhagic cystitis | |
| Adults | Acute respiratory disease | 1-7 |
| | Epidemic keratoconjunctivitis | |
| | Haemorrhagic cystitis | 19,37 |
| Immunocompromised | Pneumoia | 1-3, 7 |
| | Gastroenteris, hepatitis | |
| | Haemorrhagic cystitis, interstitial nephritis | |
| | Meningoencephalitis | |

#### *1.3.2.3.1 Enteric infections and gastroenteritis*

Gastroenteritis results in the inflammation of the stomach and intestines causing nausea, vomiting and diarrhoea (Oude Munnink and Van der Hoek, 2016). It is responsible for approximately two to three million deaths yearly (Kotloff *et al*., 2013). This causes severe diarrhoeal infections in children younger than five years old (Kotloff *et al*., 2013). The HAdV-F (type 40 and 41) and HAdV-G (type 52) are responsible for 1.5%-5.4 % of diarrhoeal cases in children younger than 2 years (Jones *et al*., 2007; Eckardt and Baumgart, 2011; GBD Diarrhoeal Disease Collaboration., 2017).

#### *1.3.2.3.2 Respiratory Diseases*

One third of the HAdV serotypes cause acute upper and lower respiratory infections, which mainly affects children with pneumonia, bronchiolitis or croup (Hong *et al*., 2001). These infections can occur endemically or in epidemics throughout the year affecting communities, hospitals or chronic care facilities (Chany *et al*., 1958; Teng, 1960; Wesley *et al*., 1993; Scott *et al*., 2016). The most common causes of adenoviral respiratory infection are: HAdV-B3, HAdV-B7, HAdV-B14 and HAdV-B21, followed by HAdV-C1, HAdV-C2 and HAdV-C5 and HAdV-E4 (Scott *et al*., 2016). The HAdV-B and HAdV-C are predominantly found to be part of the sporadic outbreaks in severe cases of infected adults (Metzgar *et al*., 2007).

#### *1.3.2.3.3 Ocular Diseases*

Adenovirus is the most important pathogen causing ocular diseases, accounting for 92% of all keratoconjunctivitis cases worldwide (Bialasiewicz, 2007). The most prevalent HAdV species associated with keratoconjunctivitis is HAdV-D, followed by HAdV-B. Keratoconjunctivitis is one of the most severe ocular diseases affecting the ocular surface causing inflammation around the cornea and conjunctiva of the eye. Symptoms include itching, tearing, burning, photophobia and in severe cases enlargement of lymph nodes. The majority of adenoviral ocular infections are subclinical and usually are self-limiting (Chigbu and Labib, 2018).

#### *1.3.2.3.4 Urinary and Genital tract infections*

Urinary tract infections (UTIs) leading to haemorrhagic cystitis is likely to be caused by the adenovirus (Paduch, 2007). The HAdV-B11 mainly causes UTIs (Asim *et al*., 2003). These infections usually affect children and immunosuppressed individuals, resulting in hypertension, fever, proteinuria, and glomerulonephritis (Mufson and Belshe, 1976; Nanmoku *et al*., 2016).

Sexually transmitted infections are associated with HAdV-C2, HadV-D8 and HAdV-D37 and cause inflammation in the mucous membrane of the genital areas resulting in genital ulcers, cervicitis and urethritis (Swenson *et al*., 1995; Hanaoka *et al*., 2019).

*1.3.2.3.5 Immunocompromised individuals*

Immunocompromised individuals, such as bone marrow transplant (BMT) recipients, acquired immunodeficiency syndrome (AIDS) and organ transplant recipients may be affected by adenoviral infections (Carrigan, 1997; Hiwarkar *et al*., 2018). There is normally more than one type of infection caused by HAdV which are usually associated with high fatality rates. The HAdV-B11 and HAdV-B35, HAdV-C1 and HAdV-D29 are the adenoviral serotypes, which can cause opportunistic infections in immunocompromised individuals. The HAdV disease is usually related to the organs involved in the illness of the immunocompromised individual (Carrigan, 1997; Lion, 2019).

## 1.4 TREATMENT AND PREVENTION

The majority of the HAdV infections are mild and therefore, do not always require professional medical care or treatment (Echavarría, 2008). For severe respiratory cases, bronchodilator medication to open the congested airways, oral rehydration and increased fluid intake is usually dispensed. In immunocompromised patients antivirals, such as ribavirin and cidofovir are prescribed (Lynch and Kajon, 2016).

A live non-attenuated, oral vaccine was developed against HAdV-E4 and HAdV-B7 for the United States (US) military only in 1971 (Russell *et al*., 2006). However, this vaccine was depleted by 1999. Thereafter, the same vaccine was reintroduced to the US military in October 2011 due to an increase in infections in the US military (Kajon *et al*., 2015). Although this vaccine provides antibodies to HAdV-E4 and HAdV-B7, it may cross protect against other serotypes as well (Trei *et al*., 2010).

## 1.5 LABORATORY DIAGNOSIS

The gold standard technique for direct detection of HAdV used to be viral isolation; however, it takes several days or weeks for results, which is impractical for diagnostics purposes (Munoz *et al*., 2015). There are several other ways of rapid detection, such as serology, enzyme immune assay using direct antigen detection methods and immunofluorescence (Rossouw, 2004). However, the disadvantage of these techniques is that they are less sensitive (Avellón *et al*., 2001). Due to the adenovirus having a broad tropism, molecular techniques are useful (Robinson *et al*., 2013).

Therefore, the new gold standard technique is a genome amplification technique, the polymerase chain reaction (PCR), which produces rapid results with increased sensitivity. In addition, it is capable of detecting all types of adenovirus within environmental samples and clinical specimens, which is ideal for a research environment (Glimåker *et al*., 1992).

### 1.5.1 Serology

A serological diagnosis can be performed using assays of paired acute and convalescent sera for adenovirus-specific antibodies (Fields *et al*., 1996). Adenovirus-specific EIA and complement fixation assays are used, to measure the adenovirus-specific anti-hexon antibodies but these techniques do not provide the serotype. The detection of hemagglutination inhibition antibodies or neutralising antibodies is more sensitive and serotype specific (Munoz *et al*. 2015).

### 1.5.2 Viral antigen assays

Viral antigen assays are based on the direct detection of adenovirus antigens in clinical samples using enzyme immune assays (EIA) and immunofluorescence (IF). The use of adenovirus-specific monoclonal antibodies reacting with common antigenic determinants on all serotypes are used commercially. These antigen assays are mainly used for the detection of fastidious adenovirus types, such as HAdV-F40 and HAdV F-41 (Herrmann *et al*., 1987).

### 1.5.3 Viral isolation

For HAdV specificity, viral cultures can also be used to detect most of the HAdV serotypes, except for HAdV-F40 and HAdV-F41 (Levent *et al*., 2009). These viral cultures usually show characteristic cytopathic effects (CPE) in human epithelial cell lines presenting with swelling and clumping of the host cells. The human epithelial cell lines usually used are HeLa and A549 as well as stable human embryonic kidney (HEK) cells. This CPE culturing usually takes 28 days (Wold and Horwitz, 2007). Although viral cultures have been replaced by PCR, this technique is still used for research purposes. An example of HAdV CPE is shown in Figure 1.4. This figure represents sub-confluent monolayers of porcine PK15 cells and primary cultures of porcine kidney cells that were infected at an MOI (Multiplicity of Infection) of 5 with HAdV-5 and mock-infected control. This image was taken seventy-two hours after infection (Jogler *et al*., 2006).

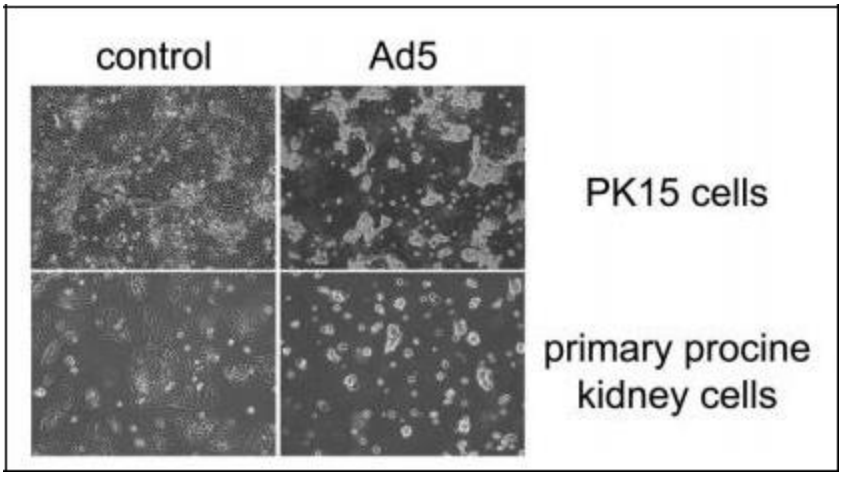


**Figure 1.4:** Adenovirus CPE in porcine kidney cells (PK 15 cells) and primary porcine kidney cells. Photographed through inverted phase-contrast microscope (original magnification, X 20) (Jogler *et al*., 2006).

### 1.5.4 Viral detection using molecular methods

Molecular methods are used for monitoring and tracking the presence of a particular pathogen (Girones *et al*., 2010). The molecular method used for adenoviral detection is PCR, which is the most important technique, since it is highly sensitive and specific. Due to the adenovirus having different genotypes that are heterogeneous at DNA level, different primers are used for the detection of specific or related genotypes (Allard *et al*., 1992). The hexon regions in the HAdV is most commonly targeted for diagnosis and types using conventional PCR (Casas *et al*., 2005; Akhil *et al*.,2016). For diagnostic purposes, qPCR is the preferred method for the detection of HAdVs (Heim *et al*., 2003). Commercial adenovirus qPCR assays that are used comprise of both universal primers and probes, which detects the majority of genotypes (Claas *et al*., 2005). Applications of PCR enable HAdVs to be detected in various specimens, such as blood and environmental samples, which were previously difficult to use for detection (Kampmann *et al*., 2005; Okoh *et al*., 2010).

### 1.5.5 Recovery of human adenoviruses in environmental water samples

There is a significant amount of human-associated pathogens present in urban sewage resulting in the contamination of these waters, which is known to be point-sourced pollution (Sinclair *et al*., 2009). Most of these pathogens are removed by sewage treatment; however, some remain and get discharged into the effluent and are likely to enter the receiving waters. The HAdV is known to be the second largest cause of documented outbreaks of water-borne diseases after norovirus and due to the high prevalence in water, it can be used as indicators of faecal pollution (Fong *et al*., 2010;

2010; Eftim *et al.*, 2017). Other important viral waterborne pathogens are Norovirus GI and GII,, Astrovirus 1-9, Hepatitis E, Sapovirus, Enterovirus A-D, Poliovirus 1-3, Aichivirus A-C, Parechovirus 1-16 and Rotavirus A-G (Rusinol and Girones, 2017).

There is usually a two-step process when analysing water for enteric viruses, firstly, the primary recovery whereby samples need to be processed to concentrate the virus into smaller volumes (less than 10 mL). This is due to the viruses being too few for direct detection (Wyn-Jones and Sellwood, 2001). The detection is the second step, whereby the virus is usually detected quantitatively and if necessary, the virus may be isolated and identified. For optimal concentration, the recovery of viruses include the following criteria: (i) the recovery method should be technically easy to perform during a short period of time, (ii) have a high viral recovery rate, (iii) must be able to concentrate a wide range of viruses, (iv) provide a small volume concentrate and (v) should not be costly (Block and Schwartzbrod, 1989). There are several primary recovery techniques, and all these techniques have one main challenge, which is to maximise the virus recovery without decreasing the viral load.

*1.5.5.1 Adsorption-elution*

The adsorption-elution technique was first described by Wallis and colleague, whereby the virus is adsorbed by a matrix under specific pH and ionic strength conditions (Wallis and Melnick, 1967). The adsorbent can be an electron-charged glasswool column, borosilicate glass beads, electropositive cartridges and membranes or other filter membranes (Sarrette *et al*., 1977; Vilaginès *et al*., 1993). Following this, the virus undergoes a secondary concentration whereby the virus is eluted from the matrix to a smaller volume using either beef extract at pH 9.5 or skimmed milk at pH 9 or polyethylene glycine /NaOH at pH 9.5-11.5 (Wyn-Jones and Sellwood, 2001).

*1.5.5.2 Skimmed milk flocculation*

The skimmed milk flocculation (SMF) is a technique that relies on the conductivity and pH of the samples. The conductivity should always be ≥ 1.5 mS and this is obtained using artificial sea salts (Calgua *et al*., 2013). This technique is an efficient low-cost method to concentrate viruses in all types of water samples. It also shows the recovery of viruses with a low variability (Gonzales-Gustavson *et al*., 2017).

*1.5.5.3 Entrapment*

Entrapment is a technique whereby the virus is held in a filter matrix based on the molecular size (Percival and Wyn-Jones, 2014). This is achieved by ultrafiltration, which filters the water under pressure through capillary membranes with hollow fibres permitting the water to flow through excluding macromolecules that attach to the membrane or fibre. This technique is usually only useful for small volumes (100 mL or less) (Percival and Wyn-Jones, 2014). Other forms of entrapment are vortex flow filtration (VFF) as well as tangential flow filtration which is similar to ultrafiltration with an added step involving the reduction of clogging (Fong and Lipp, 2005).

*1.5.5.4 Ultracentrifugation*

This technique is known as the catch-all method as it concentrates all viruses in a sample provided that there is sufficient G-force (gravitational force) and time. This catch-all method predominantly works for clean water and purified sewage. However, there are a few disadvantages when using this technique. These include processing limited volumes, high costs and the lack of portability of equipment (Wyn-Jones and Sellwood, 2001).

*1.5.5.5 Other techniques*

There are other recovery techniques, such as two-phase separation technique and immuno-affinity columns with magnetic beads technique. The two-phase separation technique is where the viruses are partitioned between two phases formed when organic polymers are dissolved in water. Immuno-affinity columns with magnetic beads technique can be used for small volumes. Iron oxide flocculation and talc-celite adsorption are techniques which are used to a lesser extent (Wyn-Jones and Sellwood, 2001).

## 1.6 EPIDEMIOLOGY

The epidemiology of the HAdV encompasses how and where the HAdV is transmitted. It also focuses on the period of communicability and the worldwide spread of the HAdV that could potentially cause severe outbreaks.

### 1.6.1 Modes of transmission

The HAdVs are likely to be transmitted *via* several routes. This commonly occurs in the case of stable viruses that lack the lipid envelope which makes them less susceptible to environmental agents and the digestive track (Girones *et al*., 2010). The predominant routes of transmission occur

through aerosols, respiratory secretions, person-to-person contact, contaminated fomites or *via* the faecal-oral route (Barnadas *et al*., 2018). Respiratory infections are airborne transmitted, and outbreaks are more likely to occur seasonally. These infections are usually transmitted through inhalation of air droplets or direct contact with infected bodily fluids of an infected person and fomites (Bonvehí and Temporiti, 2018). Ocular infections caused by the HAdV are most likely to be spread *via* person-to-person contact in overcrowded areas, or direct inoculation of contaminated fingers around the eye area (Garcia-Zalisnak *et al*., 2018). Exposure to contaminated areas such as swimming pools and other recreational water also increase the transmission rate of these infections (van Heerden *et al*., 2005). Enteric strains affecting the gastrointestinal tract are transmitted *via* faecal-oral routes after being in contact with contaminated recreational water such as swimming pools, freshwater or tap water (Mickan and Kok, 1994; Wyn-Jones *et al*., 2011; Love *et al*., 2013). There is a possibility for the virus to be spread *via* a nosocomial pathway from exposure to contaminated hands of healthcare personnel and infected medical equipment (Bialasiewicz, 2007).

### 1.6.2 Reservoirs

The HAdV is found to be ubiquitous within environmental waters, such as wastewater treatment plants where contaminated sewage is present (Gray, 2006). The virus is also found to be present in drinking waters presenting with the potential of high replication and mutability rates which can result in an increased pathogenicity (Silva *et al*., 2015). This virus is only pathogenic to the species of origin and is seldom pathogenic to animals. Infections are becoming an increasing threat to immunocompromised individuals, especially those who have received transplants (Rodríguez *et al*., 2016).

### 1.6.3 Incubation and duration periods

These infections have an incubation period ranging from two days to two weeks. These incubation periods are dependent on the adenoviral viral type, mechanism of acquisition and spectrum of clinical manifestations (Lynch *et al*., 2011). Respiratory infections, which are more common amongst children usually have an incubation period before onset of symptoms of about four to eight days (Lessler *et al*., 2009). For less severe respiratory infections, the symptoms (fever, cough, coryza and sore throat) usually last for three to five days. More severe respiratory symptoms will last for as long as two to four weeks (Tabain *et al*., 2012). For intestinal infections, the incubation period is about 3 to 10 days and the duration ranges from three days to two weeks (Orenstein, 2020). Ocular infections, depending on the severity, can persist from two to four weeks and can even cause diarrhoea lasting for two more weeks (Uhnoo *et al*., 1984; Pihos, 2013).

### 1.6.4 Period of communicability and shedding levels

The contagiousness of the human adenovirus is based on the large number of viral particles (100 000 – 1000 000 viral copies/mL) in sputum or oral secretions of an infected individual (Murphy, 2017). Enteric HAdV are excreted in faeces up to $1.0 \times 10^{11}$ virion copies per gram of stool, with an infectious dose of less than 150 plaque forming units (Allard and Vantarakis, 2015). These enteric HAdVs have a HAdV carriage that is eight times higher than any of the non-enteric HAdV carriers within the diarrhoeal specimens. The secretion levels of the non-enteric HAdV particles may persist for months, which leads to their presence within the stool (Hassan et al., 2017).

### 1.6.5 Geographical distribution

The virus is dispersed throughout the world and the strains differ and evolve over time between the various geographical regions(Ampuero *et al*., 2012). These new HAdV strains may lead to either being rare within an area or can be found to re-emerge, resulting in the replacement of the initial dominant strains causing infection (Kajon *et al*., 2010). The virus is predominantly occurring in middle to low-income countries on continents such as Asia, Africa and South America, in closed communities or contaminated environments, where water and sanitation facilities are insufficient and scant (Baker *et al*., 2016). These impoverished conditions place many children younger than the age of 5 years old as well as immunocompromised individuals at risk of being infected (Moyo *et al*., 2014). The most globally prevalent HAdVs associated with human diseases are HAdV-B3, HAdV-B7, HAdV-B21, HAdV-C1, HAdV-C2, HAdV-C5, HAdV-E4, HAdV-F40 and HAdV-F41 (Guo *et al*., 2012).

#### *1.6.5.1 South Africa*

The HAdV species F, types 40 and 41 were shown to be predominant in South African paediatric stool specimens in 1998 (Moore *et al*., 1998). Subsequently, HAdV-F40 and HAdV-41 as well as HAdV-A12 and HAdV-31 were also detected in the stool specimens of children in South Africa (Rossouw, 2004). A study based on the epidemiology of HAdV infections in SA from 2009 to 2014, detected the presence of HAdV in 656/3623 (18.1%) hospitalised children with acute gastroenteritis. Of these 656 hospitalised children, 377/656 (57.5%) were male and 279/656 (42.5%) were female. Co-infections with other enteric viruses, bacteria and parasites were found in a high number of these infections (76.3%). The causative role of HAdV in these infections were uncertain. The HAdV species that were identified include HAdV-A, HAdV-B, HAdV-C, HAdV-D, HAdV-E and HAdV-F (Netshikweta *et al*., 2019). A recent study confirmed the association of HAdV with respiratory disease within children that were

hospitalised with pneumonia in the Western Cape province, South Africa (Zampoli and Mukkendum-Sably., 2017). The HAdV was detected in contaminated treated and untreated sewage and final effluents of selected WWTPS, rivers and drinking waters. A study conducted within the Eastern Cape Province, South Africa, showed that HAdVs were detected in 64% of raw sewage samples from five WWTPS (Osuolale and Okoh, 2015). Another study showed the presence of groups F and D in rivers and drinking water within Gauteng, South Africa (van Heerden *et al*., 2005). In other studies, the detection of HAdV and other enteric viruses was shown in river waters in Eastern Cape Province (Enriquez *et al*., 1995; Sibanda and Okoh, 2012; Lin and Singh, 2015). The virus is found to be present in rivers contaminated by raw sewage, which can potentially cause a serious threat to public health (Vos and Knox, 2018).

### 1.6.6 Seasonal distribution

The occurrence of the human adenovirus may vary seasonally as the virus is constantly secreted by infected individuals that are either symptomatic or asymptomatic (Vetter *et al*., 2015). A study done in Greece showed a peak in adenovirus within domestic sewage during the winter months (Krikelis *et al*., 1985). Human adenovirus associated respiratory infections usually occur throughout the year with no particular peaked season (Price *et al*., 2019). Enteric HAdV infections are known to mainly peak during the winter months (Pang *et al*., 2019). This indicates that the virus is capable of persisting longer in the environment during winter conditions (Tao *et al*., 2016).

## 1.7 MOTIVATION

Gastroenteritis is a leading cause of morbidity and mortality worldwide. The 2015 Global Burden of Disease study showed that globally HAdV was the fourth leading cause of mortality in children younger than five years (GBD Diarrhoeal Disease Collaborators, 2017). However, there is limited data on the prevalence and types of HAdVs circulating in South Africa, specifically the Tshwane region of Gauteng. Surveillance of sewage samples for the presence of HAdV is beneficial as HAdV causing symptomatic or asymptomatic infections can be detected (Zhang et al., 2011). Therefore, the analysis and surveillance of the presence of HAdV within two WWTPS in the Tshwane region will create a broader perspective and awareness of the HAdV circulating within the surrounding communities. This will be based on the detection, quantification and genotyping of HAdV as well as determination of viral seasonality.

## 1.8 AIM

This study aimed to investigate the presence and genotypes of human adenovirus in environmental samples namely raw sewage and treated effluent, using molecular methods.

## 1.9 OBJECTIVES

The objectives of the study were:

- To recover human adenovirus from the collected raw sewage samples by primary precipitation with skim milk flocculation
- To recover human adenoviruses from the collected treated effluent samples using glass wool adsorption-elution technique followed by secondary precipitation with polyethylene glycol$_{8000}$/sodium chloride (PEG$_{8000}$/NaCl) precipitation
- To prepare a standard curve, using known dilutions of a HAdV standard for the quantitative detection of HAdVs
- To extract, detect and quantify the HAdVs in samples collected from August 2018 - January 2020, using real-time PCR
- To determine the genotypes of human adenovirus strains detected in the samples using targeted next generation sequencing as well as cloning and Sanger sequencing on selected samples.
- To compare the types identified with Sanger sequencing and next generation sequencing and to determine the genetic relatedness of the viral strains detected using phylogenetic analysis.

# CHAPTER 2

# MATERIALS AND METHODS

## 2.1 FLOW DIAGRAM

Figure 2.1 is a schematic representation of the experimental workflow for this study. All the steps were conducted by the master's candidate, apart from Illumina MiSeq which was performed at the National Institute of Communicable Diseases.

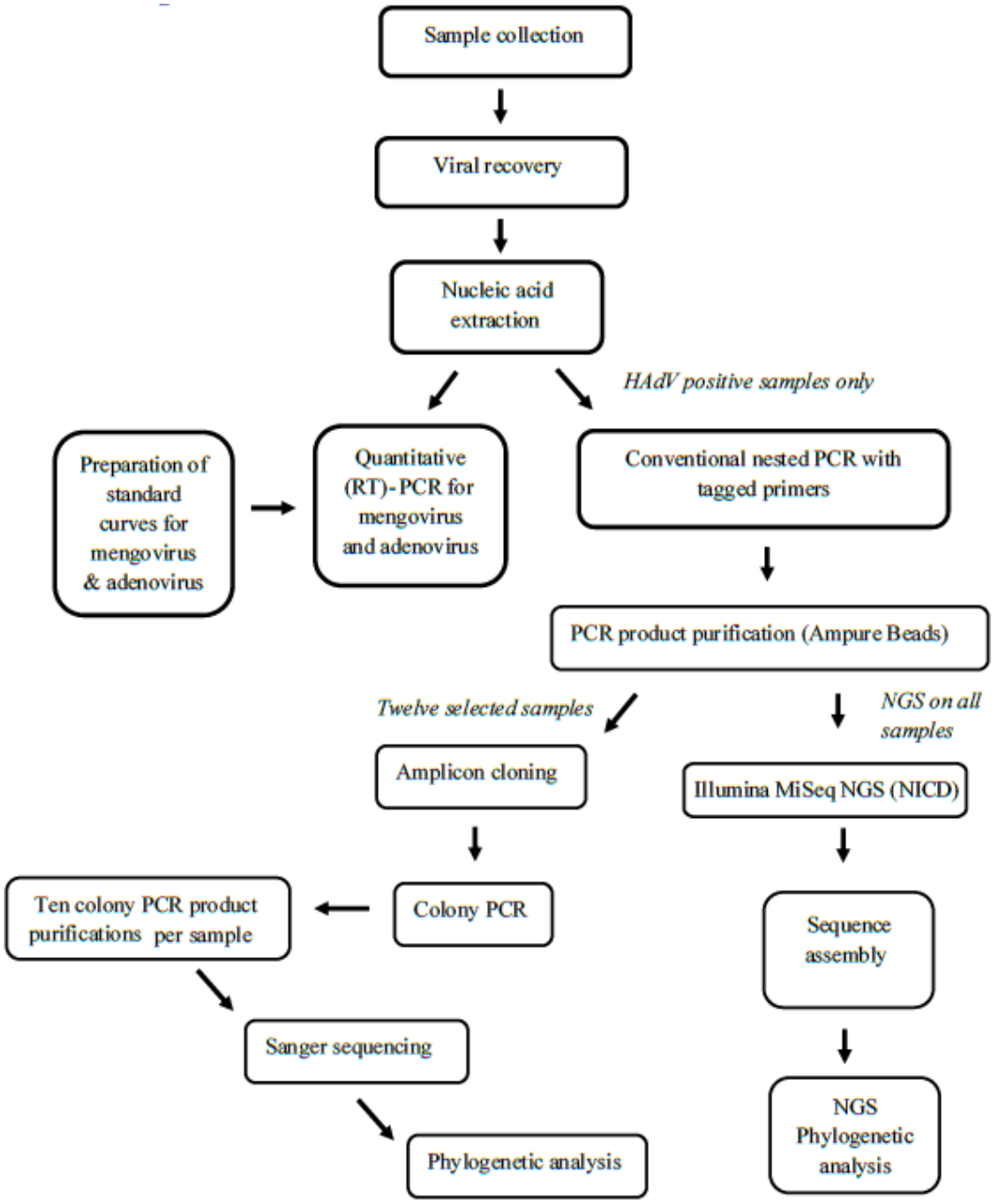


**Figure 2.1: Schematic representation of the experimental workflow.**

## 2.2 ETHICS APPROVAL

Ethical approval for this study was granted by the Research Ethics Committee of the Faculty of Health Sciences, University of Pretoria, South Africa with an approval number: 249/2019 (see appendix C for the certificate). Wastewater treatment samples were used for research purposes and no unethical procedures or tests were conducted during the study.

## 2.3 ENVIRONMENTAL SAMPLE COLLECTION

The surveillance of the environmental samples was part of a retrospective and prospective study using samples from two selected wastewater treatment plants (WWTPs) within the Tshwane region as shown in Figure 2.2. From August 2018 to January 2020 (18 months), a total of 150 samples (75 raw sewage and 75 effluent) were collected.

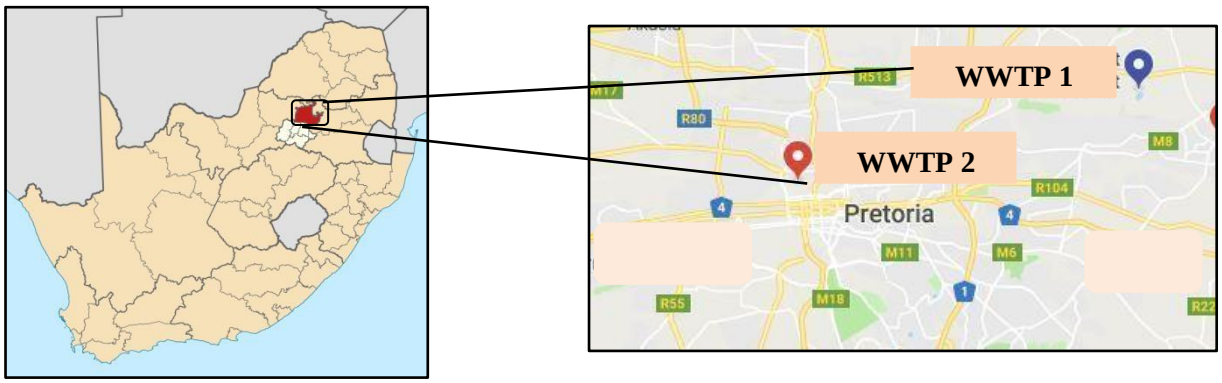


**Figure 2.2: Representative map of sampling sites in Tshwane, South Africa.** The blue beacon represents WWTP 1 and the red beacon represents WWTP 2. Maps obtained from *http://www.google.com/search?q=maps+of+Tshwane&tbm=isch&source=iu&ictx=1&fir=cooSdiBlUilTuM%253A%252CqQM-eWIoM*b and *https://www.google.com/maps/search/baviaanspoort+wastewater+treatment+plant/@25.7141116,28.207454,11z.*

The environmental samples comprised of one raw sewage sample (1 L) and one effluent sample (10 L) and were collected every month, fortnightly from two WWTPs. These collected samples were transported in a cooler box to the laboratory. Upon arrival the pH and temperature of each sample were recorded before viral recovery took place.

## 2.4 SAMPLE PROCESSING

The raw sewage samples were processed using the skimmed milk flocculation method. The treated effluent treated samples were processed using the glass wool adsorption-elution technique, followed by secondary $PEG_{8000}$/NaCl viral precipitation developed by Vilaginès *et al.,* (1993) and adapted by Mans *et al.,* (2013).

### 2.4.1 Skimmed milk flocculation

The raw sewage samples were subjected to primary precipitation with skimmed milk flocculation and centrifugation (Assis *et al.,* 2018). The pre-flocculated skimmed milk solution (PSM) (1%, w/v) was prepared by dissolving skimmed milk powder [Oxoid, Hampshire, United Kingdom (UK)] in artificial sea water (Sigma-Aldrich, St. Louis, MO) (pH 3.5). The artificial sea water solution (3.33%, w/v) was prepared in the laboratory using artificial sea salt followed by the adjustment of the pH to 3.5 with HCl [1 Molar (M)] (Merck, Darmstadt, Germany). This solution was prepared just before use or stored at 4°C for a maximum of 24 hours.

The pH of the samples was adjusted to 3.5 by adding 1 M HCl (Merck). Following this, the conductivity was measured at 25°C using the Hanna digital conductivity meter (Sigma-Aldrich) and 10 mL artificial sea salt solution was added to samples with conductivity below 1 500 µS/cm. The prepared PSM was added to samples to a final concentration of 0.01% (v/v) and the mixture was then stirred at room temperature (22'C-25'C) for eight to ten hours. Subsequently, the samples were centrifuged at 10 000 x g for 30 minutes at 4°C in the GS-6R centrifuge (Beckman Coulter, Brea, CA) and the supernatant was carefully discarded. The pellet was resuspended in 10 mL of phosphate buffered saline (PBS, pH 7.4) (Sigma-Aldrich) and 0.2 volumes of chloroform (Merck) were added. This solution was vortexed vigorously for a minute and then centrifuged at 10 000 × g for 5 minutes at 4°C in the GS-6R centrifuge (Beckman Coulter). The resulting aqueous phase was passed serially through phosphate buffer saline (PBS) (Merck). This viral concentrate was stored at -80˚C in aliquots of 1 mL until analysis.

### 2.4.2 Preparation of glass wool adsorption-elution columns

The glass wool adsorption-elution technique is a virus recovery method used for large volumes of environmental water samples and therefore was used for the 10 L effluent treated sewage

water samples. This technique was developed by Vilaginès and colleagues and the modified version of this method was used (Vilaginès *et al.,* 1993; Mans *et al.*, 2013). Glass wool columns were prepared, using 15 grams (g) of glass wool per column which was divided into three 5 g portions. Steel gauze (1 $mm^2$ pore size, 30 mm diameter) was then inserted between each glass wool portion to prevent clogging of the glass wool by debris. To positively polarise the glass wool, 200 mL of distilled water ($dH_2O$), 40 mL HCl [1 Molar (M)] (Merck), 100 mL $dH_2O$, 40 mL NaOH (1 M) (Merck) and 200 mL $dH_2O$ were passed through each glass wool column, in a sequential manner. The pH of the last flow through was checked on Whatman® pH Indicator Paper (GE Healthcare, Buckinghamshire, UK) to ensure the final pH of the glass wool columns was 7. These columns were sealed with parafilm (Merck) and stored at 4℃ until use.

#### *2.4.2.1 Viral recovery from glass wool column*

The 10 L effluent samples were filtered through the positively charged glass wool column using negative pressure that was applied by a Gast vacuum pump (Gast manufacturing, Inc. Benton Harbour, MI, USA). Thereafter, the virus was recovered from the glass wool by eluting the virus using 100 mL Glycine-beef extract buffer (GBEB) [0.05 M glycine (Merck) and 0.5% beef extract (BBL™ Benton Dickinson and Co., Sparks, MD)] with a 15-minute incubation at room temperature (22'C-25'C). Following this, the pH of the eluate was adjusted to 7 with 1 M hydrochloric acid (HCl) (Merck). This eluate (100 mL) was then subjected to secondary viral recovery using $PEG_{8000}$/NaCl viral concentration as described below.

#### *2.4.2.2 Polyethylene glycol$_{8000}$/sodium chloride viral concentration*

The $PEG_{8000}$/NaCl solution was prepared by adding 250 g of $PEG_{8000}$ (Amresco, Solon, OH) and 43.5 g NaCl (Merck) in a final volume of 500 mL with $dH_2O$. This solution was then incubated (50˚C overnight) in a Heraeus Incubator (Thermo Fisher Scientific, Waltham, CA) for the solutes to dissolve prior to sterilisation in an autoclave (Hirayama Manufacturing Corporation, Kasukabe-Shi Saitama, Japan) at 121℃ for 15 min (Minor *et al*., 1985; Lowther *et al.,* 2013).

Subsequently, 25 mL of the PEG/NaCl was added to 100 mL eluate from the glass wool column and this mixture was placed on ice in a shaking water bath (GFL, Burgwedel, Germany) for an hour. Following this, the PEG/NaCl-solution was centrifuged at 10 000 x g for 30 minutes in the Sorvall®Super T21 centrifuge (DuPont, Wilmington, DE) at 4°C. The supernatant was discarded, and the resulting pellet was resuspended in 10 mL PBS (pH 7.2). The resulting virus concentrate was clarified by adding 0.2 volumes of chloroform, followed by vigorous vortexing and centrifuging at 10 000 x g for 5 minutes in the GS-6R centrifuge (Beckman Coulter). The supernatant was removed and stored at -20°C.

## 2.5 VIRAL DETECTION

Nucleic acids were extracted from the recovered viral suspensions. Human adenovirus (HAdV) was subsequently detected and quantified using real-time PCR. For quantification of the HAdV, mengovirus (MV) was used as an extraction control.

### 2.5.1 Nucleic acid extraction

The QIAmp® UltraSens® virus kit (Qiagen, Hilden, Germany) with spin column technology, was used for nucleic acid extraction according to the manufacturer's instructions. One mL of each sample was seeded with a known concentration of mengovirus tissue culture infectious dose ($TCID_{50}$) of 0.5 $TCID_{50}$. A typical extraction run consisted of 11 samples and one negative sample, which comprised of nuclease-free water. Once the extraction was complete, the extracted nucleic acids were eluted in 100 µL, aliquoted and stored at -80℃. There were no positive control samples included to prevent contamination.

### 2.5.2 Preparation of standard curves

For viral detection, MV was used as an extraction control. Therefore, standard curves were prepared for MV and HAdV in order to quantify the HAdV that will be detected.

#### *2.5.2.1 Mengovirus*

Menogovirus is a non-pathogenic murine virus and has previously been used as an extraction control to control the efficiency of the extraction procedure for the detection of enteric viruses from food and water samples (Pinto *et al*., 2009; Bosch *et al*., 2011). This virus was an extraction control because it is unlikely for this virus to occur naturally in water sources. A cell culture stock of mengovirus was kindly provided by Prof Albert Bosch, Department of

Microbiology, Faculty of Biology, University of Barcelona, Barcelona, Spain. This cell culture stock was used to generate the mengovirus standard curve. The concentration of the culture stock was 3.28 x $10^7$ TCID50/ mL, which was used to extract 140 µL of mengovirus nucleic acids. Thereafter, the extracted nucleic acids were eluted into 60 µL and of that, 5 µL was used as the initial undiluted volume to construct the standard curve. The standard curve was generated using a ten-fold serial dilution of mengovirus. The real-time reverse transcriptase PCR (RT-qPCR) reaction mix (25 µL) consisted of the following: 5 µL mengovirus RNA, 1 x Quantifast Pathogen Master Mix, 1 x RT-PCR enzyme mix, 1 x internal control (IC) Assay and 1 x IC RNA. The protocol used for amplification is described in Table 2.1 and was done in triplicate using the QuantiFast Pathogen PCR + IC kit (Qiagen) on a QuantStudio5 instrument (Thermo Fisher Scientific). Fluorescence was acquired after the extension step. The amplification data was analysed on the QuantStudio5 software, followed by the construction of a standard curve.

**Table 2.1:** Reverse transcriptase RT- PCR conditions used for the detection of mengovirus on the QuantStudio 5 instrument

| **Step** | **Temperature (**℃) | **Time** | **Cycles** |
|---|---|---|---|
| Reverse transcription | 50 | 20 minutes | 1 |
| Activation | 95 | 10 minutes | 1 |
| Denaturation | 95 | 15 seconds | 45 |
| Annealing | 60 | 30 seconds | |
| Extension | 65 | 30 seconds | |
| Cooling | 40 | 30 seconds | 1 |

*2.5.2.2 Human adenovirus*

For the construction of the standard curve, the adenovirus-2 (AdV-2) positive control was amplified in a nested PCR as described in section 2.6.1. The positive hexon region product was cloned in the pJET plasmid using the CloningJET PCR cloning kit (as described in section 2.6.3.1). Following this, the plasmid DNA was purified using the Zymogen plasmid purification kit (Zymo Research, Irvine, CA) according to the manufacturer's instructions. The HAdV fragment was amplified from the plasmid (as described in section 2.6.3.2) and the product was purified using the Zymogen Clean and Concentrate kit (Zymo Research) according to the manufacturer's instructions. The concentration of the purified product was determined

using the Nanodrop (Thermo Fisher Scientific) and the HAdV copies was calculated using the following formula:

$$\frac{X\ ng\ (6.0221 \times 10^{23} molecules/mole)}{(N \times 660 g/mol) \times 1 \times 10^{9}\ ng/g} = number\ of\ copies\ (molecules)$$

*X=Amount if amplicon (ng)*

*N=length of dsDNA amplicon*

Thereafter, a serial dilution of the purified product containing the correct HAdV fragment was done and stored at -20℃. Real-time PCR (as described in section 2.5.3) was performed in triplicate for each dilution on a QuantStudio5 instrument (Thermo Fisher Scientific). The amplification data was analysed using the QuantStudio5 software, followed by the construction of a standard curve.

### 2.5.3 Detection and quantification using real-time PCR

Real-time PCR was used to detect and quantify the HAdVs from the environmental samples, using the QuantiFast Pathogen PCR + IC kit (Qiagen). This kit was advantageous since it contained an internal control, which monitored for the presence of any PCR inhibitors. The primers (AQ1 and AQ2) and probe (AP-probe) (Thermo Fisher Scientific) that were used for the detection of the HAdV were described by Heim and co-workers and are shown in Table 2.2 (Heim *et al.*, 2003). The primers set targeted the hexon region. An AP-probe was labelled with 6- Carboxyfluorescein (FAM) as a fluorescent reporter dye on the 5'-end, together with 5-Carboxytetramethylrhodamine (TAMRA) as a quencher dye on the 3'end.

**Table 2.2:** Real-time primers and probes used for routine screening for human adenoviruses (Heim *et al.*, 2003) (Thermo Fisher Scientific)

| **Primer/Probe** | **Sequence (5'-3')** | **Orientation** |
|---|---|---|
| AQ1 | GCCACGGTGGGGTTTCTAAACTT | Forward |
| AQ2 | GCCCCAGTGGTCTTACATGCACATC | Reverse |
| AP - probe | TGCACCAGACCCGGGCTCAGGTACTCCGA | - |

For the real-time PCR, a 25 µL master mix reaction was made up of the following reagents: 5 µL 5X PCR master mix (containing buffer, nucleotides and DNA polymerase enzyme), IC assay (2.5 µL), IC DNA (2.5 µL) and associated primers (10 pmol each) and probe (2 pmol)

described in Table 2.2. Subsequently, 5 µL of extracted nucleic acids were added to the master mix. The PCR procedure was performed on the QuantStudio 5 Instrument (Thermo Fisher Scientific) with the conditions illustrated in Table 2.3.

**Table 2.3:** Real-time PCR conditions used for the detection of human adenoviruses on the QuantStudio 5 instrument

| Step | Temperature (℃) | Time | Cycles |
|---|---|---|---|
| Activation/ Initial Denaturation | 95 | 5 minutes | 1 |
| Denaturation | 95 | 15 sec | 45 |
| Annealing | 60 | 30 sec | |
| Extension | 65 | 30 sec | |
| Cooling | 40 | 30 sec | 1 |

### 2.5.4 Quantitative analysis

Standard curves were used to determine the number of genomic copies detected in each sample. The mengovirus (MV) standard curve was used to calculate the extraction efficiency, using formula 1. The calculated extraction efficiency was then used to adjust the observed HAdV titers using formula 2.

1. $\frac{Detected\ MV}{Seeded\ MV\ copies} = Extraction\ efficiency$

2. $\frac{Quantified\ HAdV}{Extraction\ efficieny} = Total\ adenovirus\ copies$

## 2.6 CHARACTERISATION OF HAdV

All samples, in which adenovirus DNA was detected, were used for the characterisation of adenovirus. The HAdV genotypes were determined by a conventional nested PCR assay of the hexon gene (Akhil *et al.*, 2016), followed by targeted next generation sequencing (NGS) as well as cloning and Sanger sequencing of selected samples.

### 2.6.1 Conventional nested PCR

For the first round of amplification, the external primers (Adhex 1 [10 pmol] and Adhex 2 [10 pmol) (Thermo Fisher Scientific) described in Table 2.4, were added to 25 µL of OneTaq

Quickload polymerase master mix (New England Biolabs Inc, Ipswich, MA), together with nuclease free water to create a final volume of 40 µL. These primers target a conserved region on the hexon gene and is often used for the identification of HAdVs.

**Table 2.4:** Conventional nested PCR primers used for first round of amplification of adenovirus hexon gene (Akhil *et al.,* 2016)

| Primer | Sequence (5' - 3') | Orientation | Position |
|---|---|---|---|
| AdhexF1 | TIC TTT GAC ATI CGI GGI GTI CTI GA | Forward | 19135–19160 |
| AdhexR1 | CTG TCI ACI GCC TGR TTC CAC A | Reverse | 20009–20030 |

*Degenerate primer codon representation; I = U, C or A and R = A or G

Ten microliters of DNA were added to the master mix and the following cycling parameters shown in Table 2.5 were used for the conventional PCR procedure with an expected PCR product size of 764-896 base pairs for the first round (Akhil *et al.,* 2016).

**Table 2.5:** Conventional semi-nested PCR cycling parameters used for first and second round of amplification

| Step | Temperature (℃) | Time | Cycles |
|---|---|---|---|
| Activation/ Initial Denaturation | 94 | 3 minutes | 1 |
| Denaturation | 94 | 1 minutes | 35 |
| Primer annealing | 45 | 1 minutes | |
| Extension | 68 | 1 minutes 30 sec | |
| Final Extension | 68 | 7 minutes | 1 |
| Hold | 4℃ | ∞ | - |

For the second round of amplification, the internal primers (Adhex F2 and Adhex R2) as described by Akhil and co-workers were used, and the expected band size was 688-821 bp. For the purpose of NGS analysis, adapter sequences were added, which comprised of Illumina Miseq adapters at the 5'- end as illustrated in Table 2.6. The overhang adaptor sequences are indicated in red and are attached to the Adhex primer specific sequences.

**Table 2.6:** Hexon specific primer sequences with overhang adapters for second round of amplification (Akhil *et al.,* 2016)

| Primer | Sequence (overhang-locus specific sequence, (5' – 3') | Orientation | Position |
|---|---|---|---|

| | | | |
|---|---|---|---|
| Adhex F2 | TCGTCGGCAGCGTCAGATGTGTATAAGAGACAG- GCCY AGY TTY AAR CCC TAY TC | Forward | 19165-19187 |
| Adhex R2 | GTCTCGTGGGCTCGGAGATGTGTATAAGAGACAG- GGT TCT GTC ICC CAG AGA RTC IAG CA | Reverse | 19960-19985 |

*Degenerate primer codon representation; I = U, C or A; R = A or G and Y = C or T

This second round of amplification was performed by adding 1 µL of the first round PCR product to 49 µL of OneTaq Quickload polymerase master mix (New England Biolabs) and the tagged primers Adhex F2 (10 pmol) and Adhex R2 (10 pmol) (Thermo Fisher Scientific). The cycling parameters are illustrated in Table 2.7.

**Table 2.7:** Second round of amplification conditions using MiSeq adapters

| **Step** | **Temperature** (℃) | **Time** | **Cycles** |
|---|---|---|---|
| Initial denaturation | 95 | 5 minutes | 1 |
| Denaturation | 95 | 30 sec | 35 |
| Annealing | 58 | 1 minutes | |
| Extension | 68 | 1 minutes 30 sec | |
| Final extension | 68 | 7 minutes | 1 |
| Hold | 4 | ∞ | - |

*2.6.1.1 PCR product analysis and purification*

Agarose gel electrophoresis was used to analyse the PCR products. The 1.5% agarose gels were prepared using the SeaKem® LE Agarose (FMC Corporation, Philadelphia, PA) and 1 x Tris-acetate-ethylenediaminetetra acetic acid (TAE) buffer (Thermo Fisher Scientific). This solution was cooled to 55˚C and thereafter, 5 µL ethidium bromide (10 mg/mL) (Sigma Aldrich, St. Louis, MO) was added per 100 mL of agarose gel. Thereafter, the gel was poured into a casting tray, with a comb inserted to create the wells. Once solidified, the comb was removed and the gel casting tray was placed into an electrophoresis tank (Cleaver Scientific, Rugby, United Kingdom), containing TAE buffer (Thermo Fisher Scientific). A GeneRuler 1 kb DNA ladder (Thermo Fisher Scientific) was added to the first and last well of the gel for reference with HAdV samples into the rest of the wells. Subsequently, the electrophoresis tank was covered, connecting the power supply which allowed the gel to be run at 120 V for 45 minutes. For visualisation and analysis of the agarose gel, the Gel Doc™ XR+ System (Bio-

Rad, Hercules, CA) was used. Thereafter, the PCR products were purified using Ampure XP Beads, 60 mL (Beckman Coulter, Brea, CA) according to the manufacturer's instructions.

*2.6.1.2 Conventional nested PCR optimisation*

During optimisation for conventional PCR, different primers as described by Casas and co-workers as illustrated in Table 2.8. (Casas *et al.*, 2005). The primers (10 pmol each) were added to 25 µL of OneTaq Quickload polymerase (New England Biolabs) and nuclease-free water was added up to a volume of 40 µL. Ten microlitres of the extracted DNA was added. This was performed using the PCR protocol shown in Table 2.9. The expected PCR product size was 470 bp for the first round (Casas *et al.*, 2005).

**Table 2.8:** External primers used for environmental samples during first and second round of conventional semi-nested PCR optimisation (Casas *et al.*, 2005)

| Primer | Sequence (5' – 3') | Orientation | First / Second round |
|---|---|---|---|
| Adhex F1 | TICTTTGACATICGIGGIGTICTIGA | Forward | First |
| Adhex R1 | CGTTCIACIGCCTGRTTCCACA | Forward | First |
| Adhex R2 | GGYCCYAGTTYAARCCCTTAYTC | Reverse | Second |

For the second round of semi-nested amplification, the internal primer (AdhexF2) and external primer (AdhexR1) were used and is described in Table 2.8 (Thermo Fisher Scientific). This was performed by adding 1 µL of the first-round products to 49 µL of OneTaq Quickload polymerase master mix with the same cycling parameters that were used in the first round. As a result, the expected PCR size should be 375 bp (Casas *et al.*, 2005). The second round PCR products were then visualised as described in section 2.6.1.1. The sizes were compared to a commercial 100 bp DNA size standard (Thermo Fisher Scientific). The Biorad Gel Doc System (Biorad Laboratories, Inc., Hercules, CA) was used to visualise these products.

**Table 2.9:** PCR protocol for conventional nested PCR optimisation

| Step | Temperature (˚C) | Time | Cycle |
|---|---|---|---|
| Activation | 94 | 30 sec | 1 |
| Denaturation | 94 | 30 sec | 35 |
| Primer annealing | 50 | 1 minutes | |
| Extension | 68 | 1 minutes | |
| Final Extension | 68 | 5 minutes | 1 |
| Hold | 4 | ∞ | - |

Another optimisation technique was changing the annealing temperature from 68˚C to 58˚C and 65˚C. The same primers described in Table 2.4 and 2.6 with the cycling conditions described in Table 2.5 and 2.7 respectively were used.

### 2.6.2 Next generation sequencing

The adapter-tagged PCR products were purified and sequenced with Illumina MiSeq NGS in collaboration with Dr Arshad Ismail from the Sequencing Core Facility at the National Institute of Communicable Disease (NICD). The NGS and sequence assembly followed by BLAST analysis resulted in the identification of genotypes. This was followed by phylogenetic analysis.

#### *2.6.2.1 Nextera XT library preparation for NGS*

For NGS, the amplicons were transferred on ice packs to the Sequencing Core Unit at the NICD. The following steps were performed by the staff of the Sequencing Core unit at the NICD. During the library preparation, the Nextera® XT Library Preparation Kit and Nextera® XT Index Kit (Illumina, San Diego, CA), used according to the manufacturer's instructions. This procedure began with the input DNA being fragmented and tagged with Illumina-compatible index adapter sequences for multiplexing. Thereafter, the amplification proceeded using the conditions described in Table 2.10. The amplified DNA fragments were analysed

using gel electrophoresis and the DNA library was purified using AMPure® XP beads (Beckman Coulter Life Sciences, Indianapolis, IN). Following this, the DNA concentration was measured on the Qubit® 2.0 Fluorometer (Invitrogen, Carlsbad, CA) for validation and the size of the DNA library was verified using the Agilent 2100 Bioanalyzer System (Agilent Technologies, Santa Clara, CA).

**Table 2.10:** Amplification conditions using GeneAmp® PCR System (Thermo Fisher Scientific)

| **Temperature (℃)** | **Time** | **Cycles** |
|---|---|---|
| 72 | 3 minutes | 1 |
| 95 | 30 sec | 1 |
| 95 | 10 sec | 12 |
| 55 | 30 sec | |
| 72 | 30 sec | |
| 72 | 5 minutes | 1 |
| 10 | Hold | ∞ |

*2.6.2.2 Illumina sequencing*

Before multiplexing the libraries into one micro-centrifuge tube, the purified DNA was normalised to 2 nM. The libraries were then denatured and diluted to form the desired input concentration for MiSeq sequencing. For the MiSeq sequencing, the diluted DNA library was loaded onto a MiSeq reagent cartridge (MiSeq® Reagent Kit version 3, Illumina) and subjected to NGS. The MiSeq platform used base calling and sample demultiplexing as a standard, producing paired FASTQ files for each sample.

*2.6.2.3 Sequence assembly*

The FASTQ files were sent back to the University of Pretoria for further analysis. The MiSeq paired-end reads of each file was adapter- and quality-trimmed using QuasR (Gaidatzis *et al.*, 2015), followed by the assembly of read pairs into consensus sequences, which was completed on SPAdes (Bankevich *et al.*, 2012). These HAdV contigs were mapped to a list of all adenovirus complete genome sequences in GenBank. Contigs with less than 200 nucleotides were removed. The generated contigs were aligned to a single GenBank reference sequence to

confirm the orientation of the contig. The consensus sequences were generated from the mapped reads based on the overlapping nucleotide sequences and areas with low coverage (< 10-fold) were assigned the ambiguity symbol N.

*2.6.2.4 Phylogenetic analysis*

The sequences obtained were analysed on Basic Local Alignment Search Tool® [BLAST® (http://blast.ncbi.nlm.nih.gov/Blast/cgi)] (Altschul *et al.,* 1990) to assign genotypes and compare the detected sequences to the adenovirus specific sequences in GenBank. The relationship between the strains was elucidated by aligning sequences with reference strains and closely related adenovirus strains using multiple sequence alignment using Fast Fourier Transform (MAFFT) version 7 (http://maft.cbrc.jp/alignment/sorftware/). BioEdit was used for manual adjustment of alignment (Hall, 1999). Thereafter, BLAST was used to identify the HAdV genotypes and to determine, which viral strains the identified sequences were closely related to using the GenBank database. Subsequently, the MEGA V.6 software was used to construct the phylogenetic trees with the following parameters: Neighbour-Joining method with Kimura-2 parameter, 1 000 bootstrap replicates and the reference strains obtained from GenBank, to determine the genetic relationship and diversity between the HAdV positive strains detected. The reference strains that were selected, were the top hits from GenBank

**2.6.3 Sanger sequencing procedure**

Twelve of the positive samples were selected for conventional nested PCR, cloning and colony PCR followed by Sanger sequencing analysis. These samples were selected per season from spring 2018 to summer 2020 and included five raw sewage and seven effluent samples.

*2.6.3.1 DNA cloning*

The environmental samples most likely contained a mixture of different HAdV types. Therefore, cloning of the conventional nested PCR products was required, to distinguish between the different types of identified strains. The CloneJET PCR cloning kit (Thermo Fisher Scientific) was used for cloning of the nPCR products according to the manufacturer's instructions.

Terrific Broth (TB) agar plates were prepared by adding 10 g sodium chloride (NaCl) (Merck), 5 g Bacto™ Yeast Extract powder (Becton Dickinson, Franklin Lakes, NJ) and 10 g Bacto™ Tryptone (Becton Dickinson) in 1 L distilled water. Following this, 3.75 g Bacto™ Agar

(Becton Dickinson) was added to 250 mL of broth. This solution was autoclaved and once cooled, 250 µL ampicillin (100 mg/mL) (Thermo Fisher Scientific) was added. Thereafter, approximately 25 mL agar was poured onto each plate.

Firstly, the conventional PCR products were purified with the AMPure XP beads (Beckman Coulter, Brea, CA) and then eluted in 40 µL. Thereafter, the CloneJET PCR Cloning kit (Thermo Fisher Scientific) used the blunt end cloning procedure, which consisted of 5 µL buffer, 0.5 µL blunting enzyme and 1-4 µL PCR product. This reaction was incubated at 70℃ in an oven (Techne, Minneapolis, MN) for five minutes to digest any overhanging nucleotides, rendering blunt-ended products. After incubation, the reaction was put on ice for two minutes before the addition of 0.5 µL ligase and 0.5 µL linearised pJET (25 ng/µL) vector. Finally, this ligation reaction was incubated for 30 minutes at room temperature (22˚C-25˚C).

Subsequently, the resultant clones were transformed into New England Biolabs® 10-beta competent *E. coli* cells (New England Biolabs). Ten microliters of 10-beta cells (New England Biolabs) and 2 µL of ligation reaction were added together and incubated for 30 minutes on ice. Following this, the heatshock step took place at 42℃ for 30 seconds on a MJ Minicycler (MJ Reseach Inc., Hercules, CA) and thereafter, the cells were returned to ice for two minutes. A recovery medium (200 µL) was added to these cells, followed by shaking at 37℃ for one hour at 220 rpm (Labcon, Petaluma, CA). The *E. coli* cells were subsequently plated on TB agar plates, containing 100 µg/mL ampicillin (Thermo Fisher Scientific). The plates were incubated for 16 hours at 37℃ to allow growth of the transformed cells in a Labcon shaking incubator (Labcon).

*2.6.3.2 Colony PCR*

Colony PCR was performed in order to determine the clones that contained the DNA fragment insert with the correct size. Clones were not directly sequenced to ensure high quality sequencing data. Fifteen colonies were randomly selected from the TB-agar plates of each of the twelve samples to perform colony PCR assays,. Colony PCR assays were performed according to the instructions of the CloneJET PCR cloning kit manual (Thermo Fisher Scientific). The reaction consisted of 10 µL OneTaq QuickLoad 2X MasterMix (New England Biolabs) with pJET forward and reverse primers (10 pmol/µL) described in Table 2.11 in a final volume of 20 µL.

**Table 2.11:** pJET primer sequences for colony PCR (Thermo Fisher Scientific)

| Primer (10 µM) | Sequence (5'- 3') | Orientation | Position |
|---|---|---|---|
| pJETFor | CGACTCACTATAGGGAGAGCGGC | Forward | 310 - 322 |
| pJETRev | AAGAACATCGATTTTCCATGGCAG | Reverse | 428 - 405 |

These reactions were run in a SimpliAmp™ Thermocycler (Thermo Fisher Scientific) using the conditions illustrated in Table 2.12. The PCR products were analysed on a 1.5% agarose gel as described in section 2.6.1.1, to determine which clones contained the correct size fragment.

**Table 2.12:** Colony PCR cycling conditions

| Step | Temperature (℃) | Time | Cycles |
|---|---|---|---|
| Activation/ Initial Denaturation | 95 | 3 minutes | 1 |
| Denaturation | 95 | 30 sec | 30 |
| Primer annealing | 60 | 30 sec | |
| Extension | 68 | 50 sec | |
| Final Extension | 68 | 7 minutes | 1 |
| Hold | 4℃ | ∞ | - |

*2.6.3.3 Sanger sequencing*

From the colony PCR products, 10 from each sample were selected for Sanger sequencing. These 10 products were subjected to purification using the DNA Clean and Concentrator™ 25 kit (Zymo Research). The Sanger sequencing was performed using 2 µL of purified product, which was divided into 1 µL each for the forward and the reverse reaction sequences. The sequencing master mix was made up of 1 µL pJET forward or reverse primers (3.2 µM) and ABI PRISM BigDye Terminator v3.1 Cycle Sequencing Kit (Applied Biosystems, Warrington, UK) which consisted of 3 µL 5X sequencing buffer and 1 µL terminator mix for both the forward and reverse sequences. This resulted in a final volume of 20 µL for each of the respective reactions. The SimpliAmp™ Thermocycler (Thermo Fisher Scientific) was used for amplification with the conditions shown in Table 2.13. After amplification, the sequences were

submitted to Inqaba Biotech™ for purification and analysis and chromatogram files generated and sent to the student for sequence assembly and analysis.

**Table 2.13:** SimpliAmp™ Thermocycler conditions used for Sanger Sequencing

| Step | Temperature (℃) | Time | Cycles |
|---|---|---|---|
| Initial denaturation | 94 | 3 min | 1 |
| Denaturation | 94 | 30 s | 30 |
| Annealing | 50 | 10 s | |
| Elongation | 60 | 4 minutes | |
| Termination & Hold | 4 | ∞ | - |

*2.6.3.4 Genotypic assignment and phylogenetic analysis*

The forward and reverse strands were analysed using the Sequencer™ 4.10.1 software (Gene Codes Corporation, Ann Arbour, MI) to produce a contig. Following this, the contigs were aligned using BioEdit Sequence Alignment Editor®, version 7.2.5 (Hall, 1999) to create multiple alignments. Thereafter, BLASTn (Altschul *et al.*, 1990) was used to identify the HAdV genotypes based on a similarity level ranging from 98% to 100%. Thereafter, the determinations of the viral strains were classified using the GenBank database. Neighbour-joining phylogenetic trees were constructed as described in section 2.6.2.4. The nucleotide sequences were submitted to GenBank and will be made publicly available upon publication.

## 2.7 TIME AND COST ANALYSIS

The time and cost of the two sequencing methods, Sanger sequencing and NGS, were compared. This was to confirm which sequencing method was the best to use regarding the cost and time for each technique. Before the laboratory work start, a budget plan for both Sanger sequencing and NGS was drawn up. This budget included all the different reagents required for each sequencing technique. During the laboratory work, a time schedule was drawn up and consisted of the recorded time it took for each procedure in the laboratory.

# CHAPTER 3

# RESULTS

## 3.1 ENVIRONMENTAL SAMPLES COLLECTED

A total of 150 environmental samples instead of the planned 154 environmental samples were collected over a period of 18 months from August 2018 to January 2020. Due to precautionary and safety measures relating to the surrounding area at one of the wastewater treatment plants, collection could only take place once during September 2018. Of the 150 environmental samples, 75 were raw sewage and the remaining 75 were effluent samples.

## 3.2 PREPARATION OF STANDARD CURVE

Mengovirus (MV) was used as an extraction control. For the quantification of human adenovirus (HAdV), standard curves were prepared for MV and HAdV.

### 3.2.1 Preparation of the standard curve for quantification using mengovirus

The eluted concentration of the MV after extraction amounted to $4.59 \times 10^{6}$ $TCID_{50}$/60µL. The concentration per reaction resulted in $3.83 \times 10^{5}$ $TCID_{50}$/5 µL. Table 3.1 illustrates the real-time *rt*-PCR 10-fold triplicate serial dilution values with the average MV cycle threshold (Ct) values and corresponding MV concentration per dilution. As shown in this table, the averaged cycle threshold values were approximately 3.3 cycles apart. The lower limit of detection (LLOD) was $3.83 \times 10^{-02}$ $TCID_{50}$/5 µL which represented the lowest concentration of MV that the real-time *rt*-PCR could detect. Subsequently, all the concentrations lower than the lower limit of detection (LLOD) was regarded as negative. The dilution that was selected to be used as the standard for quantification was the $10^{-5}$ dilution, with a concentration of $3.83 \times 10^{00}$ $TCID_{50}$/5 µL.

**Table 3.1:** Real-time *rt*-PCR cycle threshold average values and concentration of the mengovirus 10-fold triplicate serial dilution

| Sample name | Mengovirus Ct value | Mengovirus Ct value average | Difference in Ct value | Mengovirus concentration [$TCID_{50}$/5 µL] |
|---|---|---|---|---|
| Undiluted A | 11.99 | 12.23 | - | $3.83 \times 10^{5}$ |
| Undiluted B | 12.12 | | | |
| Undiluted C | 12.49 | | | |
| $10^{-1}$ A | 15.11 | 15.45 | 3.22 | $3.83 \times 10^{04}$ |
| $10^{-1}$ B | 15.74 | | | |
| $10^{-1}$ C | 15.51 | | | |
| $10^{-2}$ A | 18.49 | 18.87 | 3.42 | $3.83 \times 10^{03}$ |
| $10^{-2}$ B | 19.06 | | | |
| $10^{-2}$ C | 19.05 | | | |
| $10^{-3}$ A | 22.25 | 21.98 | 3.11 | $3.83 \times 10^{02}$ |
| $10^{-3}$ B | 21.37 | | | |
| $10^{-3}$ C | 22.32 | | | |
| $10^{-4}$ A | 25.92 | 25.28 | 3.30 | $3.83 \times 10^{01}$ |
| $10^{-4}$ B | 25.48 | | | |
| $10^{-4}$ C | 24.97 | | | |
| $10^{-5}$ A | 29.00 | 28.89 | 3.61 | $3.83 \times 10^{00}$ |
| $10^{-5}$ B | 28.83 | | | |
| $10^{-5}$ C | 28.83 | | | |
| $10^{-6}$ A | 33.20 | 32.81 | 3.92 | $3.83 \times 10^{-01}$ |
| $10^{-6}$ B | 32.55 | | | |
| $10^{-6}$ C | 32.67 | | | |
| $10^{-7}$ A | 35.90 | 36.16 | 3.34 | $3.83 \times 10^{-02}$ |
| $10^{-7}$ B | 36.09 | | | |
| $10^{-7}$ C | 36.46 | | | |

The MV amplification plot of the 10-fold dilution series, done in triplicate is shown in Figure 3.1. Each dilution exhibited three sigmoidal curves and the curves that clustered closely together were regarded as good representatives for a standard curve. Amplification of eight 10-fold dilutions (Ct values ranging between 10 to 37) were obtained. This resulted in a coverage of a wide range of mengovirus concentrations as shown in Figure 3.1. Figure 3.2 illustrates the amplification plot of the internal control, showing no PCR inhibition.

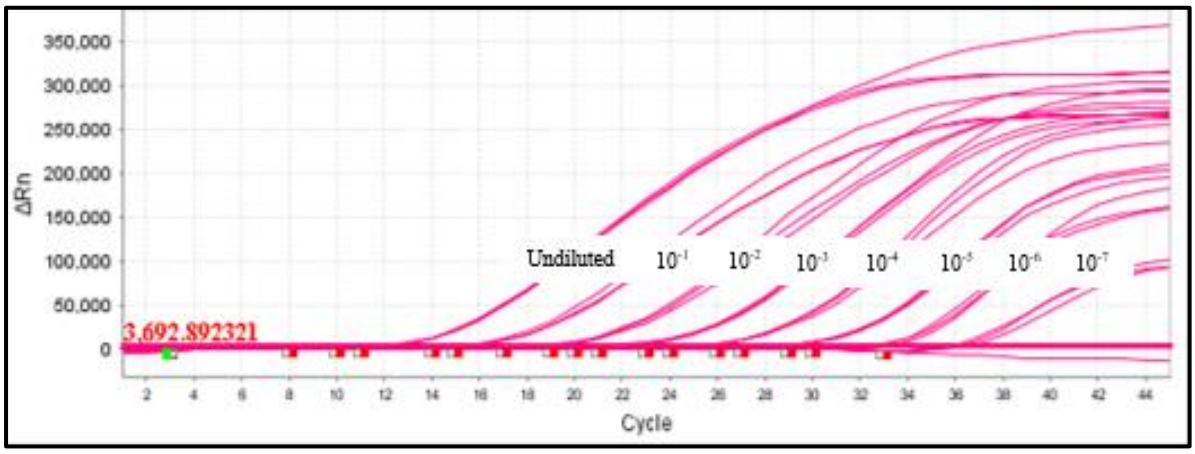


**Figure 3.1: Amplification curves of 10-fold dilution series of mengovirus.** Dilution series done in triplicate ranging from undiluted to $10^{-7}$ for the preparation of the mengovirus standard curve as shown in pink ■. Each dilution series is labelled on the right-hand side.

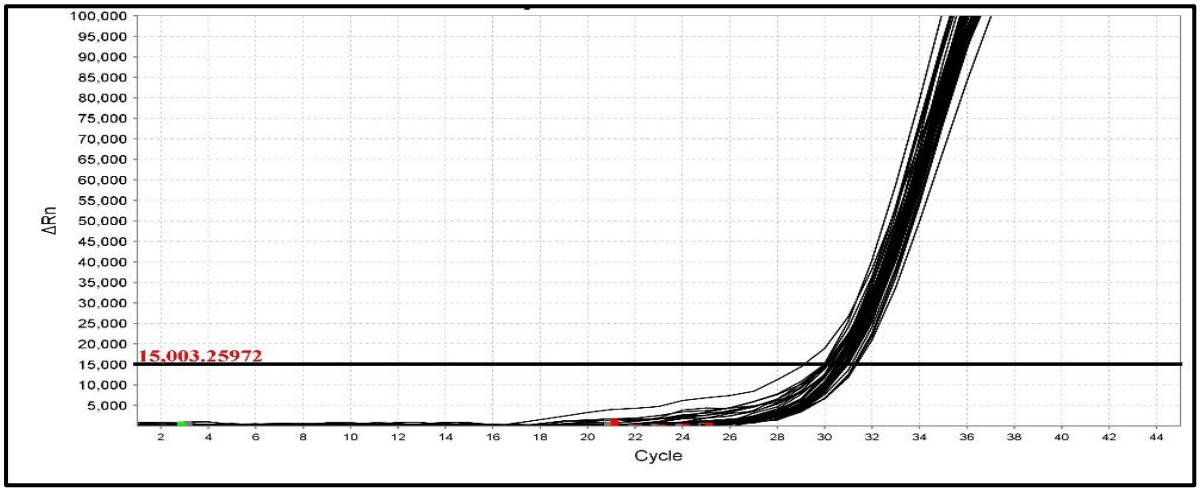


**Figure 3.2: Amplification curves of the internal control for the 10-fold dilution series of mengovirus.** The amplification of the internal control was done in triplicate shown in black ■.

Following this, the standard curve as shown in Figure 3.3 was generated, using the QuantStudio 5 software. This curve displayed properties of a good standard curve with the equation y = -3.424 $x$ + 31.09. Accordingly, the PCR efficiency was 95.91% with a slope of -3.42 which appears in within the -3.6 ≥ slope ≤ -3.3, with the regression amounting to 0.998.

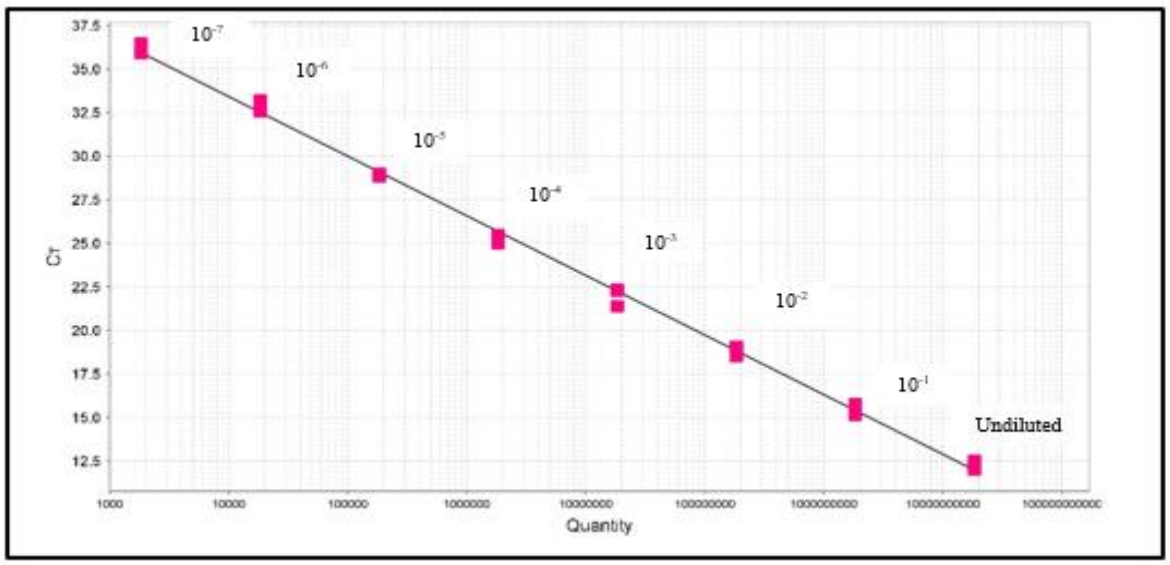


**Figure 3.3: Mengovirus standard curve generated from the 10-fold triplicate dilution series**. This standard curve was generated for the quantification of mengovirus to estimate nucleic extraction efficiency. Each dilution point represents specific dilutions as indicated by the labels.

## 3.2.2 Human adenovirus standard curve preparation for quantification

The HAdV-2 concentration as determined using the NanoDrop was 14.14 ng/µL, amounting to a copy number of 5.04 x $10^9$ gc/5 µL. The real-time PCR 10-fold triplicate serial dilution values are shown in Table 3.2. This table shows that the LLOD for the HAdV was 5.04 x $10^{03}$ gc/5 µL. The dilution that was selected for quantification was HAdV $10^{-4}$ with the HAdV concentration of 5.04 x $10^{05}$ gc/5 µL. The sample (HAdV $10^{-6}$) presented with the lowest concentration of 5.00 x $10^{03}$ gc/5 µL where HAdV was detected consistently in all three triplicates.

**Table 3.2:** Real-time PCR cycle threshold average values and concentrations of the human adenovirus 10-fold triplicate serial dilution

| Sample name | Human adenovirus Ct value | Human adenovirus Ct value average | Difference in Ct value | Human adenovirus concentration [gc/5 µL] |
|---|---|---|---|---|
| Undiluted A | 14.07 | 14.09 | - | $5.00 \times 10^{09}$ |
| Undiluted B | 13.90 | | | |
| Undiluted C | 14.48 | | | |
| $10^{-1}$ A | 18.66 | 18.30 | 4.21 | $5.00 \times 10^{08}$ |
| $10^{-1}$ B | 18.55 | | | |
| $10^{-1}$ C | 17.98 | | | |
| $10^{-2}$ A | 21.34 | 21.32 | 3.02 | $5.00 \times 10^{07}$ |
| $10^{-2}$ B | 21.46 | | | |
| $10^{-2}$ C | 21.47 | | | |
| $10^{-3}$ A | 25.09 | 24.90 | 3.58 | $5.00 \times 10^{06}$ |
| $10^{-3}$ B | 24.84 | | | |
| $10^{-3}$ C | 25.10 | | | |
| $10^{-4}$ A | 28.30 | 28.18 | 3.28 | $5.00 \times 10^{05}$ |
| $10^{-4}$ B | 28.32 | | | |
| $10^{-4}$ C | 28.14 | | | |
| $10^{-5}$ A | 31.50 | 31.50 | 3.32 | $5.00 \times 10^{04}$ |
| $10^{-5}$ B | 31.56 | | | |
| $10^{-5}$ C | 31.80 | | | |
| $10^{-6}$ A | 34.61 | 34.46 | 2.96 | $5.00 \times 10^{03}$ |
| $10^{-6}$ B | 33.98 | | | |
| $10^{-6}$ C | 35.05 | | | |

The amplification plot of the HAdV real-time PCR 10-fold serial dilution is represented in Figure 3.4. Apart from the $10^{-06}$ dilution, all the amplification curves per dilution set were closely clustered. The MV Ct values (ranging from 12 to 36) were comparable to the HAdV Ct values (ranging from 13 to 35) as both resulted in similar Ct value ranges. Figure 3.5 illustrates the amplification curve of the internal control used which indicated that there was no PCR inhibition.

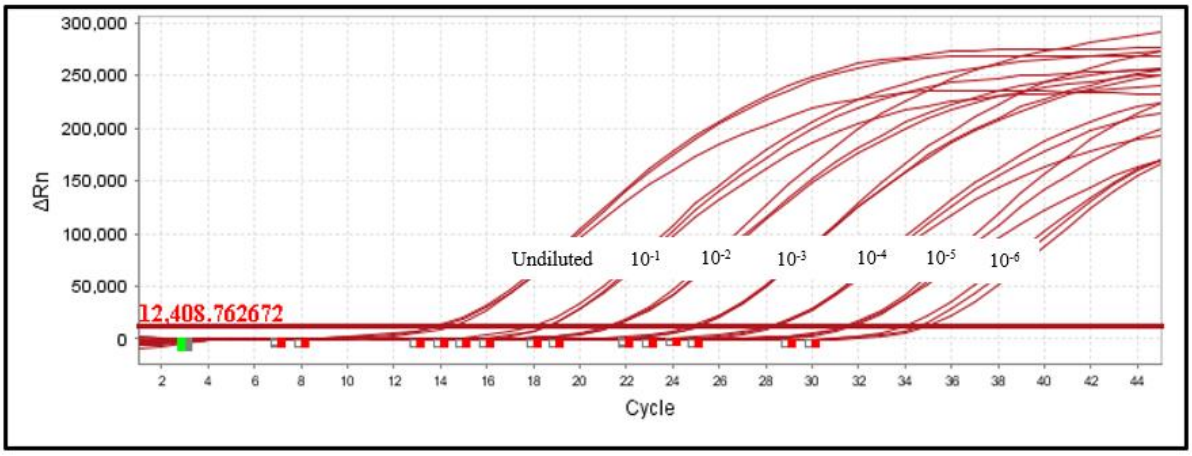


**Figure 3.4: Amplification curves of the human adenovirus for the 10-fold dilution series**. The amplification curve was done in triplicate ranging from undiluted to $10^{-6}$ for the preparation of the human adenovirus standard curve as shown in red . Each amplification curve is labelled at the bottom right-hand side.

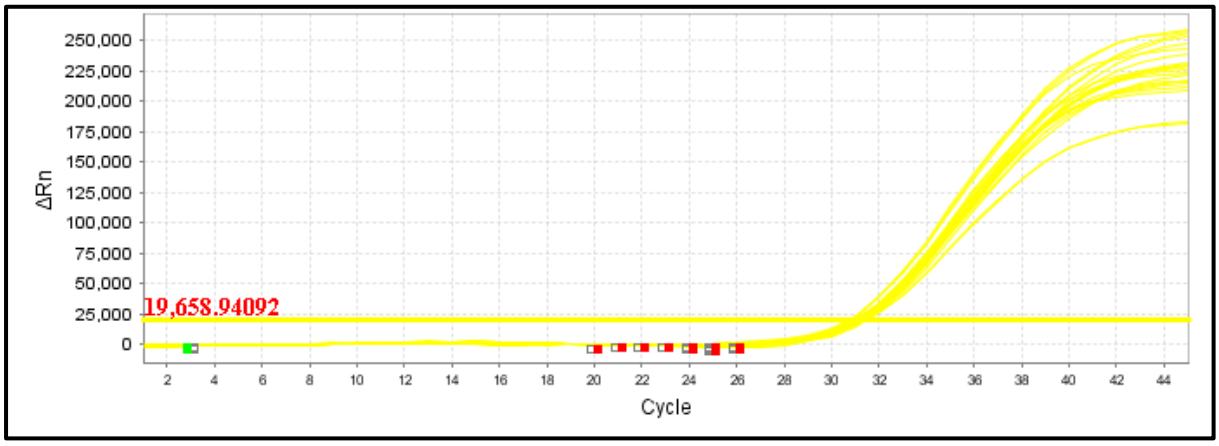


**Figure 3.5: Amplification of the internal control for the 10-fold dilution series of the human adenovirus.** The amplification of the internal control was done in triplicate as shown in yellow .

The HAdV standard curve is shown in Figure 3.6, resulting in the equation y = -3.71 $x$ + 50.41. This standard curve did not have a consistent difference of 3.3 cycles between the cycle threshold values and the slope amounted to -3.71. The PCR efficiency amounted to 86.11% and the regression was 0.968.

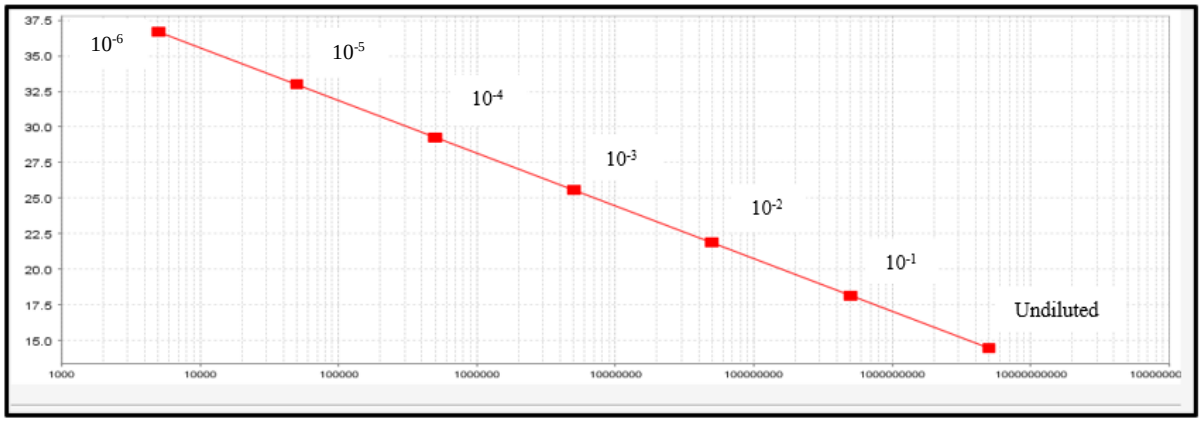


**Figure 3.6: Human adenovirus standard curve generated from the 10-fold triplicate dilution series**. The human adenovirus standard curve was generated for the preparation of the human adenovirus quantification. Each dilution point represents specific dilutions as indicated by the labels.

## 3.3 DETECTION OF THE HUMAN ADENOVIRUS

Human adenoviruses were detected in 140/150 (93%) of the environmental samples that were analysed. Figure 3.7 illustrates an example of HAdV amplification curves of both HAdV and internal control. Graph A represents the detection of HAdV and graph B illustrates that no PCR inhibition occurred. In all the real-time amplification experiments, the extraction negative controls and PCR negative controls did not show any amplification. Therefore, no cross contamination was suspected.

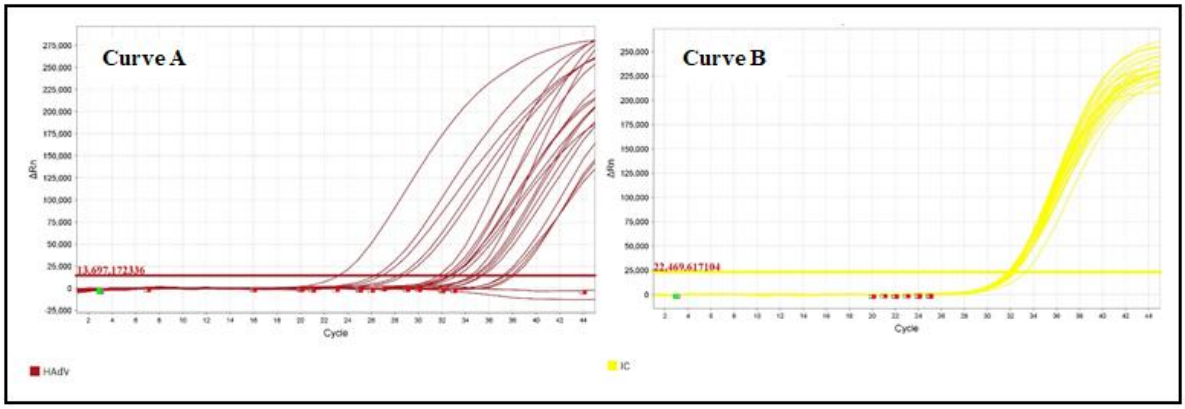


**Figure 3.7: Amplification curves of human adenovirus and human adenovirus internal control.** Curve A represents the human adenovirus amplification curve as illustrated in red curves ( ). Curve B represents the internal control amplification curve as illustrated in yellow curves ( ).

Human adenoviruses were detected in 69/75 (92%) of the raw sewage samples and in 71/75 (95%) of the effluent samples as presented in Figure 3.8. The months that presented with the most HAdV detection in both raw sewage ranged from August 2018 to May 2019, June and August 2019 as well as January 2020. Human adenoviruses were detected most frequently in effluent samples in August 2018 to May 2019, August and September 2019 as well as January 2020. The lowest level of detection for raw sewage occurred in September 2019 and December 2019. There was a consistent detection of HAdV in the effluent samples throughout the 18 months with the lowest detection occurring during the months in 2019.

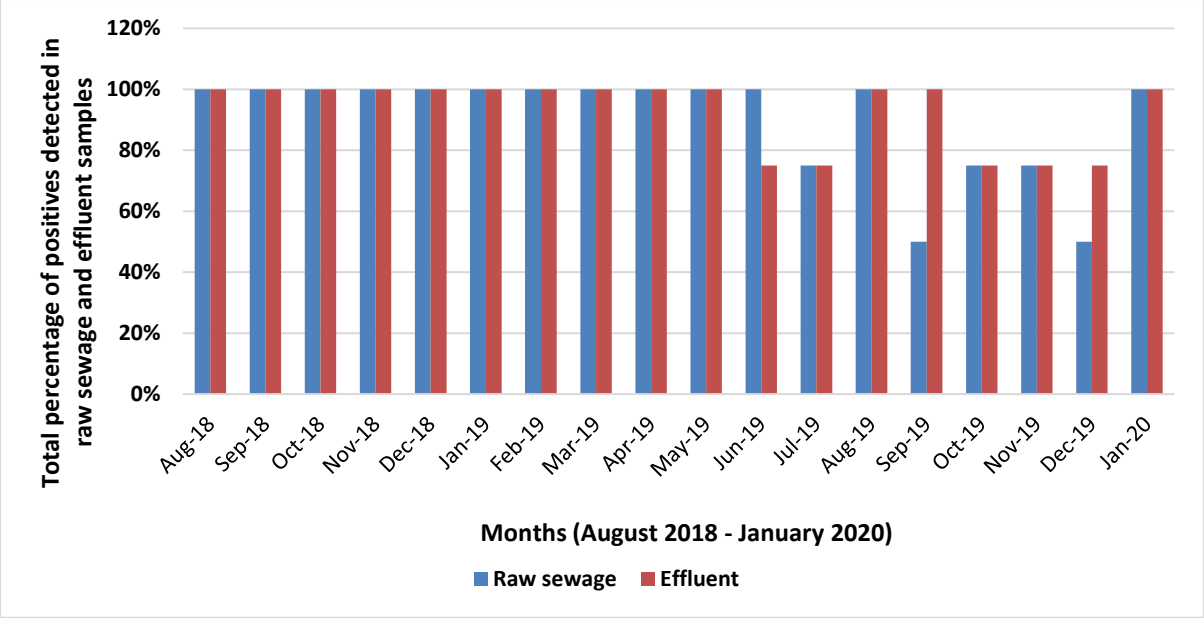


**Figure 3.8: The detection of human adenovirus in environmental samples.** The bar graph represents the total percentage of positives detected in raw sewage (blue ) and effluent samples (red ) from August 2018 to January 2020 (18 months).

## 3.4 QUANTIFICATION OF THE HUMAN ADENOVIRUS

Mengovirus was detected in a total of 126/150 (82%) of the samples. The remaining 24 negative samples were re-tested with 1:10 diluted nucleic acids. However, only 16/24 (67%) became positive. Unfortunately, there were insufficient samples remaining in each sample for re-extraction. Therefore, the samples that remained negative after 1:10 dilution (12/24, 50%) were declared as undetectable. The MV concentrations ranged from 2.6 x $10^{01}$ $TCID_{50}$/L to 8.6 x $10^{08}$ $TCID_{50}$/L. Figure 3.9 represents an example of a real-time PCR amplification curve for the detection of MV for quantification.

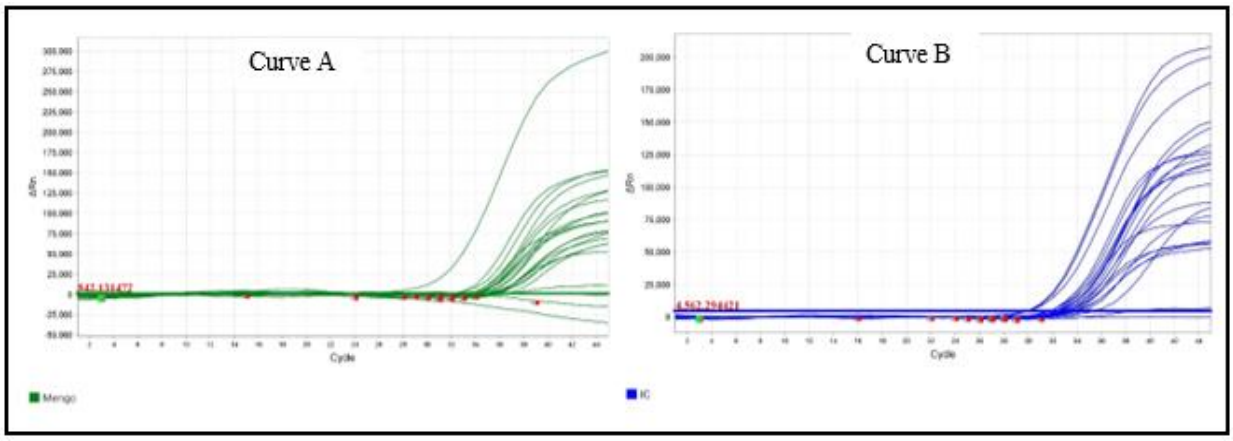


**Figure 3.9: Amplification curves of mengovirus and internal control.** Curve A represents the mengovirus amplification curve as illustrated in green curve . Curve B represents the internal control curves as illustrated in blue curves .

The HAdV was successfully quantified presenting with a wide range of concentrations as shown in Table 3.3. In WWTP 1, the HAdV concentration ranged from 1.38 x $10^{05}$gc/L to 4.50 x $10^{09}$gc/L in raw sewage and 5.08 x $10^{03}$ gc/L to 4.30 x $10^{08}$gc/L in effluent samples. In WWTP 2, the HAdV concentration ranged from 6.84 x $10^{04}$gc/L to 1.69 x $10^{12}$gc/L in raw sewage and 5.27 x $10^{03}$ gc/L to 1.16 x $10^{08}$gc/L in effluent samples. The complete data set of the adenovirus concentrations detected in the environmental samples is shown in Appendix 2.

**Table 3.3:** The human adenovirus concentrations detected in both wastewater treatment plants ranging from lowest concentration to highest concentration

| WWTP | Sample type | Sample ID | Date | Lowest concentration (gc/L) | Sample ID | Date | Highest concentration (gc/L) |
|---|---|---|---|---|---|---|---|
| 1 | Raw | 112 | Jun'19 | 1.38 x $10^{05}$ | 31 | Sep'18 | 4.50 x $10^{09}$ |
| | Effluent | 116 | Jul'19 | 5.08 x $10^{03}$ | 94 | May'19 | 4.30 x $10^{08}$ |
| 2 | Raw | 111 | Jun'19 | 6.84 x $10^{04}$ | 33 | Sep'18 | 1.69 x $10^{12}$ |
| | Effluent | 76 | Feb'19 | 5.27 x $10^{03}$ | 100 | May'19 | 1.16 x $10^{08}$ |

## 3.5 GENOTYPING

Conventional nested PCR was used for the amplification of the hexon region. Sanger sequencing and NGS of the hexon region was subsequently used to determine the genotypes of the HAdVs detected in the environmental samples.

### 3.5.1 Human adenovirus hexon amplification

The HAdV hexon region was successfully amplified from nucleic acids of 43/140 (31%) of the environmental samples. Of the 43 HAdV samples, 17 (40%) were raw sewage and 26 (60%) were effluent samples. This resulted in a conventional nested PCR amplification success rate of below 50%. The remaining samples (97/140) had Ct values ranging from 25 to 45. Figure 3.10 and Figure 3.11 illustrate an example of conventional first round and nested PCR amplification on an agarose gel.

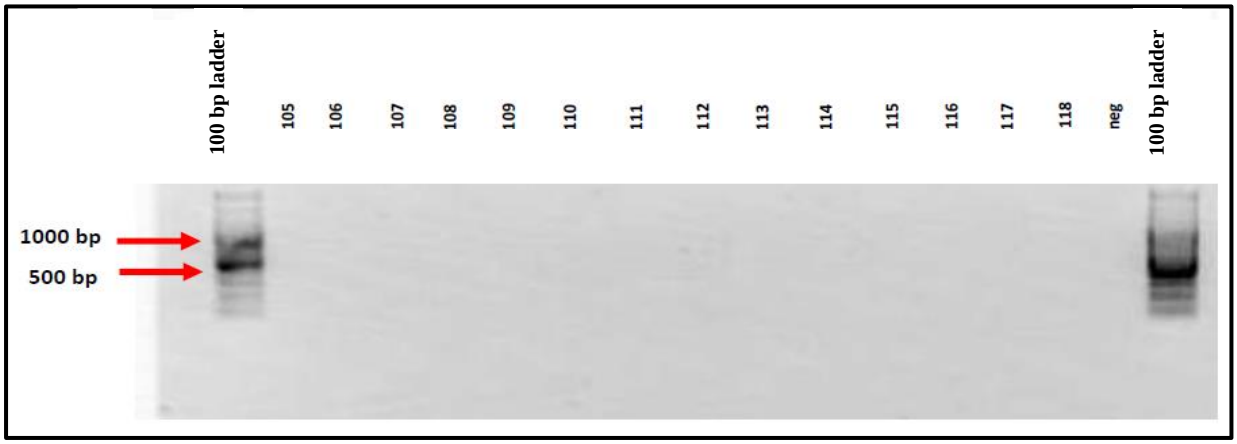


**Figure 3.10: Agarose gel electrophoresis of first round products of the hexon region genotyping PCR from HAdV positive samples.** The HAdV samples were collected from June 2019 and July 2019. No PCR positive sample was included to avoid cross contamination.

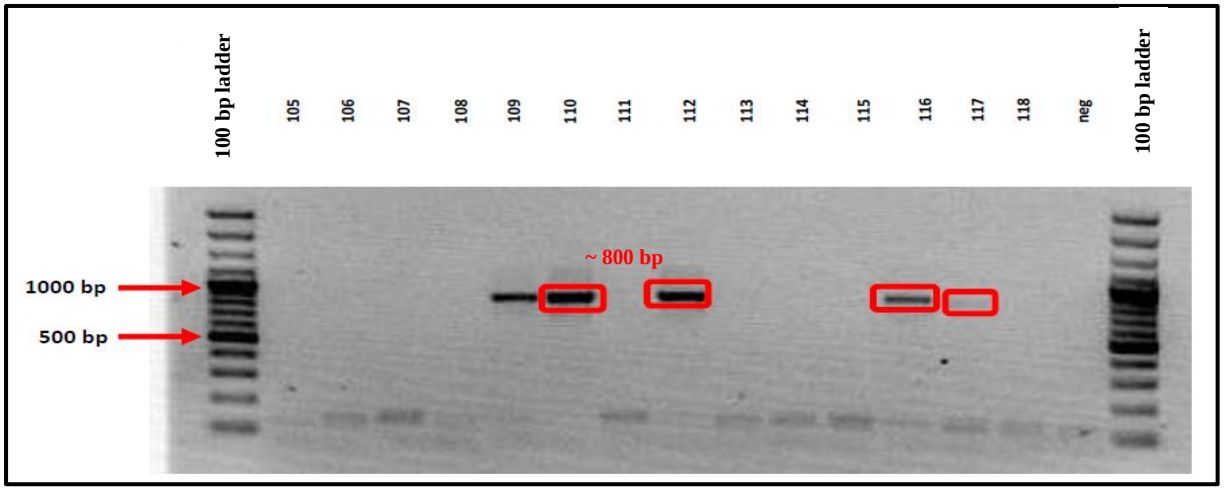


**Figure 3.11: Agarose gel electrophoresis of second round products of the hexon region genotyping PCR from HAdV positive samples collected from June 2019 and July 2019.** Ladder = 100 bp DNA molecular weight marker.

No PCR products, detectable by gel electrophoresis were amplified in the first round of the nested PCR. There was successful amplification of the target hexon gene during the second round as shown in the gel electrophoresis example in Figure 3.11. This is illustrated by the ~ 800 bp dark bands with the expected band size being between 688-821 bp. A PCR negative control was included in both rounds of the nested PCR as shown in Figure 3.10 and Figure 3.11. These figures confirm that there was no contamination during the PCR reaction as no bands were present. To minimise the probability of contamination, a positive control was not added to these PCR reactions.

Wastewater treatment plant 1 presented with the most samples (24/43, 56%) in which HAdV nested PCR product amplification was achieved. Wastewater treatment plant 2 presented with the least samples (19/43, 44%) in which HAdV nested PCR product amplification was achieved.

## 3.5.2 Optimisation of conventional PCR

Due to the low conventional nested PCR product amplification success rate (31%), PCR optimisation was implemented. There were two optimisation techniques tested. However, these optimisation techniques were not successful as it resulted in no significant difference when compared to the initial PCR amplification.

The first optimisation technique was evaluating another PCR primer, namely Casas primers. A total of 5 randomly selected samples were tested using the Casas primers and compared to that using the Akhil primers. When using the Akhil primers, amplification was achieved in 4 of the

5 randomly selected samples. The Casas primers resulted in the amplification of 3 HAdV PCR products during second round of PCR. As shown in Figure 3.12, the amplification of these 3 HAdV PCR products were faint bands with several nonspecific bands of larger size. The expected band size was ~369 bp. The PCR negative reaction confirmed that there was no contamination during the PCR reaction. These HAdV PCR products presented with bold, dark bands with no nonspecific binding. The expected band size was between 688 – 821 bp as shown in Figure 3.13. These results showed that the Akhil primers were the best option as it yielded the optimum results.

The second optimisation technique was altering the annealing temperature. For this optimisation, there were 8 samples selected with three being positive (sample number 60, 62 and 64) during the initial PCR reaction. The initial temperature used during conventional PCR was 67˚C. The two different temperatures used for optimisation were 58˚C and 65˚C as shown in Figure 3.14. There was no significant difference when altering the annealing temperature. These temperatures resulted in a combination of faint, light and broad dark bands. Subsequently, these results showed that altering the annealing temperature did not improve the positivity rate. In all the conventional PCR reactions (Figure 3.12, Figure 3.13 and Figure 3.14), a PCR negative control was added to ensure that no PCR contamination occurred. The presence of no bands in each agarose gel's negative control lane confirms that there was no PCR contamination.

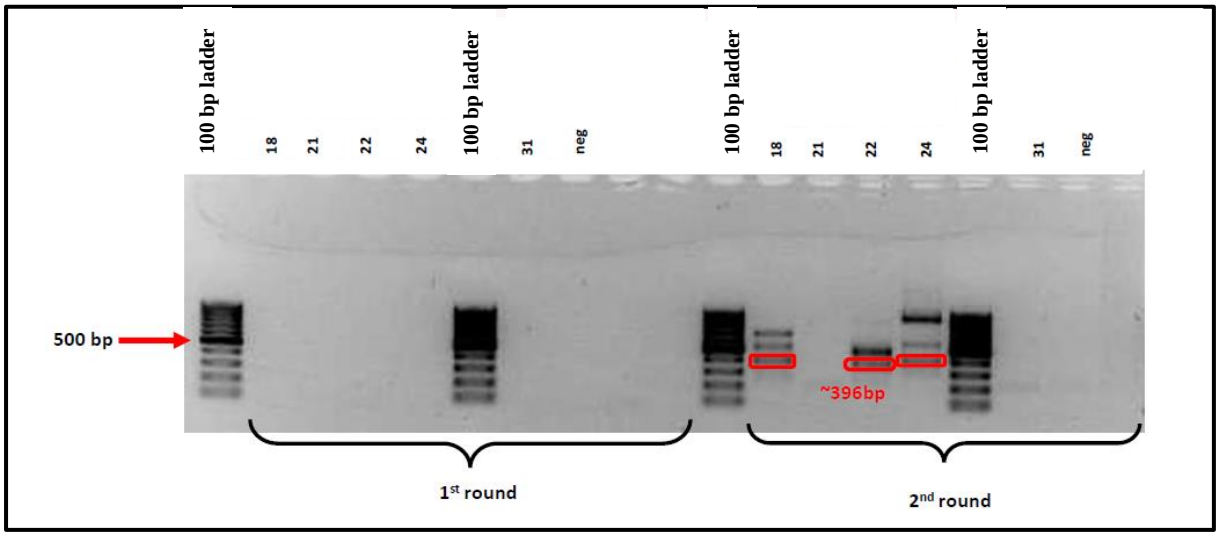


**Figure 3.12: Amplification of the human adenovirus hexon region using the Casas primers.** The ~ 396 bp faint bands in the second round PCR products indicate successful amplification of the target gene. Ladder = 100 bp DNA molecular weight marker.

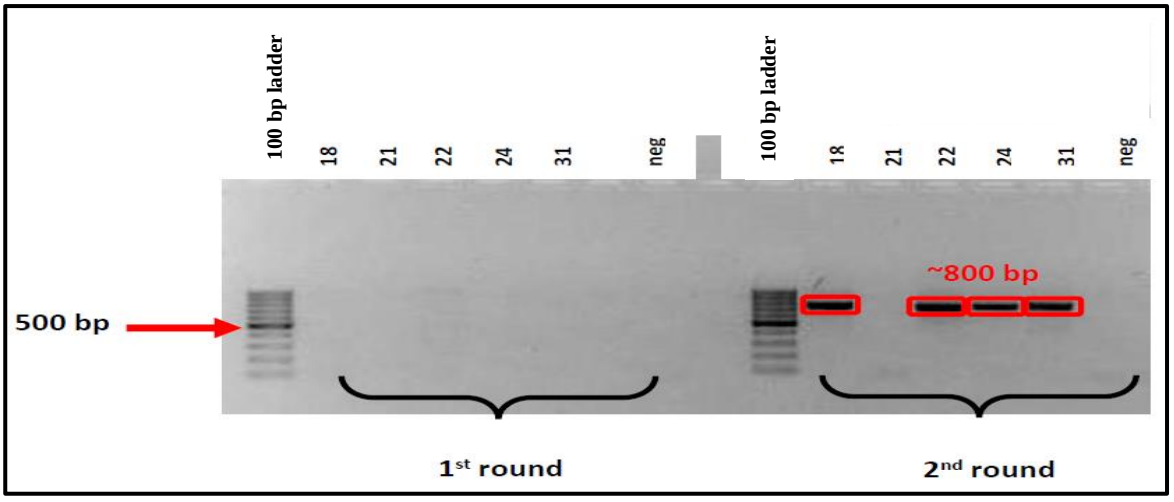


**Figure 3.13: Amplification of the human adenovirus hexon region using the Akhil primers.** The ~ 800 bp bands in the second round PCR products indicate successful amplification of the target gene. Ladder = 100 bp DNA molecular weight marker.

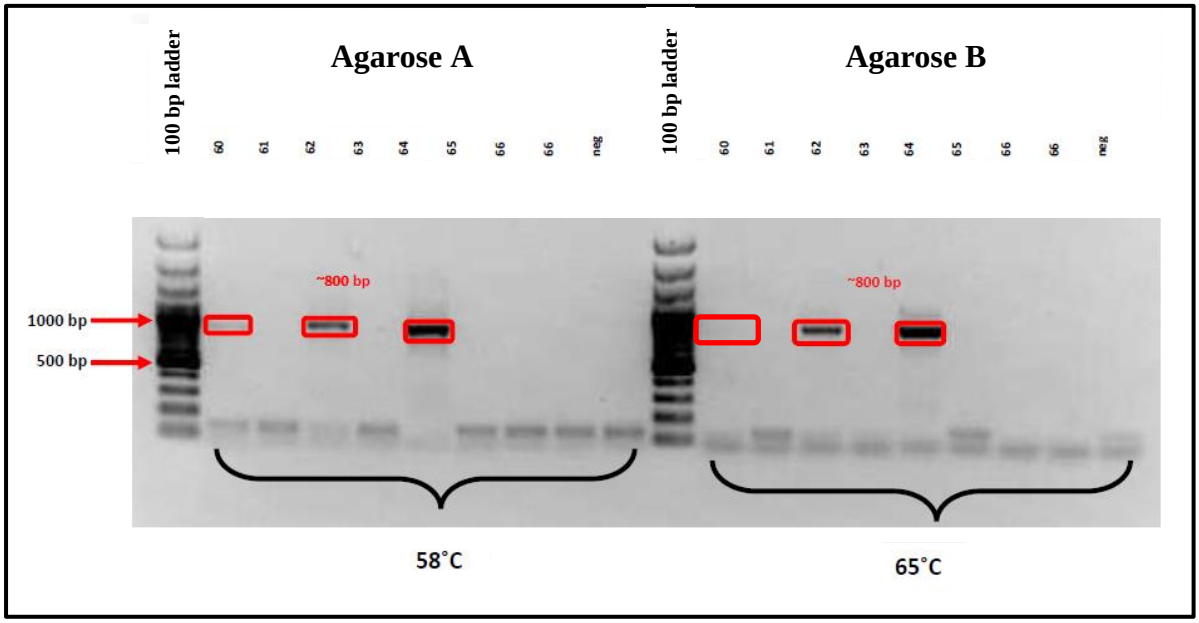


**Figure 3.14: Comparison of two annealing temperatures to amplify the hexon region with the Akhil primer set.** These two agarose gels (A and B) are a representation of second round PCR. The ~ 800 bp faint bands in the second round PCR products indicate successful amplification of the target gene. Agarose A represents the HAdV PCR products at 58˚C and agarose B represents the HAdV PCR products at 65˚C. Ladder = 100 bp DNA molecular weight marker.

### 3.5.3 Colony PCR

A total of 12 HAdV PCR positive products were successfully cloned and 15 clones were selected from each sample. Figure 3.15 shows a typical agarose gel electrophoresis result obtained after colony PCR of samples 76 to 90. The expected band size was ~925 bp due to vector added on the 5'- and 3'- region of the hexon gene. Although these bands were not all the same size, they were within the range of 900 bp to 925 bp.

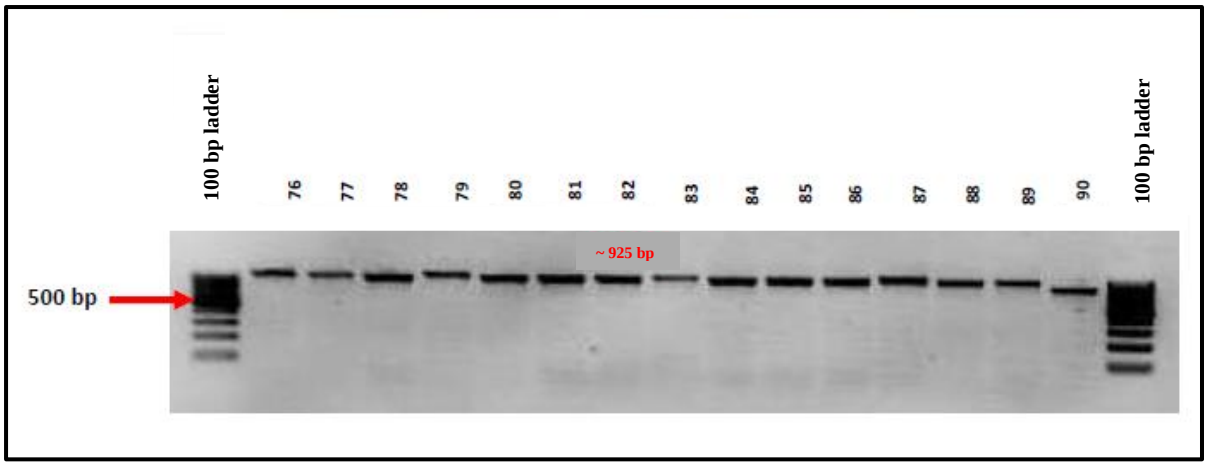


**Figure 3.15: Gel electrophoresis analysis of colony PCR products obtained after cloning of the HAdV hexon gene region from 12 HAdV PCR products.** Ladder = 100 bp DNA molecular weight marker.

## 3.6 GENOTYPIC CHARACTERISATION OF HUMAN ADENOVIRUS

Genotypes were determined by Sanger sequencing and NGS. Sanger sequencing was performed on the nested PCR products originating from 12 samples, while NGS was performed on all the nested PCR products obtained in this study.

### 3.6.1 Human adenovirus species and genotypic characterisation with Sanger sequencing

Eighteen HAdV genotypes were successfully characterised with Sanger sequencing from 12 HAdV positive samples. Figure 3.16 illustrate the HAdV species identified in WWTP 1 and WWTP 2, respectively using Sanger sequencing. The HAdV-D was the most dominant species identified in both WWTPs. The HAdV species; HAdV-A, HAdV-B, HAdV-D and HAdV-F were identified in WWTP 1. In WWTP 2, HAdV-B, HAdV-D and HAdV-E were identified. The HAdV species that was least identified was HAdV-A. There was no presence of HAdV-C and HAdV-G amongst the 12 samples.

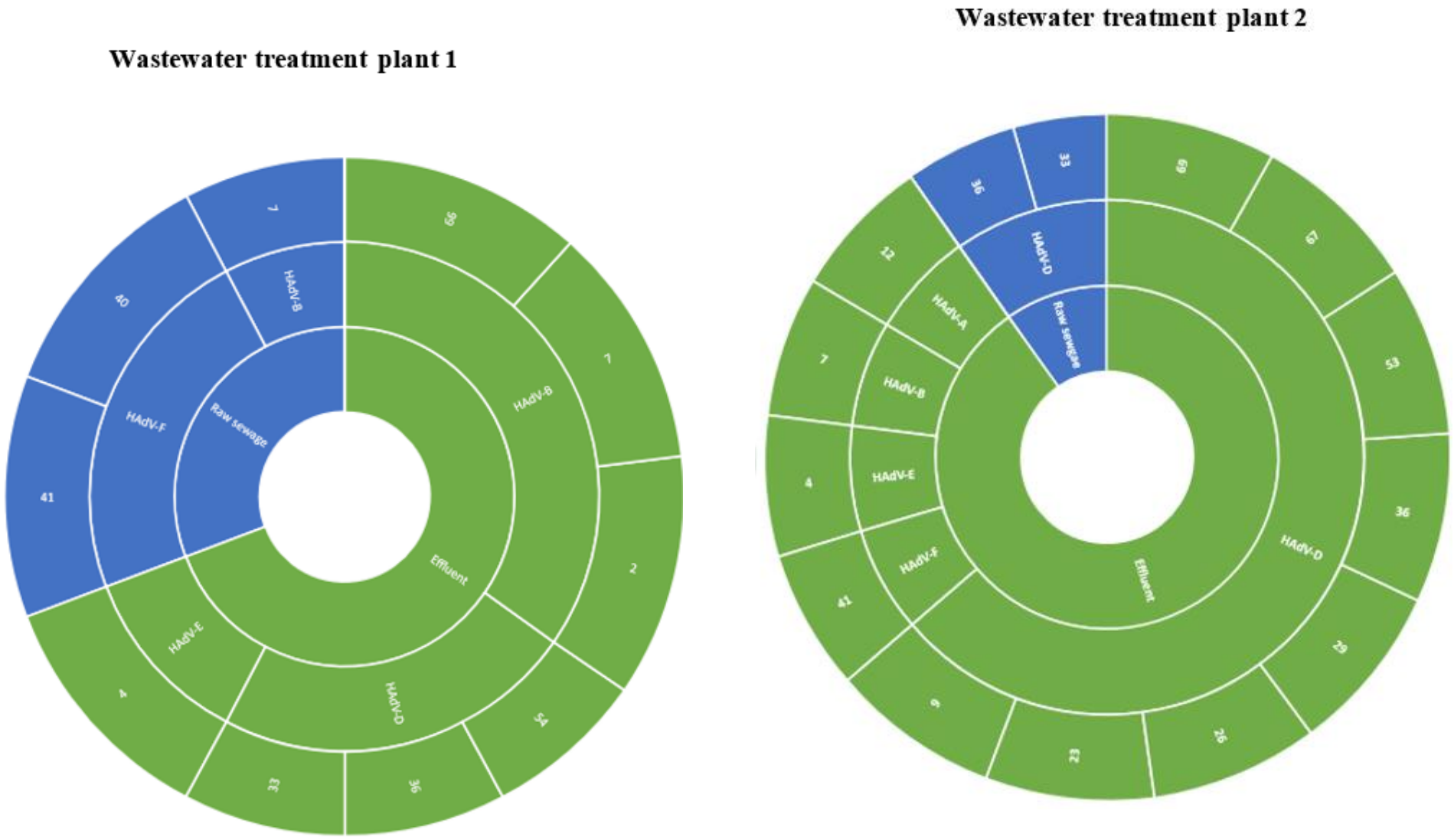


**Figure 3.16: Distribution of human adenovirus species and genotypes characterised using Sanger sequencing from two wastewater treatment plants.** Each wastewater treatment plant comprises of raw sewage and effluent samples. These sample types are colour -coded accordingly; Raw sewage (Blue ●) and Effluent (Green ●).

### 3.6.2. The prevalence of human adenovirus species and genotypes characterised using next generation sequencing

Conventional nested PCR products, obtained from 43 samples, were characterised using NGS. Data was obtained for 30/43 (70%) PCR products. The remaining 13/43 (30%) HAdV PCR products were untypeable. A total of 77 different HAdV types were identified in both WWTPs. More types could be characterised from effluent samples (44/77, 57%) than the raw sewage (33/77, 43%). Twenty-two HAdV types were identified in raw sewage from WWTP 1 and 27 HAdV types in effluent samples. The results of WWTP 2 showed the presence of 11 HAdV types in raw sewage and 17 HAdV types in the effluent samples. Subsequently, WWTP 1 contained the highest number of HAdV types (49/77, 64%) and WWTP 2 contained the lowest number of HAdV types (28/77, 36%). The number of HAdV types identified in each WWTP is shown in Table 3.4.

**Table 3.4: Total amount of human adenovirus types identified in two wastewater treatment plants**

| | **WWTP 1** | **WWTP 2** | **Total** |
|---|---|---|---|
| **Raw sewage** | 22 | 11 | **33** |
| **Effluent** | 27 | 17 | **44** |
| **Total** | **49** | **28** | **77** |

The HAdV NGS data is summarised in Table 3.5. This table represents the overall reads obtained after the data quality control and contig assembly. These samples originally had Ct values ranging from 27.9 to 38.2. Most of the samples passed quality trimming reads with percentages above 90% except for 4 samples (sample 32, sample 38, sample 94 and sample 132). The largest number of contigs after assembly using SPAdes were obtained for sample 48 and sample 165. The least number of contigs after assembly were sample 32, sample 38, sample 110 and sample 127. All the samples presented with more than 96% HAdV contigs.

Figure 3.17 illustrates the different HAdV species and genotypes characterised from WWTP 1 and WWTP 2. The broadness of each pie section is dependent on the number of HAdV species and genotypes identified. The HAdV-D (51/77, 66%) was the most prevalent HAdV species identified in both WWTPs. Furthermore, samples from WWTP 1 (35/77, 45%) consisted of more HAdV-D types than samples from WWTP 2 (16/77, 21%). These mainly occurred in the effluent samples of each WWTPs. The HAdV-A12 and HAdV-E4 types were only identified

in WWTP 1 occurring in both raw sewage and effluent samples. The HAdV-C1 strain was the only strain identified in the raw sewage of WWTP 1 with no presence in WWTP 2. The HAdV-B and HAdV-F species were co-dominant in both WWTPs occurring in both raw sewage and effluent samples. Neither WWTP 1 nor WWTP 2 showed the presence of HAdV-G types.

**Table 3.5: Summary of next generation sequencing quality control and contig assembly**

| Collection Date | Sample ID | Ct-Value | Reads before analysis | % of reads that passed quality trimming | Number of HAdV contigs (SLIM) | % of HAdV contigs |
|---|---|---|---|---|---|---|
| August 2018 | 25 | 32.6 | 25643 | 98.22 | 244 | 98.3 |
| August 2018 | 26 | 37.7 | 70490 | 97.69 | 599 | 99.6 |
| September 2018 | 29 | 31.6 | 21120 | 90.70 | 244 | 98.3 |
| September 2018 | 30 | 32.7 | 26936 | 97.22 | 822 | 99.5 |
| September 2018 | 32 | 33.2 | 146209 | 89.23 | 2 | 100 |
| September 2018 | 38 | 28.8 | 23529 | 21.77 | 12 | 100 |
| November 2018 | 47 | 27.9 | 34097 | 96.78 | 523 | 99.4 |
| November 2018 | 48 | 31.7 | 202776 | 97.26 | 19060 | 98.6 |
| December 2018 | 60 | 35.5 | 109600 | 97.62 | 1727 | 99.7 |
| January 2019 | 62 | 32.3 | 62462 | 96.46 | 353 | 99.4 |
| January 2019 | 64 | 29.8 | 381592 | 97.02 | 2025 | 99.8 |
| February 2019 | 70 | 31.9 | 34567 | 98.03 | 550 | 99.4 |
| April 2019 | 86 | 29.6 | 22430 | 97.40 | 181 | 96.6 |
| April 2019 | 87 | 35.1 | 32106 | 97.49 | 1099 | 99.3 |
| April 2019 | 88 | 33.9 | 128771 | 98.16 | 3289 | 98.1 |
| April 2019 | 89 | 32.6 | 33997 | 97.38 | 403 | 99.9 |
| May 2019 | 94 | 29.3 | 32699 | 83.85 | 770 | 99.7 |
| May 2019 | 98 | 33.3 | 89417 | 97.74 | 315 | 98.7 |
| June 2019 | 110 | 31.1 | 134101 | 97.25 | 79 | 97.5 |
| July 2019 | 113 | 37.8 | 93103 | 97.58 | 1346 | 99.4 |
| July 2019 | 117 | 35.1 | 35035 | 97.69 | 1106 | 99.2 |
| July 2019 | 118 | 35.9 | 40972 | 97.49 | 3998 | 99.7 |
| August 2019 | 126 | 33.1 | 89172 | 97.55 | 5016 | 99.9 |
| August 2019 | 127 | 36.8 | 51071 | 97.82 | 58 | 96.5 |
| September 2019 | 132 | 34.1 | 26342 | 87.96 | 865 | 99.4 |
| October 2019 | 140 | 36.9 | 167727 | 95.92 | 510 | 96.2 |
| December 2019 | 160 | 38.2 | 249169 | 97.02 | 113 | 93.7 |
| January 2020 | 165 | 32.6 | 296427 | 97.55 | 35961 | 99.6 |
| January 2020 | 167 | 33.7 | 378726 | 97.15 | 8741 | 98.9 |
| January 2020 | 170 | 32.8 | 224560 | 97.09 | 1247 | 99.1 |

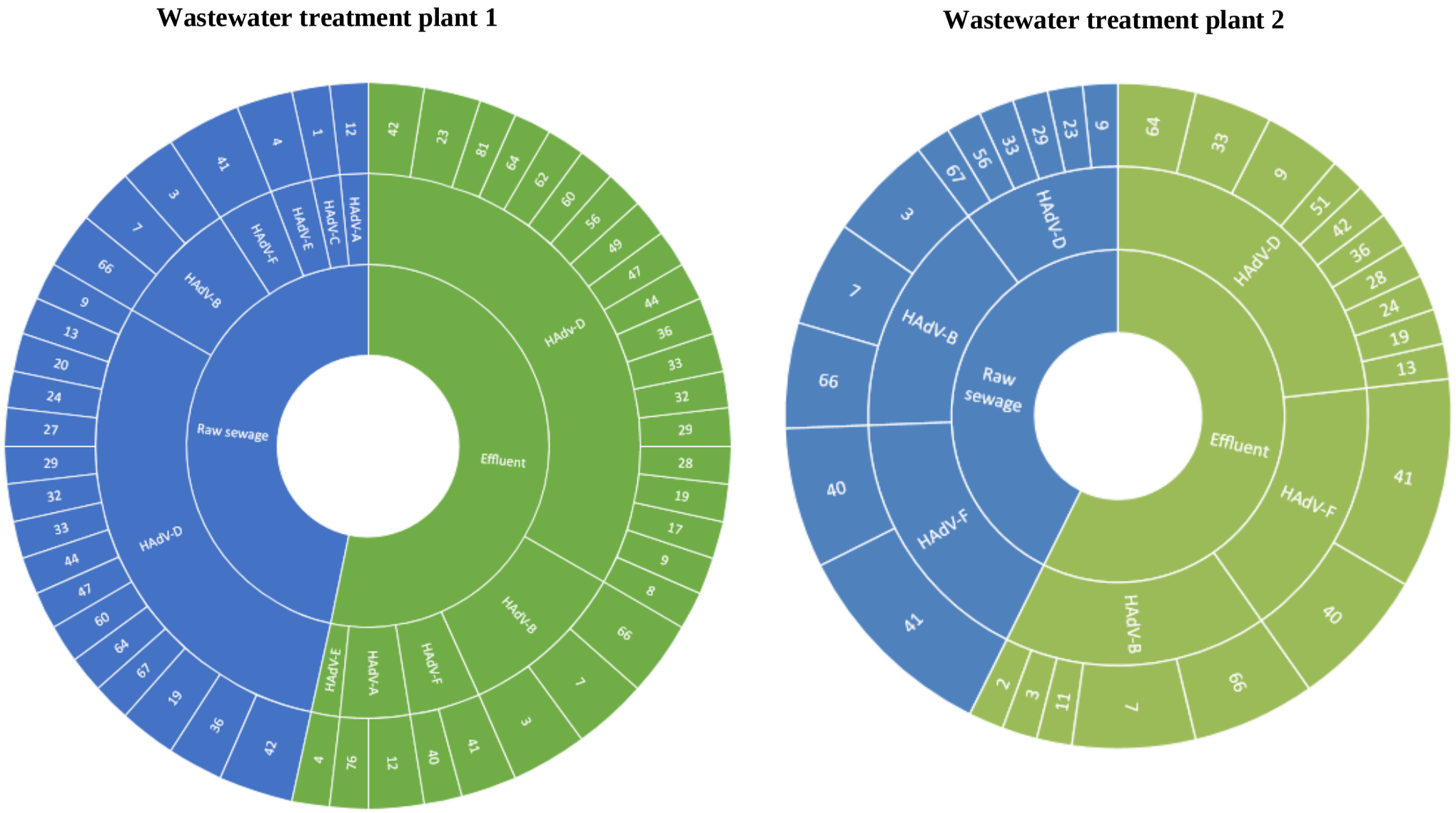


**Figure 3.17: Distribution of human adenovirus species and genotypes characterised using next generation sequencing from two wastewater treatment plants.** Each wastewater treatment plant comprises of raw sewage and effluent samples. These sample types are colour -coded accordingly; Raw sewage (Blue ) and Effluent (Green )

### 3.6.3 The human adenovirus species and genotypes identified using Sanger sequencing and next generation sequencing

When comparing the distribution of the HAdV species and genotypes identified in Sanger sequencing and NGS, it is evident that NGS yields a more diverse range of HAdV types compared to Sanger sequencing. This is shown in Figure 3.18. As many as nine different HAdV types were identified in sample 126 (August 2019, effluent, WWTP 2) (HAdV-B7, HAdV-D9, HAdV-D13, HAdV-D19, HAdV-D28, HAdV-D36, HAdV-D42, HAdV-D51, HAdV-D64) using NGS. The most HAdV types that were identified with Sanger sequencing in sample 125 were three and this was seen with most of the samples. Sample 38 (October 2019, Effluent, WWTP 1) was the only sample that presented with the same HAdV types (HAdV-D9, HAdV-53, HAdV-D67) that were identified using both sequencing techniques. Most of the samples had at least one HAdV strain that was the same in both sequencing techniques. However, sample 132 (September 2019, Effluent, WWTP 1) consisted of different HAdV types for the two sequencing techniques.

| Sanger sequencing | Next generation sequencing |
|---|---|
| **Sample 38: October 2019, Effluent, WWTP1** | |
| 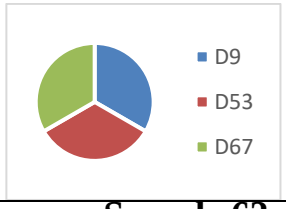 | 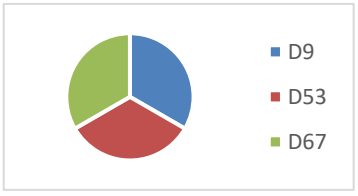 |
| **Sample 62: January 2019, Effluent, WWTP1** | |
| 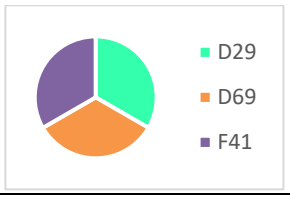 | 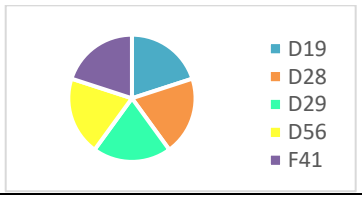 |

**Sample 64: January 2019, Effluent, WWTP 2**

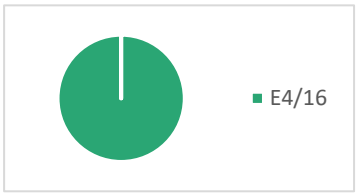


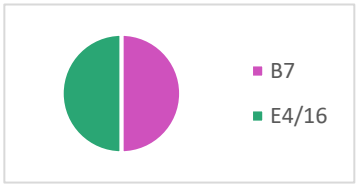


**Sample 70: February 2019, Effluent, WWTP 1**

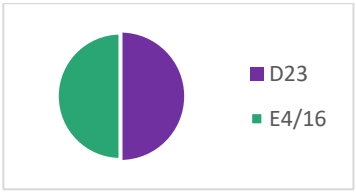


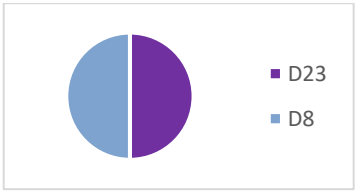


**Sample 87: April 2019, Effluent, WWTP1**

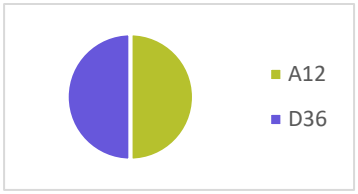


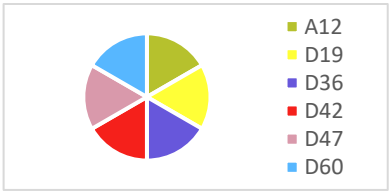


**Sample 98: May 2019, Effluent, WWTP1**

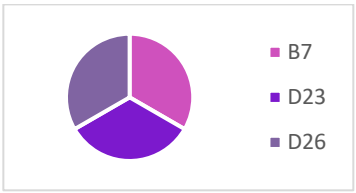



**Sample 110: June 2019, Effluent, WWTP2**

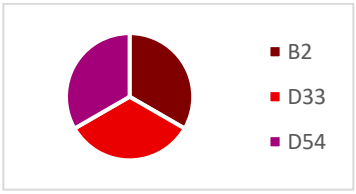


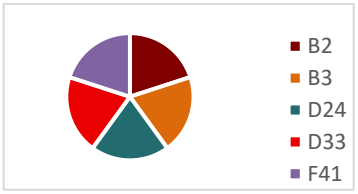


**Sample 113: July 2019, Raw, WWTP1**

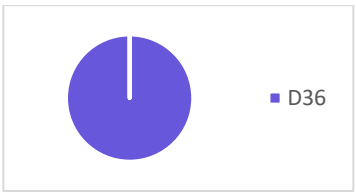


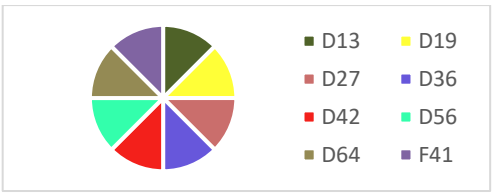

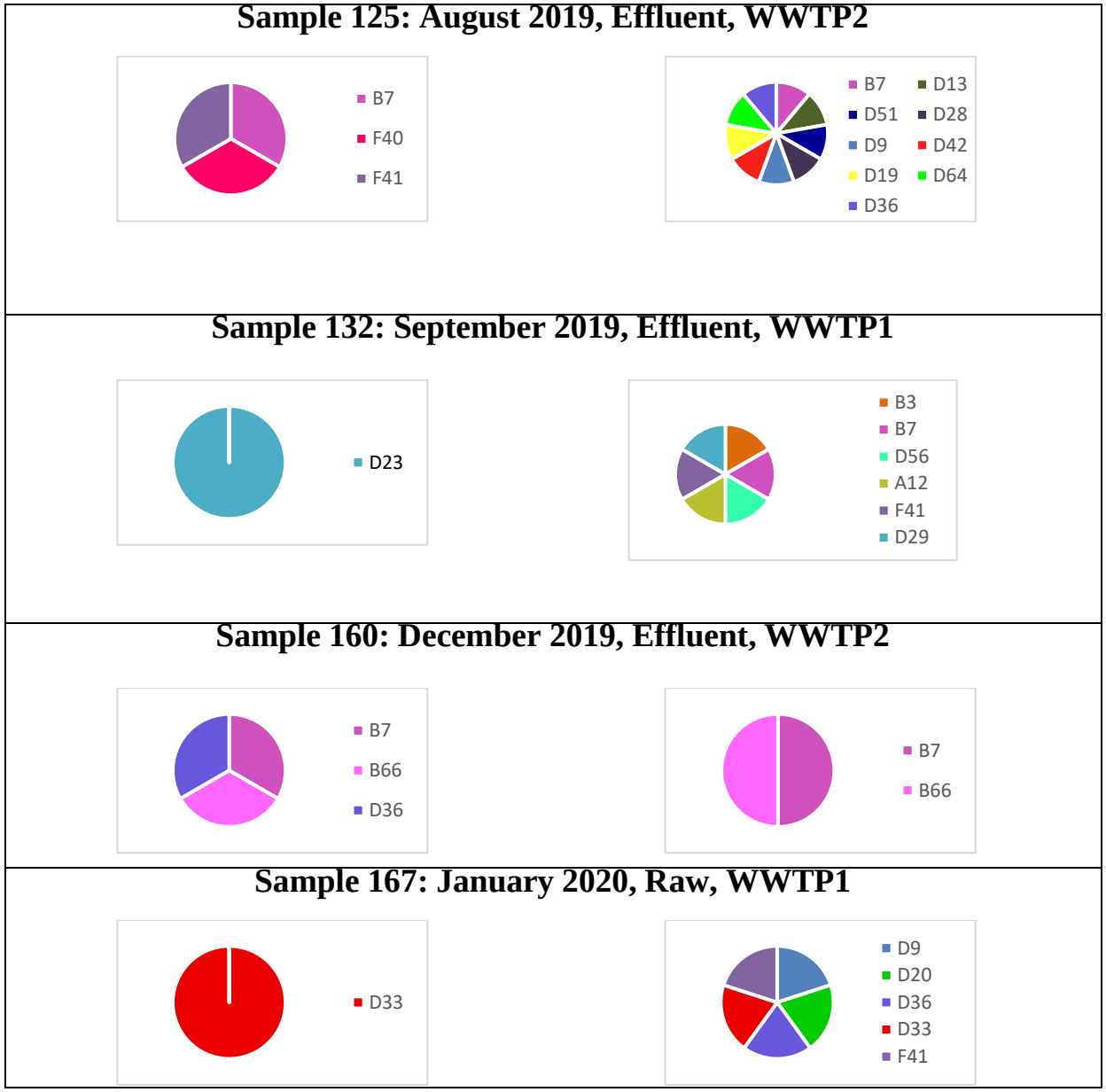


**Figure 3.18: Distribution of human adenovirus species and genotypes identified in 12 samples using Sanger sequencing and next generation sequencing**. Each sample represents a particular month from October 2019 to January 2020. The HAdV types that were identified in each sample are colour coded as shown in the key represented in each section. Abbreviation: WWTP: Wastewater treatment plants 1 / 2.

### 3.6.4 Seasonal prevalence of the human adenovirus species

The predominant species characterised throughout the seasons from Autumn 2018 to summer 2019 was HAdV-D as shown in purple in Figure 3.19. To a lesser extent, other species such as HAdV-B and HAdV-F were also present during each season. The highest number of HAdV species were detected in Spring 2018 (HAdV-B, HAdV-C, HAdV-D, HAdV-E and HAdV-F) and Summer 2019 (HAdV-A, HAdV-B, HAdV-D, HAdV-E and HAdV-F). The presence of HAdV-C was only detected in spring 2018. There was no evidence of the presence of HAdV-G. Furthermore, Figure 3.20 indicates that the presence of the HAdV species occurs throughout the year, with no pattern.

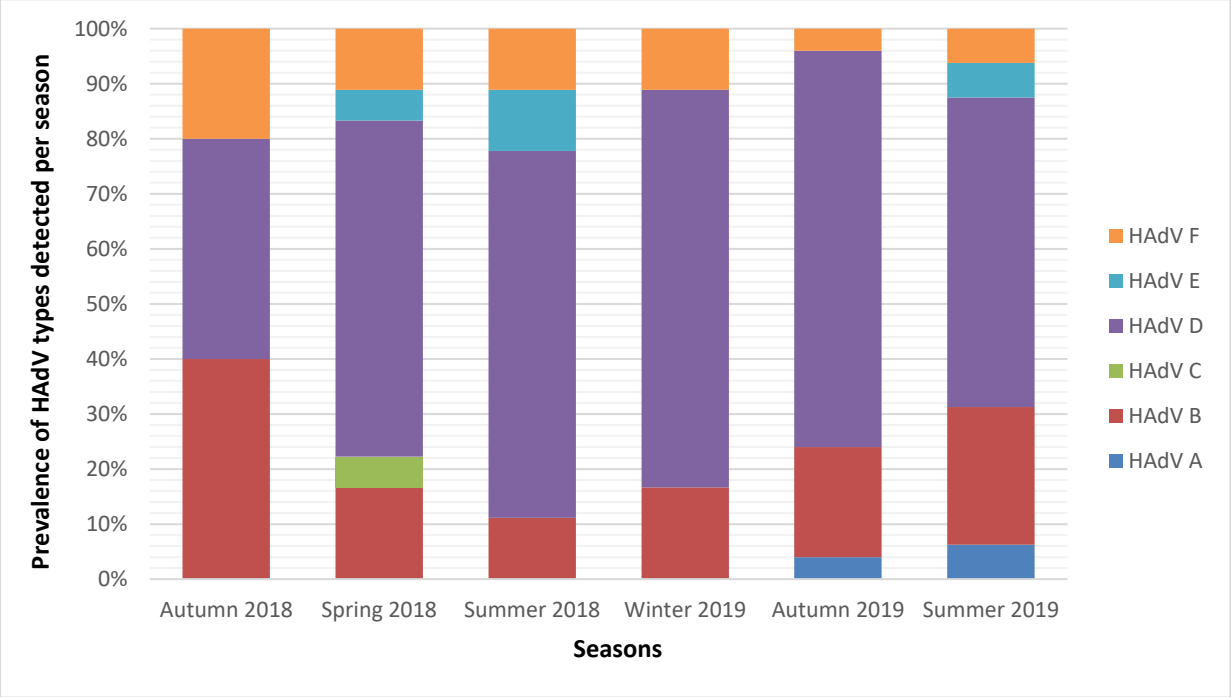


**Figure 3.19: Distribution of HAdV genotypes occurring in each season from Autumn 2018 to Summer 2019.** Each HAdV strain is colour coded, HAdV-A (Blue ) , HAdV-B (Red ), HAdV-C (Green ), HAdV-D (Purple ), HAdV-E (Light blue ), HAdV-F (Orange ),

## 3.7 PHYLOGENETIC ANALYSIS OF HUMAN ADENOVIRUS

The HAdV types detected were subjected to phylogenetic analysis. The HAdV types that were involved in this analysis were from both Sanger sequencing and NGS. These phylogenetic trees illustrate the types that are grouped into WWTP 1 and WWTP 2, respectively. For Sanger sequencing, the majority of HAdV types formed part of HAdV-D clusters as shown in Figure 3.20 and Figure 3.21. This phylogenetic analysis with types detected using Sanger sequencing, reveals a high diversity of HAdV-D types as there are four clusters with several sub-clusters within. For Sanger sequencing, the majority of HAdV types in WWTP 1 and WWTP 2 occurred during the summer and winter season, respectively. These types with their corresponding top hits from BLAST are illustrated in Appendix 2.1. The size fragments used for Sanger sequencing were approximately 800-925 bp. For both WTTPs, only the contigs with length fragments of 500 bp were selected and analysed. These types are represented in Appendix 2.3. Using BLAST, all the top hits presented with HAdV top hits but not all of them were selected for the construction of phylogenetic trees. The NGS assembly yielded in different regions of the hexon gene. Therefore, for phylogenetic analysis to take place, these contigs were trimmed to 180 bps. The majority of HAdV types from NGS analysis were HAdV-B and HAdV-D clusters, as shown in Figure 3.22 and Figure 3.23. There is a diverse range of HAdV clusters in WWTP 1 compared to WWTP 2. Most of the HAdV types were from the spring season in WWTP 1 and winter season for WWTP 2.

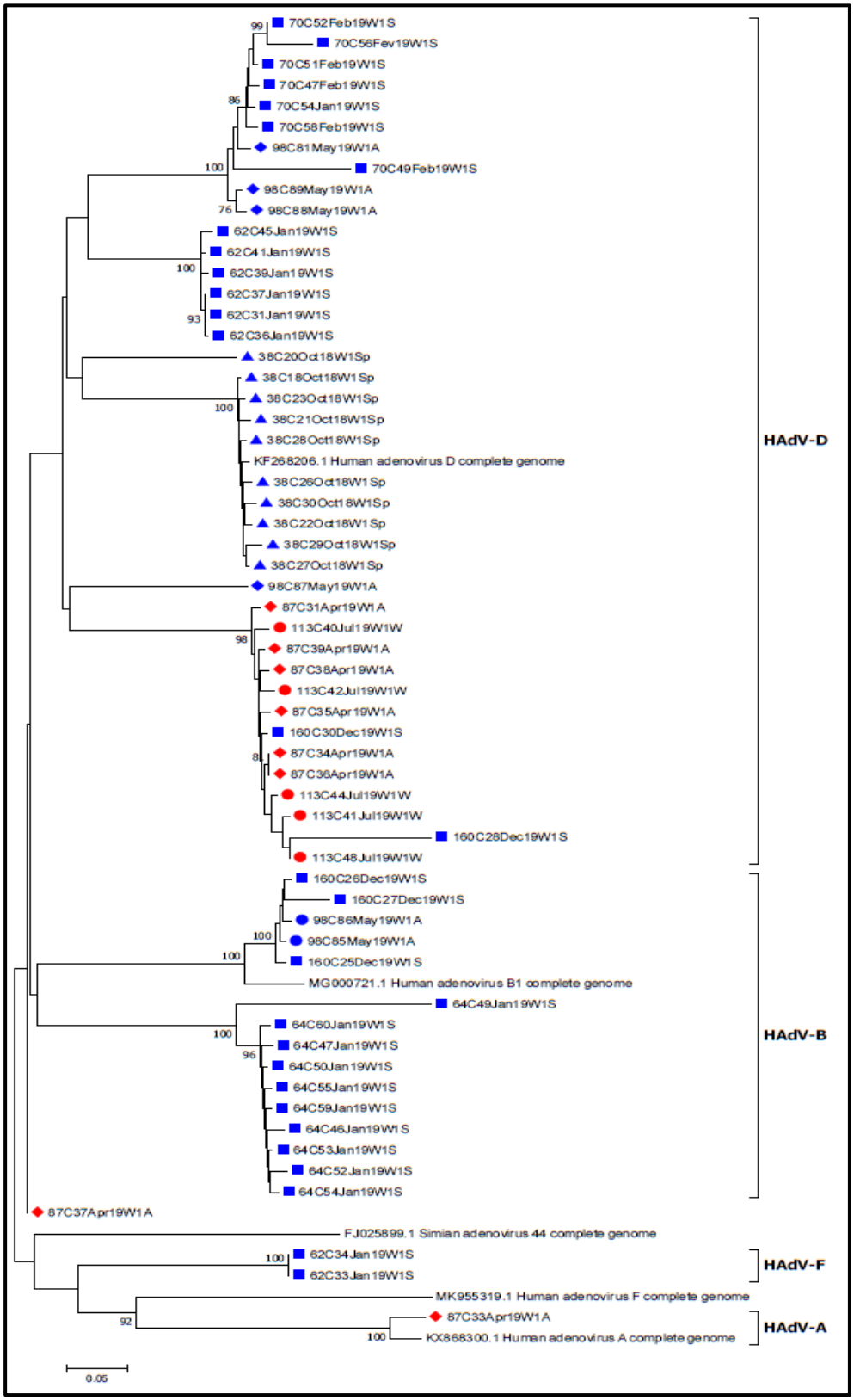


**Figure 3.20: The neighbour-joining phylogenetic tree of human adenovirus nucleotide sequences identified from wastewater treatment plant 1 using Sanger sequencing.** The evolutionary distances were determined using the Kimura 2-parameter method, conducted in MEGA6 (Tamura *et al.*, 2013). Closely related strains from GenBank indicated by accession numbers serve as reference. The percentage of replicate trees in which the associated strains clustered together in the bootstrap test (1000 replicates) is shown next to the branches. The scale bar indicates 0.05 nucleotide differences per site, over the indicated region. The tree is drawn to scale, with branch lengths in the same units as those of the evolutionary distances used to infer the phylogenetic tree. The analysis involved 64 nucleotide sequences. All ambiguous positions were removed for each sequence pair. There were a total of 1000 positions in the final dataset. Key: Raw sewage samples (Red) and effluent samples (Blue). Each season is represented by a shape; Summer (Square ■ ), Autumn (Diamond ◆), Winter (Circle ●) and Spring (Triangle ▲)

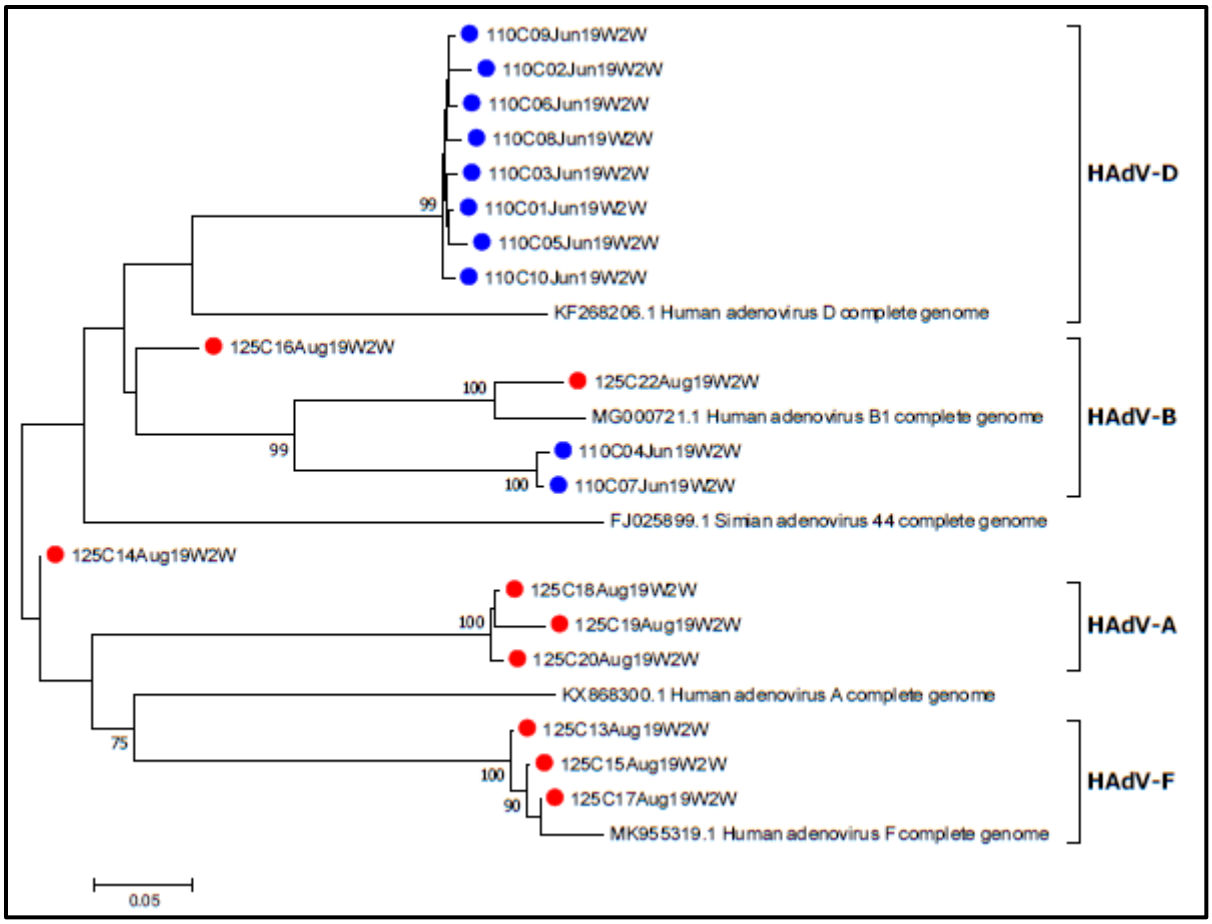


**Figure 3.21: The neighbour-joining phylogenetic tree of human adenovirus nucleotide sequences identified from wastewater treatment plant 2 using Sanger sequencing.** The evolutionary distances were determined using the Kimura 2-parameter method, conducted in MEGA6 (Tamura *et al.*, 2013). Closely related strains from GenBank indicated by accession numbers serve as reference. The percentage of replicate trees in which the associated strains clustered together in the bootstrap test (1000 replicates) is shown next to the branches. The tree is drawn to scale, with branch lengths in the same units as those of the evolutionary distances used to infer the phylogenetic tree. The analysis involved 24 nucleotide sequences. The scale bar indicates 0.05 nucleotide differences per site, over the indicated region. Key: Raw sewage samples (Red) and effluent samples (Blue). Each season is represented by a shape; Summer (Square ■), Autumn (Diamond ◆), Winter (Circle ●) and Spring (Triangle ▲)

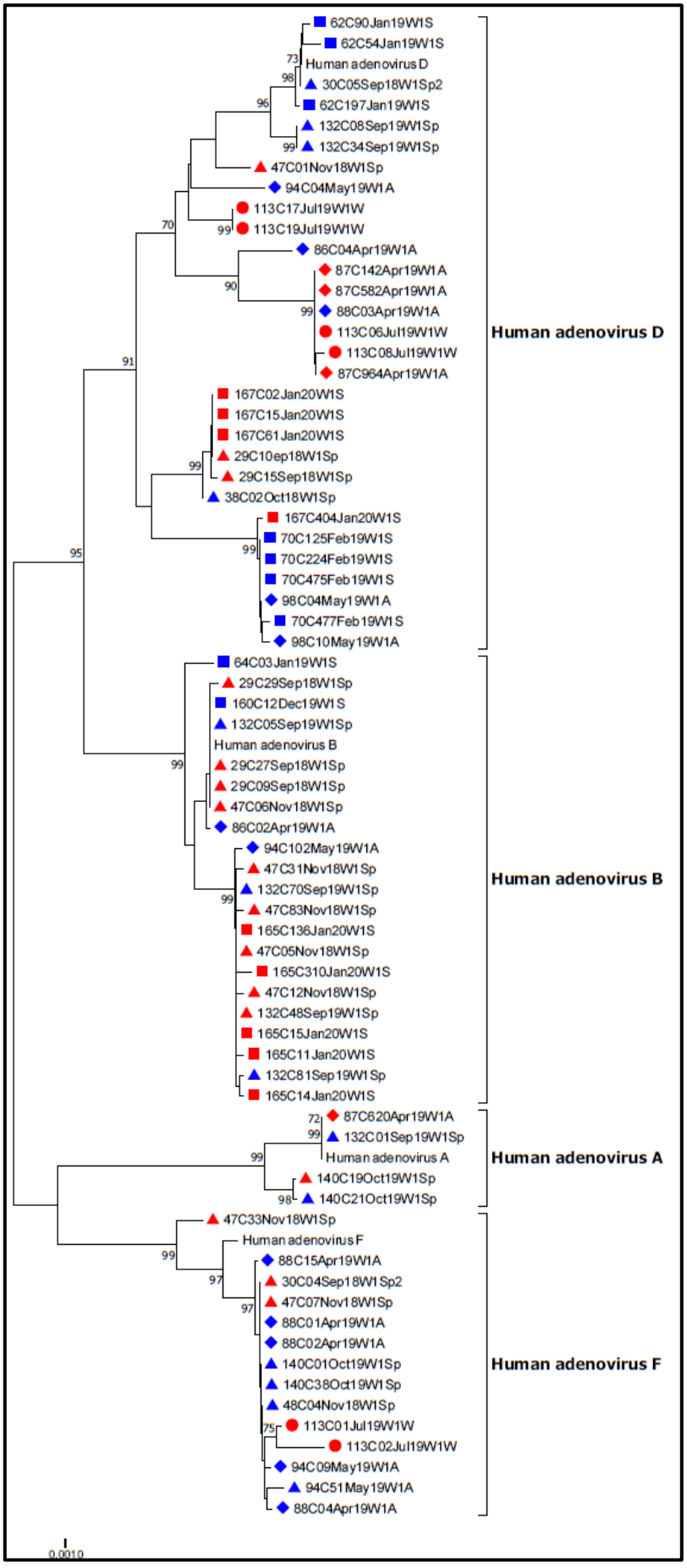
62C90Jan19W1S
62C54Jan19W1S
Human adenovirus D
30C05Sep18W1Sp2
62C197Jan19W1S
132C08Sep19W1Sp
132C34Sep19W1Sp
47C01Nov18W1Sp
94C04May19W1A
113C17Jul19W1W
113C19Jul19W1W
86C04Apr19W1A
87C142Apr19W1A
87C582Apr19W1A
88C03Apr19W1A
113C06Jul19W1W
113C08Jul19W1W
87C964Apr19W1A
167C02Jan20W1S
167C15Jan20W1S
167C61Jan20W1S
29C10ep18W1Sp
29C15Sep18W1Sp
38C02Oct18W1Sp
167C404Jan20W1S
70C125Feb19W1S
70C224Feb19W1S
70C475Feb19W1S
98C04May19W1A
70C477Feb19W1S
98C10May19W1A
Human adenovirus D
64C03Jan19W1S
29C29Sep18W1Sp
160C12Dec19W1S
132C05Sep19W1Sp
Human adenovirus B
29C27Sep18W1Sp
29C09Sep18W1Sp
47C06Nov18W1Sp
86C02Apr19W1A
94C102May19W1A
47C31Nov18W1Sp
132C70Sep19W1Sp
47C83Nov18W1Sp
165C136Jan20W1S
47C05Nov18W1Sp
165C310Jan20W1S
47C12Nov18W1Sp
132C48Sep19W1Sp
165C15Jan20W1S
165C11Jan20W1S
132C81Sep19W1Sp
165C14Jan20W1S
Human adenovirus B
87C620Apr19W1A
132C01Sep19W1Sp
Human adenovirus A
140C19Oct19W1Sp
140C21Oct19W1Sp
Human adenovirus A
47C33Nov18W1Sp
Human adenovirus F
88C15Apr19W1A
30C04Sep18W1Sp2
47C07Nov18W1Sp
88C01Apr19W1A
88C02Apr19W1A
140C01Oct19W1Sp
140C38Oct19W1Sp
48C04Nov18W1Sp
113C01Jul19W1W
113C02Jul19W1W
94C09May19W1A
94C51May19W1A
88C04Apr19W1A
Human adenovirus F
0.0010

**Figure 3.22: The neighbour-joining phylogenetic tree of human adenovirus nucleotide sequences identified from wastewater treatment plant 1 using NGS.** The evolutionary distances were determined using the Kimura 2-parameter method, conducted in MEGA6 (Tamura *et al.*, 2013). Closely related strains from GenBank indicated by accession numbers serve as reference. The percentage of replicate trees in which the associated strains clustered together in the bootstrap test (1000 replicates) is shown next to the branches. The tree is drawn to scale, with branch lengths in the same units as those of the evolutionary distances used to infer the phylogenetic tree. The analysis involved 73 nucleotide sequences. The scale bar indicates 0.05 nucleotide differences per site, over the indicated region. Key: Raw sewage samples (Red) and effluent samples (Blue). Each season is represented by a shape; Summer (Square ■), Autumn (Diamond ◆), Winter (Circle ●) and Spring (Triangle ▲)

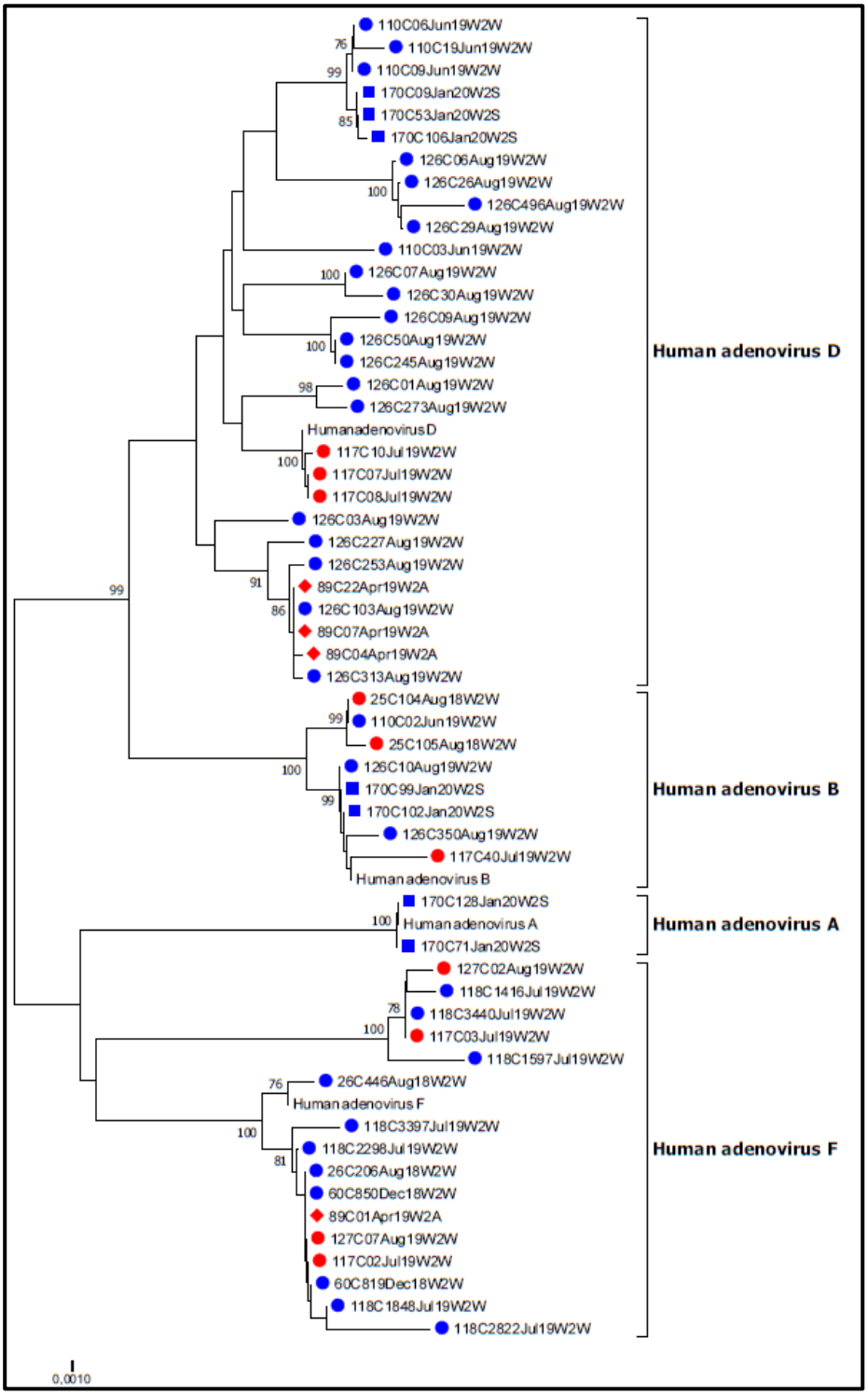


**Figure 3.23: The neighbour-joining phylogenetic tree of human adenovirus nucleotide sequences identified from wastewater treatment plant 2 using NGS.** The evolutionary distances were determined using the Kimura 2-parameter method, conducted in MEGA6 (Tamura *et al.*, 2013). Closely related strains from GenBank indicated by accession numbers serve as reference. The percentage of replicate trees in which the associated strains clustered together in the bootstrap test (1000 replicates) is shown next to the branches. The tree is drawn to scale, with branch lengths in the same units as those of the evolutionary distances used to infer the phylogenetic tree. The analysis involved 59 nucleotide sequences. The scale bar indicates 0.05 nucleotide differences per site, over the indicated region. Key: Raw sewage samples (Red) and effluent samples (Blue). Each season is represented by a shape; Summer (Square ■), Autumn (Diamond ◆), Winter (Circle ●) and Spring (Triangle ▲)

## 3.8 TIME AND COST ANALYSIS

The two sequencing techniques have a vast difference with respect to time and cost as shown in Table 3.6. The Sanger sequencing costs three times as much as the next generation sequencing, which amounted to R 6 300 and R 27 000 for 12 samples, respectively. However, the time it took to receive feedback from the sequencing institutes was the opposite to the cost for each. The laboratory procedures for Sanger sequencing also took longer than next generation sequencing. Due to a collaboration with the Sequencing Core Facility at the NICD, only the cost price was paid for the NGS. The waiting period for NGS took approximately 2 months whereas with Sanger sequencing took 2 to 3 days. The NGS time may vary at the NICD as outbreaks such as listeriosis and SARS-CoV-2 get first preference at the Sequencing Core Facility Unit. Following this, the analysis and editing of the next generation sequencing was quite laborious due to the extreme load of content for each sample. The analysis and editing for the Sanger sequencing data took at most only 24 hours.

**Table 3.6: Time and cost analysis comparing next generation sequencing and Sanger sequencing**

| Method | Next generation sequencing | | Sanger sequencing | |
|---|---|---|---|---|
| | Time | Cost | Time | Cost |
| Cloning & colony PCR | | | 18 hours | R 4 500 |
| Zymo recovery kit, DNA clean and concentrate | | | 2 hours | R 4 500 |
| Sequencing | 3.5 hours | R 6 300 | 3,5 hours | R 18 000 |
| Sequencing TOTAL | 3.5 hours | R 6 300 | 23.5 hours | R 27 000 |
| Sequencing cost per sample | | R 525 | | R 2 250 |

# CHAPTER 4

# DISCUSSION AND CONCLUSION

The human adenovirus is distributed worldwide and is a causative agent of several infections such as respiratory tract, gastrointestinal, ophthalmologic, genitourinary, and neurologic infections (Khanal *et al*., 2018). This ubiquitous virus is a waterborne pathogen as several human adenovirus (HAdV) types are present at high concentrations in aqueous environments throughout the year (Murphy, 2017). The HAdV is extremely resistant to environmental stressors and tertiary wastewater treatments. This property of HAdV resistance is beneficial to the public health sector as the virus can be used as an index for viral environmental contamination (Rigotto, 2010). This allows for viral monitoring and characterisation that provides rapid detection and quantification of viruses that are potential risks for communities surrounding these waters.

This study represented the surveillance of 75 raw sewage samples and 75 effluent environmental samples for the presence of HAdVs. These samples (n=150) were collected from two wastewater treatment plants (WWTPs) over a period of 18 months. The aim of the study was to provide a broader perspective and knowledge of the different HAdV types circulating within the surrounding communities in the Tshwane region, South Africa. Theoretically, raw sewage samples should contain more virus than effluent samples. This is because the effluent samples undergo a primary and secondary wastewater treatment before it is released into surface water sources, which may be used for domestic, irrigation or recreational purposes (Qiu *et al*., 2015). Therefore, to ensure that sufficient amount of virus was detected in the effluent samples, a larger volume (10 L) was used in comparison to the raw sewage samples (1 L). The successful detection of the HAdVs allowed for further analysis. This analysis comprised of determining the viral concentration, HAdV diversity amongst the two WWTPS and viral seasonality. The comparison of the sequencing techniques namely, Sanger sequencing and next generation sequencing (NGS), confirmed that NGS was the superior technique based on the laboratory preparation time, cost per sample and the ability to detect greater genotypic diversity.

The human adenovirus was successfully detected and quantified from raw sewage (69/75, 92%) and effluent samples (71/75, 95%) from two WWTPs, over a period of 18 months. In this study, HAdV was detected at a comparable detection rate in the raw and effluent samples. A high detection rate in the raw sewage were also shown in Tunisian study which was based on the detection of HAdVs in hospital wastewater. This study was conducted by Ibrahim and colleagues and detected 65/102 (64%) HAdV positives from two WWTPs (Ibrahim *et al*., 2018). Another study performed in Japan showed a higher detection rate in raw sewage compared to effluent samples (Thongprachum *et al*., 2018). In the current study, the remaining raw sewage (6/75, 8%) and effluent samples (4/75, 5%) that tested negative could be due to various reasons. These include the turbidity of the water, low viral recovery efficiency and PCR inhibitors such as humic acids, oils and several detergents (Gibson *et al*., 2012). For the same reasons, a minority of samples mengovirus could not be detected (24/150, 16%). Human adenoviruses were detected throughout the 18-month period, with most positives detected during the autumn and winter seasons. These detection peaks could represent a seasonal pattern as a previous study done in the Eastern Cape province, South Africa showed similar detection peaks during the autumn and winter season (Osuolale and Okoh, 2015). A study done in Egypt in 2019 presented with similar seasonality where Elmahdy and colleagues, 2020, found the seasonality occurrence rate of HAdV in sewage to be throughout the year with peaks in winter season (100%, 16/16 sewage samples) and autumn (69%, 11/16) (Elmahdy *et al*., 2020). A recent study done in Sydney, Australia, showed their highest seasonal peaks occurring during their summer seasons (January and March) and their lowest seasonal peaks occurring during their winter seasons (July) (Lun *et al*., 2019). However, a study collecting samples for 24-36 months will provide a more accurate representation of the HAdV seasonality.

During the first round of conventional nested PCR, there were no HAdV positive bands present. This is due to the environmental samples having a lower viral titer, which makes it less sensitive for the first-round detection. Environmental samples consist of many other organisms and pathogens which could lead to non-specific amplification. However, there were no nonspecific bands present during the second round of conventional nested PCR. The majority of the HAdV positive samples detected could not be amplified during conventional nested PCR as the amplification success rate was 31%. Various strategies, including using a different primer set and varying the annealing temperature, were used to increase the success rate. A study done in 2019 in Brazil, where Rames and colleagues looked at enteric viruses, also presented with a HAdV amplification success rate of below 50% (16/84, 19%) (Rigotto *et al*., 2010). Another

study done in 2011 in Greece by Kokkinos and colleagues achieved a genotyping success rate of HAdV below 50% during a 21-month study (November 2007 - July 2009), where they could genotype 22/48 (46%) HAdV positives in raw sewage samples from the municipal WWTP (Kokkinos *et al*., 2011). There are many reasons for this low success rate such as choice of polymerase enzymes, annealing temperature and primer mismatches. The current study did not investigate the possibility of primer mismatches. In spite of these difficulties, the hexon gene region has become the universal target for detecting and typing the HAdV (Okada et al., 2007). The qPCR (hexon gene position 18861 bp to 18981 bp as described by Heim and co-worker) and conventional nested PCR (hexon gene position 19135 bp to 20030 bp as described by Akhil and co-workers) targeted different areas on the hexon coding region. This could explain the difference in detection rates using these two molecular methods. Another study which found better genotyping efficiencies is a study done by Laconelli and colleagues, 2017, where they assessed the presence of HAdV in urban wastewaters of Italy. Laconelli and colleagues were able to genotype 85/141 samples (60%) (Laconelli *et al*., 2017).

Quantification of HAdVs detected in the environmental samples was done using standard curves for HAdV and MV, which served as an extraction control. The HAdV concentrations were adjusted according to the extraction efficiencies. However, these concentrations were probably an underestimation of the true quantity of the HAdV present in the wastewater. This is because, when HAdV concentrations were calculated, the efficiency of viral recovery with glass wool adsorption-elution and $PEG_{8000}$/NaCl as well as with skimmed milk flocculation, was not taken into consideration. A previous study done in our department found the efficiency of virus recovery for HAdVs from surface water and tap water to be 8% and 33% respectively, using the glass wool adsorption-elution technique (Ruhanya, 2013). The efficiency of recovery of HAdV from wastewater samples is not known. In addition, the efficiency of recovery for the skimmed milk flocculation method was not determined. Wastewater treatment plant 2 samples contained higher concentrations of HAdV (raw sewage samples [$1.69 \times 10^{12}$ gc/L] and effluent samples [$1.16 \times 10^{8}$ gc/L]) compared to WWTP 1 samples (raw sewage samples [$4.5 \times 10^{9}$ gc/L] and effluent samples [$4.3 \times 10^{8}$ gc/L]) This suggests that WWTP 2 tertiary treatments were more effective than that of WWTP 1 for the removal of HAdVs. These results confirm that the HAdV is present at high concentrations. It also corresponds to concentrations reported in a recent study that reviewed the prevalence of enteric viruses in environmental water sources. The results showed that HAdVs were detected in various studies at a

concentration range of $10^7$ -$10^9$ gc/L in raw sewage and $10^4$-$10^5$ gc/L in effluent samples (Katayama *et al*., 2008; Kitajima et al., 2014; Haramoto *et al*., 2018).

Two sequencing techniques targeting the hexon coding region were used for the identification of the HAdV species and genotypes. These included Sanger sequencing and NGS and the data obtained between the two methods were compared accordingly. The NGS was the most cost effective and required less laboratory preparation time compared to Sanger sequencing. The collaboration with the Sequencing Core Facility at the NICD enabled this study to pay cost price for NGS. Should this collaboration not be possible, the NGS would have been substantially more expensive. The NGS (77 HAdV types) also identified substantially more HAdV diversity than Sanger sequencing (18 HAdV types). These results are expected since a limited number of clones can be sequenced with Sanger sequencing compared to a substantially large number of reads using NGS. However, the NGS analysis took much longer than Sanger sequencing due to the vast diversity of the sequencing data. These results were expected and confirms that NGS is a single run assay, which yields multiple strains in many samples simultaneously. In addition, strains present at a low concentration would probably be undetectable using Sanger sequencing. This in turn reduces the time and cost involved in sample processing (Margulies *et al*., 2005). These results also clarify that Sanger sequencing is not a feasible approach when analyzing environmental samples, due to the presence of a vast diversity of strains in these samples. Environmental samples contain a high diversity of HAdV species and types, because it is a collection of viruses shed, both symptomatically and asymptomatically, by an entire community (La Rosa et al., 2014). This contrasts with the shedding of usually one type of HAdVs by a symptomatic individual. Therefore, in the case of a clinical specimen, Sanger sequencing may be the preferred technique, because of cost implications. For the analysis of environmental samples using Sanger sequencing, an additional step namely, cloning of the nested PCR products, to separate the individual strains is needed (Hajibabaei *et al.,* 2011). In addition, only a limited number of clones (n=10) can be subjected to Sanger sequencing, due to cost and time constraints.

The PCR products that were subjected to NGS but resulted in unidentifiable strains (13/43) using BLASTn analysis suggest that non-specific bands were amplified in the typing nested PCR. The phylogenetic analysis of both Sanger sequencing and NGS based sequence data could resolve 18 and 77 HAdV species respectively. The HAdV species that were prevalent during this 18-month study period were HAdV-B, HAdV-D and HAdV-F. These results partially correlate to similar studies based on the prevalence of HAdV in water environments

in South Africa. The HAdV species that were identified in these South African studies were HAdV-B, HAdV-C and HAdV-F (van Heerden *et al*., 2005; Chigor and Okoh, 2012; Sibanda and Okoh, 2012; Adefisoye *et al*., 2016) with only one other study detecting HAdV-D as well (Sibanda and Okoh, 2012). A clinical study was done in our department by Netshikweta based on the epidemiology of HAdV infections in hospitalised children with gastroenteritis in South Africa from 2009 to 2014 (Netshikweta, 2019). Over the five- year period, the detection of HAdV from stool specimens amounted to 656/3623 (18.1%), with the identification of HAdV species; HAdV-A, HAdV- B, HAdV-C, HAdV-D, HAdV-E and HAdV-F (Netshikweta, 2019). These results identified similar HAdV species as detected in the current study. The similarity between the two studies could be an indication of possible HAdVs that are predominantly circulating within South African communities. Interestingly, no HAdV-G was identified in either of the two studies. This is unexpected as this species (HAdV-G52) is associated with gastroenteritis (Jones et al., 2007).

The HAdV-D species is known to be the largest and most rapidly growing HAdV species (Ismail *et al*., 2018). This is evident in this master's study as most of the strains identified were from the HAdV-D species. This HAdV species contains viruses that are associated with epidemic keratoconjunctivitis and respiratory infections. The majority of the HAdV-D top hit strains from BLAST analysis originated from the USA. The two main HAdV strains that originated from USA resulted in two different clinical manifestations. The first originated in 1995 and was related to HAdV-D (HAdV-D88) causing respiratory infections. These strains were detected in a clinical specimen collected from a one-year-old male with bronchitis. The second USA top hit originated in 1963 and was relating to the HAdV-D (HAdV-D19) causing keratoconjunctivitis (Ismail *et al*., 2018). In 2016, there was a keratoconjunctivitis outbreak in the Virgin Islands, USA (Killerby *et al*., 2017). A total of 78 patients were affected with HAdV-D and the patients presented to various institutes such as family practices, eye care facilities and hospitals. Another outbreak of HAdV-D causing keratoconjunctivitis occurred in Los Angeles, USA in 2017 affecting seven patients which also included the health care workers and assistants (Oyong *et al*., 2018).

There were several other countries where the HAdV-D top hit strains were identified from countries, such as China, Uganda, Democratic Republic of Congo, Germany, Canada, Cote d' Ivoire and Japan. The most recent keratoconjunctivitis outbreaks have occurred in two boarding schools in southwest China, affecting 331 children in 2018 (Li *et al*., 2019). It was found that HAdV-D8 was the cause of these two outbreaks (Li *et al*., 2019). The HAdV-D8

was also the cause of an increase in keratoconjunctivitis cases in Germany from 2011 – 2013 (Hage *et al*., 2017). A nationwide keratoconjunctivitis outbreak occurred in Japan from 2015 to 2018 and was caused by HAdV-D54. In Japan, the leading cause of keratoconjunctivitis was from the HAdV-D54 (Tsukahara-Kawamura et al., 2020). In 2019, an outbreak caused by HAdV-D54 occurred in Canada affecting patients at an ophthalmology clinic and the immediate cause of the outbreak was unknown (Marwah *et al*., 2020). Magwalivha and colleagues found that HAdV-D22 and HAdV-D42 were prevalent in stool specimens from human immunodeficiency virus (HIV) children with diarrhoea in Kenya (Magwalivha *et al.,* 2010).

The current study the HAdV-B species were originally described in Argentina, followed by China, Singapore and Malaysia. The majority of HAdV strains circulating in Buenos Aires, Argentina was HAdV-B strains (Barrero *et al*., 2011). This HAdV-B species mainly causes respiratory infections in children. Several outbreaks caused by HAdV-B have occurred in military training camps in Shandong and Beijing, China and at large gathering events in Beijing and Guangzhou, China (Dongliu *et al*., 2016; Zhang *et al*., 2017; Lu *et al*., 2020).

The HAdV-F species predominantly causes acute gastroenteritis and is the predominant HAdV species causing infantile gastroenteritis (Banerjee *et al*., 2017). Many of the study strains were closely related to sequences from Genbank, which were detected in Italy, Japan, China and South Africa (See appendix B). The HAdV-F top hit strain from Italy was detected in a sewage sample and based on that study, the HAdV concentration was the highest amongst all the other enteric viruses identified from the environmental samples (La Rosa *et al*., 2010). A recent study described an outbreak of acute gastroenteritis in children in Northern Italy (Biscaro *et al*., 2018). Human adenovirus-F41 was found to be the second most predominant enteric viruses detected in these specimens (Biscaro *et al*., 2018). The HAdV-F strain originating from Japan is based on a study done in 2003 where eight types of HAdV-F41 strains were isolated from clinical samples (Li *et al*., 2004). This HAdV-F strain was detected in Italy in 2003. This is an indication that this particular strain is currently circulating in South African communities.

The HAdV-A12 strain that was used as the top hit strain in this master's study originated from Netherlands where the first isolation occurred (van der Avoort *et al*., 1989). This same strain was found in Sweden six years later (1988) in a pediatric ward at a hospital in Stockholm and thereafter occurred sporadically (Johansson *et al*., 1994). The HAdV-A12 is known to be associated with gastroenteritis which suggests viral replication in the gut. A study based on the

2013 gastroenteritis outbreak in a low-income community in Rio de Janeiro, Brazil showed that HAdV-A12 was excreted at a higher viral load than HAdV- F41 (Portes *et al*., 2016). This study by Portes and colleagues was also the first time HAdV-A12 was detected in gastroenteritis patients in Brazil.

Limitations of this study included the 18-month research period as a longer study period could have confirmed the accuracy of the seasonal distribution observed during these 18 months. More WWTPs could also be tested around the Tshwane region to determine the true prevalence of the HAdV types circulating. Despite troubleshooting, the conventional PCR remained inconsistent yielding a low genotyping success rate. Therefore, for future studies, more optimisation should be performed or new primers could be designed targeting a different region of the hexon gene. For the purpose of this study, the sensitivity of the qPCR and conventional nested PCR was not compared. Therefore, a higher sensitivity of the qPCR may explain the lower typing efficiency. This study was based solely on molecular techniques, which is unable to discriminate between viable and inactivated virions. In future, cell cultures or viability assays should be done to measure the infectivity of the quantified HAdVs identified in the aqueous environment. Additionally, the PCR and sequencing-based method used was only focused on a limited area of the hexon coding region, which could have resulted in the missed or mistyped HAdV variants. Another focus for future studies could be metagenomic study of the HAdV virome.

This study provided conclusive evidence on the prevalence and diversity of the HAdV circulating in both raw sewage and effluent environmental samples. These results provide more knowledge on the various HAdV types currently circulating within the Tshwane communities. This is indicative to a high diversity of HAdVs within the Tshwane region. The detection of these HAdVs act as an indicator of both symptomatic and asymptomatic infection and thus provided a broader knowledge compared to screening of clinical specimens. This study also confirmed that NGS would be the ideal sequencing technique for the surveillance of HAdVs in aqueous environmental samples. This is due to it resulting in a wealth of information regarding the species and genotypes of the pathogens in that particular area. In conclusion, there is a great need for continuous surveillance of the different enteric viruses, which are present in wastewaters and surface waters as it may serve as an early warning system for outbreaks. It is evident that the presence of these viruses is of environmental and public health concern, due to its presence in surface water. These waters may be utilised by surrounding communities, downstream from WWTPs for domestic and /or recreational purposes.

# CHAPTER 5
# REFERENCES


ABDOLI, A. & MASPI, N. 2018. Commentary: estimates of global, regional, and national morbidity, mortality, and aetiologies of diarrhoeal diseases: a systematic analysis for the global burden of disease study 2015. *Frontiers in Medicine,* 5**,** 11.

ABUBAKAR, I. I., TILLMANN, T., BANERJEE, A. 2015 Global, regional, and national age-sex specific all-cause and cause specific mortality for 240 causes of death, 1990-2013: a systematic analysis for the Global Burden of Disease Study 2013. *Lancet,* 385, 117-171.

ADEFISOYE, M. A., NWODO, U. U., GREEN, E. & OKOH, A. I. 2016. Quantitative detection and characterisation of human adenovirus, rotavirus and hepatitis A virus in discharged effluents of two wastewater treatment facilities in the Eastern Cape, South Africa. *Food and Environmental Virology, PCR* 8, 262-274.

AKHIL, C., SURESHA, P. G., SABEENA, S., HINDOL, M., ARUNKUMAR, G. 2016. Genotyping of human adenoviruses circulating in Southwest India. *Virus Disease*, 27, 266-270.

ALLARD, A., ALBINSSON, B. & WADELL, G. 1992. Detection of adenoviruses in stools from healthy persons and patients with diarrhea by two-step polymerase chain reaction. *Journal of Medical Virology,* 37**,** 149-157.

ALLARD, A. AND VANTARAKIS, A. 2017. Adenoviruses. In: J.B. Rose and B. Jiménez-Cisneros, (eds) Global Water Pathogen Project. http://www.waterpathogens.org (J.S Meschke, and R. Girones (eds) Part 3 Viruses) http://www.waterpathogens.org/book/adenoviruses

ALTSCHUL SF, GISH W, MILLER W, MYERS EW, LIPMAN DJ. 1990. Basic local alignment search tool. *Journal of Molecular Biology*, 215:403-410.

AMPUERO, J. S., OCAÑA, V., GÓMEZ, J., GAMERO, M. E., GARCIA, J., HALSEY, E. S. & LAGUNA-TORRES, V. A. 2012. Adenovirus respiratory tract infections in Peru. *PLoS One,* 7**,** e46898, doi.org10.1371

APARICIO O, RAZQUIN N, ZARATIEGUI M, NARVAIZA I, FORTES P. 2006. Adenovirus virus-associated RNA is processed to functional interfering RNAs involved in virus production. Journal of virology, 80,1376-84.

ARNBERG, N., EDLUND, K., KIDD, A. H. & WADELL, G. 2000. Adenovirus type 37 uses sialic acid as a cellular receptor. *Journal of Virology,* 74**,** 42-48.

ARNOLD, A. & MACMAHON, E. 2017. Adenovirus infections. *Medicine,* 45**,** 777-780.

ASIM, M., CHONG-LOPEZ, A. & NICKELEIT, V. 2003. Adenovirus infection of a renal allograft. *American Journal of Kidney Diseases,* 41**,** 696-701.

ASSIS, AS., FUMIAN, TM., MIAGOSTOVICH, MP., DRUMOND, BP., E SILVA, ML. 2018. Adenovirus and rotavirus recovery from a treated effluent through an optimized skimmed-milk flocculation method. *Environmental Science and Pollution Research,* 25, 17025-17032.

AVELLÓN, A., PÉREZ, P., AGUILAR, J. C., ORTIZ DE LEJARAZU, R. & ECHEVARRíA, J. E. 2001. Rapid and sensitive diagnosis of human adenovirus infections by a generic polymerase chain reaction. *Journal of Virological Methods,* 92**,** 113-120.

BABISS, L. E., GINSBERG, H. S., DARNELL, J. E. 1985. Adenovirus E1B proteins are required for accumulation of late viral mRNA and for effects on cellular mRNA translation and transport. Molecular and cellular biology, 5, 2552-2558.

BAKER, K. K., O'REILLY, C. E., LEVINE, M. M., KOTLOFF, K. L., NATARO, J. P., AYERS, T. L., FARAG, T. H., NASRIN, D., BLACKWELDER, W. C. & WU, Y. 2016. Sanitation and hygiene-specific risk factors for moderate-to-severe diarrhea in young children

in the global enteric multicenter study, 2007–2011: Case-control study. *PLoS Medicine***,** e1002010, doi.org10.1371.

BANERJEE, A., DE, P., MANNA, B., CHAWLA-SARKAR, M. 2017. Molecular characterization of enteric adenovirus genotypes 40 and 41 identified in children with acute gastroenteritis in Kolkata, India during 2013–2014. *Journal of Medical Virology*, 89, 606-614.

BANKEVICH, A., NURK, S., ANTIPOV, D., GUREVICH, A. A., DVORKIN, M., KULIKOV, A. S., LESIN, V. M., NIKOLENKO, S. I., PHAM, S., PRJIBELSKI, A. D., PYSHKIN, A. V. 2012. SPAdes: a new genome assembly algorithm and its applications to single-cell sequencing. Journal of Computational Biology, 19, 455-477.

BARLAN, A., GRIFFIN, T., MCGUIRE, K. & WIETHOFF, C. 2011. Adenovirus membrane penetration activates the NLRP3 inflammasome. *Journal of Virology,* 85**,** 146-155.

BARNADAS, C., SCHMIDT, D. J., FISCHER, T. K. & FONAGER, J. 2018. Molecular epidemiology of human adenovirus infections in Denmark, 2011–2016. *Journal of Clinical Virology*, 104**,** 16-22.

BARRERO, P. R., VALINOTTO, L. E., TITTARELLI, E., MISTCHENKO, A. S. 2012. Molecular typing of adenoviruses in pediatric respiratory infections in Buenos Aires, Argentina (1999–2010). *Journal of Clinical Virology*, 53, 145-150.

BERK, A. 2013. Fields Virology. Adenoviridae sixth. Lippincott Williams & Wilkins.Chapter 55.

BIALASIEWICZ, A. 2007. Adenoviral keratoconjunctivitis. *Sultan Qaboos University Medical Journal*, 7**,** 15.

BINDER, A. M., BIGGS, H. M., HAYNES, A. K., CHOMMANARD, C., LU, X., ERDMAN, D. D., WATSON, J. T. & GERBER, S. I. 2017. Human adenovirus surveillance—United States, 2003–2016. *Morbidity and Mortality Weekly Report,* 66**,** 1039.

BINN, L., HILLEMAN, M., RODRIGUEZ, J. & GLABERE, R. 1958. Antigenic relationships among adenoviruses with appraisal of reliability of complement-fixation test for typing isolates. *The Journal of Immunology,* 80**,** 501-508.

BISCARO, V., PICCINELLI, G., GARGIULO, F., IANIRO, G., CARUSO, A., CACCURI, F., DE FRANCESCO, MA. 2018. Detection and molecular characterization of enteric viruses in children with acute gastroenteritis in Northern Italy. *Infection, Genetics and Evolution,* 60, 35-41.

BLOCK, J. & SCHWARTZBROD, L. 1989. Detection and identification of viruses in water systems. New York: VCH Publishers.

BONVEHÍ, P. E. & TEMPORITI, E. R. 2018. Transmission and control of respiratory viral infections in the healthcare setting. *Current Treatment Options in Infectious Diseases,* 10**,** 182-196.

BURGERT, H.-G., RUZSICS, Z., OBERMEIER, S., HILGENDORF, A., WINDHEIM, M. & ELSING, A. 2002. Subversion of host defense mechanisms by adenoviruses. *Viral Proteins Counteracting Host Defenses.* Springer.

BURNETT, R. M., GRÜTTER, M. G., WHITE, J. L. The structure of the adenovirus capsid: I. An envelope model of hexon at 6 Å resolution. Journal of molecular biology. 1985 Sep 5;185(1):105-23.

CARRIGAN, D. R. 1997. Adenovirus infections in immunocompromised patients. *The American Journal of Medicine,* 102**,** 71-74.

CASAS I, AVELLON A, MOSQUERA M, JABADO O, ECHEVARRIA JE, CAMPOS RH, REWERS M, PEREZ-BREÑA P, LIPKIN WI, PALACIOS G. 2005. Molecular identification of adenoviruses in clinical samples by analysing a partial hexon genomic region. *Journal of Clinical Microbiology,* 43, 6176-6182.

CAUET, G., STRUB, J.-M., LEIZE, E., WAGNER, E., DORSSELAER, A. V. & LUSKY, M. 2005. Identification of the glycosylation site of the adenovirus type 5 fiber protein. *Biochemistry,* 44**,** 5453-5460.

CHANY, C., LEPINEI, P., LELONG, M., SATGE, P. & VIKAT, J. 1958. Severe and fatal pneumonia in infants and young children associated with adenovirus infections. A*merican Journal of Hygiene,* 67**,** 367-378.

CHARMAN, M., HERRMANN, C., WEITZMAN, M.D. 2019. Viral and cellular interactions during adenovirus DNA replication. FEBS letters., 593, 3531-3550.

CHIGBU, D. I. & LABIB, B. A. 2018. Pathogenesis and management of adenoviral keratoconjunctivitis. *Infection and Drug Resistance,* 11**,** 981.

CHIGOR, V. N. & OKOH, A. I. 2012. Quantitative detection and characterization of human adenoviruses in the Buffalo River in the Eastern Cape Province of South Africa. *Food and environmental virology,* 4, 198-208

CHRISTENSEN, J. B., BYRD, S. A., WALKER, A. K., STRAHLER, J. R., ANDREWS, P. C., IMPERIALE, M. J. 2008 Presence of the adenovirus IVa2 protein at a single vertex of the mature virion. Journal of virology, 15;82, 9086-9093.

CLAAS, E. C., SCHILHAM, M. W., DE BROUWER, C. S., HUBACEK, P., ECHAVARRIA, M., LANKESTER, A. C., VAN TOL, M. J. & KROES, A. C. 2005. Internally controlled real-time PCR monitoring of adenovirus DNA load in serum or plasma of transplant recipients. *Journal of Clinical Microbiology,* 43**,** 1738-1744.

COOK, J. & RADKE, J. 2017. Mechanisms of pathogenesis of emerging adenoviruses. *F1000Research,* 6.

COOK, J. L., WALKER, T. A., WORTHEN, G. S. & RADKE, J. R. 2002. Role of the E1A Rb-binding domain in repression of the NF-κB-dependent defense against tumor necrosis factor-α. *Proceedings of the National Academy of Sciences,* 99**,** 9966-9971.

DE JONG, J. C., WERMENBOL, A. G., VERWEIJ-UIJTERWAAL, M. W., SLATERUS, K. W., WERTHEIM-VAN DILLEN, P., VAN DOORNUM, G. J., KHOO, S. H. & HIERHOLZER, J. C. 1999. Adenoviruses from human immunodeficiency virus-infected individuals, including two strains that represent new candidate serotypes Ad50 and Ad51 of species B1 and D, respectively. *Journal of Clinical Microbiology,* 37**,** 3940-3945.

DE JONG, R. N., VAN DER VLIET, P. C., BRENKMAN, A. B. 2003. Adenovirus DNA replication: protein priming, jumping back and the role of the DNA binding protein DBP. Adenoviruses: Model and Vectors in Virus-Host Interactions, 187-211.

DEHGHAN, S., LIU, E. B., SETO, J., TORRES, S. F., HUDSON, N. R., KAJON, A. E., METZGAR, D., DYER, D. W., CHODOSH, J. & JONES, M. S. 2012. Five genome sequences of subspecies B1 human adenoviruses associated with acute respiratory disease. *American Society of Microbiology*.

DEHGHAN, S., SETO, J., LIU, E. B., WALSH, M. P., DYER, D. W., CHODOSH, J. & SETO, D. 2013. Computational analysis of four human adenovirus type 4 genomes reveals molecular evolution through two interspecies recombination events. *Virology,* 443**,** 197-207.

DONGLIU, Y., GUOLIANG, Y., HAOCHENG, X., SHUAIJIA, Q., LI, B., YANGLEI, J. 2016. Outbreak of acute febrile respiratory illness caused by human adenovirus B P14H11F14 in a military training camp in Shandong China. *Archives of Virology,* 161, 2481-2489.

DHINGRA, A., HAGE, E., GANZENMUELLER, T., BÖTTCHER, S., HOFMANN, J., HAMPRECHT, K., OBERMEIER, P., RATH, B., HAUSMANN, F., DOBNER, T., HEIM, A. 2019. Molecular evolution of human adenovirus (HAdV) species C. Scientific reports, 9, 1-3.

ECHAVARRÍA, M. 2008. Adenoviruses in immunocompromised hosts. *Clinical Microbiology reviews,* 21**,** 704-715.

EFTIM, S. E., HONG, T., SOLLER, J., BOEHM, A., WARREN, I., ICHIDA, A., NAPPIER, S. P. 2017. Occurrence of norovirus in raw sewage–a systematic literature review and meta-analysis. Water research.111:366-374.

ELMAHDY, E. M., AHMED, N. I., SHAHEEN, M. N., MOHAMED, E.-C. B. & LOUTFY, S. A. 2019. Molecular detection of human adenovirus in urban wastewater in Egypt and among children suffering from acute gastroenteritis. *Journal of water and health,* 17, 287-294.

ELMAHDY, E.M., SHAHEEN, M.N., RIZK, N.M., SAAD-HUSSEIN, A. 2020 May 9. Detection of Human Adenovirus and Human Rotavirus Group A in Wastewater and El-Rahawy Drainage Canal Influencing River Nile in the North of Giza, Egypt. *Food and Environmental Virology.*

ELOY, G.-G., MARTA, R., GERTJAN, M., MIQUEL, C. & ROSINA, G. 2019. Quantitative risk assessment of norovirus and adenovirus for the use of reclaimed water to irrigate lettuce in Catalonia. *Water Research*.

ENDERS JF, BELL JA, DINGLE JH, FRANCIS JR TH, HLLLEMAN MR, HUEBNER RJ, PAYNE AM. " Adenoviruses": 1956. Group name proposed for new respiratory-tract viruses. Science (Washington), 124:119-120

ENRIQUEZ, C. E., HURST, C. J. & GERBA, C. P. 1995. Survival of the enteric adenoviruses 40 and 41 in tap, sea, and waste water. *Water Research,* 29**,** 2548-2553.

ESPÍNOLA, E. E., BARRIOS, J. C., RUSSOMANDO, G., MIRAZO, S. & ARBIZA, J. 2017. Computational analysis of a species D human adenovirus provides evidence of a novel virus. *Journal of General Virology,* 98**,** 2810-2820.

FENG, Y., SUN, X., YE, X., FENG, Y., WANG, J., ZHENG, X., LIU, X., YI, C., HAO, M. & WANG, Q. 2018. Hexon and fiber of adenovirus type 14 and 55 are major targets of neutralizing antibody but only fiber-specific antibody contributes to cross-neutralizing activity. *Virology,* 518**,** 272-283.

FELSENSTEIN J. (1985). Confidence limits on phylogenies: An approach using the bootstrap. Evolution 39:783-791.

FIELDS, B. N., KNIPE, D. M. & HOWLEY, P. M. 1996. *Fields virology,* Lippincott-Raven.

FLOMENBERG, P. 2009. Adenovirus infections. *Medicine,* 37**,** 676-678.

FONG, T.-T. & LIPP, E. K. 2005. Enteric viruses of humans and animals in aquatic environments: health risks, detection, and potential water quality assessment tools. *Microbiology and Molecular Biology Reviews,* 69**,** 357-371.

FONG, T.-T., PHANIKUMAR, M. S., XAGORARAKI, I. & ROSE, J. B. 2010. Quantitative detection of human adenoviruses in wastewater and combined sewer overflows influencing a Michigan river. *Appied Environmental Microbiology,* 76**,** 715-723.

FOX, J. P., HALL, C. E. & COONEY, M. K. 1977. The Seattle virus watch: VII. Observations of adenovirus infections. *American Journal of Epidemiology,* 105**,** 362-386.

FU, Y., TANG, Z., YE, Z., MO, S., TIAN, X., NI, K., REN, L., LIU, E. & ZANG, N. 2019. Human adenovirus type 7 infection causes a more severe disease than type 3. *BioMed Central Infectious Diseases,* 19**,** 36.

GAGGAR, A., SHAYAKHMETOV, D. M. & LIEBER, A. 2003. CD46 is a cellular receptor for group B adenoviruses. *Nature Medicine,* 9**,** 1408.

GARCIA-ZALISNAK, D., RAPUANO, C., SHEPPARD, J. D. & DAVIS, A. R. 2018. Adenovirus ocular infections: Prevalence, pathology, pitfalls, and practical pointers. *Eye & Contact Lens,* 44**,** S1-S7.

GARNETT, C., ERDMAN, D., XU, W. & GOODING, L. R. 2002. Prevalence and quantitation of species C adenovirus DNA in human mucosal lymphocytes. *Journal of Virology,* 76**,** 10608-10616.

GAIDATZIS, D., LERCH, A., HAHNE, F., STADLER, M. B. 2015. QuasR: quantification and annotation of short reads in R. *Bioinformatics,* 31, 1130-1132.

GBD DIARRHOEAL DISEASES COLLABORATORS (2017) Estimates of global, regional and national morbidity, mortality and aetiologies of diarrhoeal diseases: a systematic analysis for the Global Burden of Disease Study 2015. ~~Doi.org/10.1016/S1473-3099(17)~~ 30276-30281.

GHEBREMEDHIN, B. 2014. Human adenovirus: Viral pathogen with increasing importance. *European Journal of Microbiology and Immunology,* 4**,** 26-33.

GIBSON KE, SCHWAB KJ, SPENCER SK, BORCHARDT MA. 2012. Measuring and mitigating inhibition during quantitative real time PCR analysis of viral nucleic acid extracts from large-volume environmental water samples. *Water Research,* 46, 4281-4291.

GIRONES, R., FERRUS, M. A., ALONSO, J. L., RODRIGUEZ-MANZANO, J., CALGUA, B., DE ABREU CORRÊA, A., HUNDESA, A., CARRATALA, A. & BOFILL-MAS, S. 2010. Molecular detection of pathogens in water–the pros and cons of molecular techniques. *Water Research,* 44**,** 4325-4339.

GLIMÅKER, M., ABEBE, A., JOHANSSON, B., EHRNST, A., OLCÉN, P. & STRANNEGÅRD, O. 1992. Detection of enteroviral RNA by polymerase chain reaction in faecal samples from patients with aseptic meningitis. *Journal of Medical Virology,* 38**,** 54-61.

GONZALES-GUSTAVSON, E., CÁRDENAS-YOUNGS, Y., CALVO, M., DA SILVA, M. F. M., HUNDESA, A., AMORÓS, I., MORENO, Y., MORENO-MESONERO, L., ROSELL, R. & GANGES, L. 2017. Characterization of the efficiency and uncertainty of skimmed milk flocculation for the simultaneous concentration and quantification of water-borne viruses, bacteria and protozoa. *Journal of Microbiological Methods,* 134**,** 46-53.

GRAY, G. C. 2006. Adenovirus transmission—worthy of our attention. *The Journal of Infectious Diseases,* 194**,** 871-873.

GREBER, U. F., SUOMALAINEN, M., STIDWILL, R. P., BOUCKE, K., EBERSOLD, M. W. & HELENIUS, A. 1997. The role of the nuclear pore complex in adenovirus DNA entry. *The EMBO journal,* 16**,** 5998-6007.

GREBER, U. F., WEBSTER, P., WEBER, J. & HELENIUS, A. 1996. The role of the adenovirus protease on virus entry into cells. *The EMBO journal,* 15**,** 1766-1777.

GROUP, H. A. W. 2014. Human adenovirus genotype classification.

GROUP, H. A. W. 2019. *Human Adenovirus Genotype Classification* [Online]. Available: http;//hadvwg.gmu.edu/ [Accessed 27 February 2019].

GUO, L., GONZALEZ, R., ZHOU, H., WU, C., VERNET, G., WANG, Z. & WANG, J. 2012. Detection of three human adenovirus species in adults with acute respiratory infection in China. *European journal of Clinical Microbiology & Infectious Diseases,* 31**,** 1051-1058.

HAGE, E., ESPELAGE, W., ECKMANNS, T., LAMSON, D.M., PANTÓ, L., GANZENMUELLER, T., HEIM, A. 2017. Molecular phylogeny of a novel human adenovirus type 8 strain causing a prolonged, multi-state keratoconjunctivitis epidemic in Germany. *Scientific reports,* 7, 1-9.

HAJIBABAEI, M., SHOKRALLA, S., ZHOU, X., SINGER, G. A. & BAIRD, D. J. 2011. Environmental barcoding: a next-generation sequencing approach for biomonitoring applications using river benthos. *PLoS one,* 6, e17497.

HALL, T. A. (1999). BioEdit: a user-friendly biological sequence alignment editor and analysis program for Windows 95/98/NT. *Nucleic acids symposium series*, [London]: Information Retrieval Ltd., c1979c2000.

HAMZA, I. A., JURZIK, L., ÜBERLA, K. & WILHELM, M. 2011. Methods to detect infectious human enteric viruses in environmental water samples. *International Journal of Hygiene and Environmental Health,* 214, 424-436.

HANAOKA, N., ITO, S., KONAGAYA, M., NOJIRI, N., YASUDA, M., FUJIMOTO, T. & DEGUCHI, T. 2019. Infectious human adenoviruses are shed in urine even after disappearance of urethral symptoms. *PLoS One,* 14**,** e0212434.

HARAMOTO, E., KITAJIMA, M., HATA, A., TORREY, J. R., MASAGO, Y., SANO, D.& KATAYAMA, H. 2018. A review on recent progress in the detection methods and prevalence of human enteric viruses in water. *Water Research,* 135, 168-186.

HARTMAN, Z. C., KIANG, A., EVERETT, R. S., SERRA, D., YANG, X. Y., CLAY, T. M. & AMALFITANO, A. 2007. Adenovirus infection triggers a rapid, MyD88-regulated transcriptome response critical to acute-phase and adaptive immune responses in vivo. *Journal of Virology,* 81**,** 1796-1812.

HASHIMOTO, S., GONZALEZ, G., HARADA, S., OOSAKO, H., HANAOKA, N., HINOKUMA, R. & FUJIMOTO, T. 2018. Recombinant type Human mastadenovirus D85 associated with epidemic keratoconjunctivitis since 2015 in Japan. *Journal of Medical Virology*, 90**,** 881-889.

HASSAN M, TASNUVA A, JAHURUL A, WARDA H, ENAYET M, AFM H, RAHMAN R, AHMED S, SYED A, FARUQUE G, ZIAUR M. 2017. Detection of enteric-and non-enteric adenoviruses in.

HE, F., JOSHI, S. B., MOORE, D. D., SHINOGLE, H. E., OHTAKE, S., LECHUGA-BALLESTEROS, D., MARTIN, R. A., TRUONG-LE, V. L. & MIDDAUGH, C. R. 2010. Using spectroscopic and microscopic methods to probe the structural stability of human adenovirus type 4. *Human Vaccines,* 6**,** 202-211.

HEERDEN, J., EHLERS, M., HEIM, A. & GRABOW, W. 2005. Prevalence, quantification and typing of adenoviruses detected in river and treated drinking water in South Africa. *Journal of Applied Microbiology,* 99**,** 234-242.

HEIM A, EBNET C, HARSTE G, PRING-ÅKERBLOM P. Rapid and quantitative detection of human adenovirus DNA by real-time PCR. *Journal of Medical Virology*. 2003 June;70(2):228-39.

HERRMANN, J. E., PERRON-HENRY, D. M. & BLACKLOW, N. R. 1987. Antigen detection with monoclonal antibodies for the diagnosis of adenovirus gastroenteritis. *Journal of Infectious Diseases,* 155**,** 1167-1171.

HIERHOLZER, J. C. 1992. Adenoviruses in the immunocompromised host. *Clinical microbiology reviews,* 5**,** 262-274.

HIWARKAR, P., KOSULIN, K., CESARO, S., MIKULSKA, M., STYCZYNSKI, J., WYNN, R. & LION, T. 2018. Management of adenovirus infection in patients after haematopoietic stem cell transplantation: state-of-the-art and real-life current approach: a position statement on behalf of the Infectious Diseases Working Party of the European Society of Blood and Marrow Transplantation. *Reviews in Medical Virology,* 28**,** e1980.

HLLLEMAN, M. & WERNER, J. H. 1954. Recovery of new agent from patients with acute respiratory illness. *Proceedings of the Society for Experimental Biology and Medicine,* 85**,** 183-188.

HOEBEN, R. C., UIL, T. G. Adenovirus DNA replication. 2013. Cold Spring Harbor perspectives in biology, 5

HONG, J.-Y., LEE, H.-J., PIEDRA, P. A., CHOI, E.-H., PARK, K.-H., KOH, Y.-Y. & KIM, W.-S. 2001. Lower respiratory tract infections due to adenovirus in hospitalized Korean children: epidemiology, clinical features, and prognosis. *Clinical Infectious Diseases,* 32**,** 1423-1429.

HORWITZ, M. S. 2001. Adenovirus immunoregulatory genes and their cellular targets. *Virology,* 279**,** 1-8.

HORWITZ M. S. 2004. Function of adenovirus E3 proteins and their interactions with immunoregulatory cell proteins. A cross-disciplinary journal for research on the science of gene transfer and its clinical applications. *The Journal of Gene Medicine,* 6, 172-183.

IP, W. H., DOBNER, T. 2020. Cell transformation by the adenovirus oncogenes E1 and E4. FEBS letters, 594,1848-1860.

ISMAIL, A. M., LEE, J. S., LEE, J. Y., SINGH, G., DYER, D. W., SETO, D., CHODOSH, J. & RAJAIYA, J. 2018. Adenoviromics: mining the human adenovirus species D genome. *Frontiers in Microbiology,* 9.

IBRAHIM, C., HASSEN, A., POTHIER, P., MEJRI, S., HAMMAMI, S. 2018. Molecular detection and genotypic characterization of enteric adenoviruses in a hospital wastewater. *Environmental Science and Pollution Research,* 25, 10977-10987.

ISMAIL, A. M., ZHOU, X., DYER, D. W., SETO, D., RAJAIYA, J. & CHODOSH, J. 2019. Genomic foundations of evolution and ocular pathogenesis in human adenovirus species D. *Federal of European Biomedical Sciences letters,* 593**,** 3583-3608.

ISMAIL AM, CUI T, DOMMARAJU K, SINGH G, DEHGHAN S, SETO J, SHRIVASTAVA S, FEDOROVA NB, GUPTA N, STOCKWELL TB, MADUPU R. 2018. Genomic analysis of a large set of currently—and historically—important human adenovirus pathogens. Emerging microbes & infections, 7, 1-22.

J ECKARDT, A. & C BAUMGART, D. 2011. Viral gastroenteritis in adults. *Recent Patents on anti-infective drug discovery,* 6**,** 54-63.

JAWETZ, E., KIMURA, S., NICHOLAS, A., THYGESON, P. & HANNA, L. 1955. new type of APC virus from epidemic keratoconjunctivitis. *Science (Washington),* 122**,** 1190-91.

JERNIGAN, J. A., LOWRY, B. S., HAYDEN, F. G., KYGER, S. A., CONWAY, B. P., GROSCHEL, D. H. & FARR, B. M. 1993. Adenovirus type 8 epidemic keratoconjunctivitis in an eye clinic: risk factors and control. *Journal of Infectious Diseases,* 167**,** 1307-1313.

JOGLER, C., HOFFMANN, D., THEEGARTEN, D., GRUNWALD, T., ÜBERLA, K., WILDNER, O. 2006.Replication properties of human adenovirus in vivo and in cultures of primary cells from different animal species. *Journal of Virology*, 8, 3549-3558.

JOHANSSON, M. E., M. A. ANDERSSON, AND P. A. THORNER. 1994. Adenoviruses isolated in the Stockholm area during 1987-1992: restriction endonuclease analysis and molecular epidemiology. *Archive. Virology.*

JONES, M. S., HARRACH, B., GANAC, R. D., GOZUM, M. M., DELA CRUZ, W. P., RIEDEL, B., PAN, C., DELWART, E. L. & SCHNURR, D. P. 2007. New adenovirus species found in a patient presenting with gastroenteritis. *Journal of Virology,* 81**,** 5978-5984.

KAJON, A. E., HANG, J., HAWKSWORTH, A., METZGAR, D., HAGE, E., HANSEN, C. J., KUSCHNER, R. A., BLAIR, P., RUSSELL, K. L. & JARMAN, R. G. 2015. Molecular

epidemiology of adenovirus type 21 respiratory strains isolated from US military trainees (1996–2014). *The Journal of Infectious Diseases,* 212**,** 871-880.

KAJON, A. E., LAMSON, D. M., BAIR, C. R., LU, X., LANDRY, M. L., MENEGUS, M., ERDMAN, D. D. & GEORGE, K. S. 2018. Adenovirus type 4 respiratory infections among civilian adults, Northeastern United States, 2011–2015. *Emerging Infectious Diseases,* 24**,** 201.

KAJON, A. E., LAMSON, D. M. & GEORGE, K. S. 2019. Emergence and re-emergence of respiratory adenoviruses in the United States. *Current opinion in virology,* 34**,** 63-69.

KAJON, A. E., LU, X., ERDMAN, D. D., LOUIE, J., SCHNURR, D., ST GEORGE, K., KOOPMANS, M. P., ALLIBHAI, T. & METZGAR, D. 2010. Molecular epidemiology and brief history of emerging adenovirus 14—associated respiratory disease in the United States. *The Journal of Infectious Diseases,* 202**,** 93-103.

KÄLIN, S., AMSTUTZ, B., GASTALDELLI, M., WOLFRUM, N., BOUCKE, K., HAVENGA, M., DIGENNARO, F., LISKA, N., HEMMI, S. & GREBER, U. F. 2010. Macropinocytotic uptake and infection of human epithelial cells with species B2 adenovirus type 35. *Journal of Virology,* 84**,** 5336-5350.

KAMPMANN, B., CUBITT, D., WALLS, T., NAIK, P., DEPALA, M., SAMARASINGHE, S., ROBSON, D., HASSAN, A., RAO, K. & GASPAR, H. 2005. Improved outcome for children with disseminated adenoviral infection following allogeneic stem cell transplantation. *British Journal of Haematology,* 130**,** 595-603.

KENMOE, S., VERNET, M.-A., LE GOFF, J., PENLAP, V. B., VABRET, A. & NJOUOM, R. 2018. Molecular characterization of human adenovirus associated with acute respiratory infections in Cameroon from 2011 to 2014. *Virology Journal,* 15, 153.

KENNEDY, M. A. & PARKS, R. J. 2009. Adenovirus virion stability and the viral genome: size matters. *Molecular Therapy,* 17**,** 1664-1666.

KHANAL. S., GHIMIRE, P., DHAMOON, A.S. 2018. The repertoire of adenovirus in human disease: the innocuous to the deadly. *Biomedicines,* 6, 30.

KIDD, A. & MADELEY, C. 1981. In vitro growth of some fastidious adenoviruses from stool specimens. *Journal of Clinical Pathology,* 34**,** 213-216.

KILLERBY, M.E., STUCKEY, M.J., GUENDEL, I., SAKTHIVEL, S., LU, X., ERDMAN, D.D., SCHNEIDER, E., FAGAN, R., DAVIS, M.S., WATSON, J.T., GERBER, S.I. 2017. Notes from the field: epidemic keratoconjunctivitis outbreak associated with human adenovirus type 8—US Virgin Islands, June–November 2016. *Morbidity and Mortality Weekly Report*, 66, 811

KIMURA M. (1980). A simple method for estimating evolutionary rate of base substitutions through comparative studies of nucleotide sequences. Journal of Molecular Evolution 16:111-120.

KUMAR S., STECHER G., AND TAMURA K. (2016). MEGA7: Molecular Evolutionary Genetics Analysis version 7.0 for bigger datasets.Molecular Biology and Evolution 33:1870-1874.

KOKKINOS, P.A., ZIROS, P.G., MPALASOPOULOU, A., GALANIS, A., VANTARAKIS, A. 2011. Molecular detection of multiple viral targets in untreated urban sewage from Greece. *Virology Journal*, 8, 195.

KOREN, M. A., ARNOLD, J. C., FAIRCHOK, M. P., LALANI, T., DANAHER, P. J., SCHOFIELD, C. M., RAJNIK, M., HANSEN, E. A., MOR, D. & CHEN, W. J. 2016. Type-specific clinical characteristics of adenovirus-associated influenza-like illness at five US military medical centers, 2009–2014. *Influenza and other Respiratory Viruses,* 10**,** 414-420.

KOTLOFF, K. L., NATARO, J. P., BLACKWELDER, W. C., NASRIN, D., FARAG, T. H., PANCHALINGAM, S., WU, Y., SOW, S. O., SUR, D. & BREIMAN, R. F. 2013. Burden and aetiology of diarrhoeal disease in infants and young children in developing countries (the Global Enteric Multicenter Study, GEMS): a prospective, case-control study. *The Lancet,* 382**,** 209-222.

KRIKELIS, V., SPYROU, N., MARKOULATOS, P. & SERIE, C. 1985. Seasonal distribution of enteroviruses and adenoviruses in domestic sewage. *Canadian Journal of Microbiology,* 31**,** 24-25.

LA ROSA, G., POURSHABAN, M., IACONELLI, M., MUSCILLO, M. 2010. Quantitative real-time PCR of enteric viruses in influent and effluent samples from wastewater treatment plants in Italy. *Annali dell'Istituto superiore di sanita*, 46, 266-73.

LA ROSA G, DELLA LIBERA S, IACONELLI M, CICCAGLIONE AR, BRUNI R, TAFFON S, EQUESTRE M, ALFONSI V, RIZZO C, TOSTI ME, CHIRONNA M. 2014. Surveillance of hepatitis A virus in urban sewages and comparison with cases notified in the course of an outbreak, Italy 2013. BMC Infectious Diseases,14, 1-1.

LACONELLI, M., VALDAZO-GONZÁLEZ, B., EQUESTRE, M., CICCAGLIONE, A.R., MARCANTONIO, C., DELLA LIBERA, S., LA ROSA, G. 2017. Molecular characterization of human adenoviruses in urban wastewaters using next generation and Sanger sequencing. *Water Research,* 121,240-247.

LEEN, A.M., ROONEY, C.M. 2005. Adenovirus as an emerging pathogen in immunocompromised patients. British journal of haematology,135-144.

LEEN, A. M., BOLLARD, C. M., MYERS, G. D. & ROONEY, C. M. 2006. Adenoviral infections in hematopoietic stem cell transplantation. *Biology of Blood and Marrow Transplantation,* 12**,** 243-251.

LESSLER, J., REICH, N. G., BROOKMEYER, R., PERL, T. M., NELSON, K. E. & CUMMINGS, D. A. 2009. Incubation periods of acute respiratory viral infections: a systematic review. *The Lancet Infectious Diseases,* 9**,** 291-300.

LEVENT, F., GREER, J. M., SNIDER, M. & DEMMLER-HARRISON, G. J. 2009. Performance of a new immunochromatographic assay for detection of adenoviruses in children. *Journal of Clinical Virology,* 44**,** 173-175.

LI D, ZHOU JN, LI H, HE CY, DAI QS, LI XL, HE JF, HE H, LI MB, JIANG LI, CHEN YY. 2019. An outbreak of epidemic keratoconjunctivitis caused by human adenovirus type 8 in primary school, southwest China. *BioMedical Centre Infectious Diseases*, 624.

LI, L., SHIMIZU, H., DOAN, L. T. P., TUNG, P. G., OKITSU, S., NISHIO, O., SUZUKI, E., SEO, J. K., KIM, K. S. & MÜLLER, W. E. 2004. Characterizations of adenovirus type 41 isolates from children with acute gastroenteritis in Japan, Vietnam, and Korea. *Journal of Clinical Microbiology,* 42**,** 4032-4039.

LI, Q.-G. & WADELL, G. 1988. The degree of genetic variability among adenovirus type 4 strains isolated from man and chimpanzee. *Archives of Virology,* 101**,** 65-77.

LI Q. G., WADELL, G. 1999. Genetic variability of hexon loops 1 and 2 between seven genome types of adenovirus serotype 7. Archives of virology, 144, 1739-1749.

LIN, J. & SINGH, A. 2015. Detection of human enteric viruses in Umgeni River, Durban, South Africa. *Journal of Water and Health,* 13**,** 1098-1112.

LION, T. 2014. Adenovirus infections in immunocompetent and immunocompromised patients. *Clinical Microbiology Reviews,* 27**,** 441-462.

LION, T. 2019. Adenovirus persistence, reactivation, and clinical management. *Federation of European Biomedical Sciences letters,* 593**,** 3571-3582.

LORD, A., BAILEY, A. S., KLAPPER, P. E., SNOWDEN, N. & KHOO, S. H. 2000. Impaired humoral responses to subgenus D adenovirusenovirus infections in HIV-positive patients. *Journal of Medical Virology,* 62**,** 405-409.

LOVE, D. C., RODRIGUEZ, R. A., GIBBONS, C. D., GRIFFITH, J. F., YU, Q., STEWART, J. R. & SOBSEY, M. D. 2013. Human viruses and viral indicators in marine water at two recreational beaches in Southern California, USA. *Journal of Water and Health,* 12**,** 136-150.

LOWTHER J, SCHULTZ AC, TC275 CE, TAG W. ISO TS/15216; an international standard method for the detection and quantification of norovirus in high risk foodstuffs. *In 5th International Conference Caliciviruses 2013.*

LU G, PENG X, LI R, LIU Y, WU Z, WANG X, ZHANG D, ZHAO J, SUN Y, ZHANG L, YANG P. 2020. An outbreak of acute respiratory infection at a training base in Beijing, China due to human adenovirus type B55. *BioMedical Centre Infectious Diseases,*1-0.

LUN, J.H., CROSBIE, N.D., WHITE, P.A. 2019. Genetic diversity and quantification of human mastadenoviruses in wastewater from Sydney and Melbourne, Australia. *Science of The Total Environment*, 675:305-312.

LYNCH, B. L., DEAN, J., BRADY, D. & DE GASCUN, C. 2018. Adenovirus Type 4 Respiratory Infections among Civilian Adults, Northeastern United States, 2011–2015.

LYNCH, J. P. & KAJON, A. E. Respiratory Viral Infections: Adenovirus: Epidemiology, Global Spread of Novel Serotypes, and Advances in Treatment and Prevention. Seminars in respiratory and critical care medicine, 2016. *Thieme Medical Publishers*, 586.

LYNCH, J. P., FISHBEIN, M. & ECHAVARRIA, M. Adenovirus. Seminars in respiratory and critical care medicine, 2011. © *Thieme Medical Publishers*, 494-511.

MADISCH, I., WÖLFEL, R., HARSTE, G., POMMER, H. & HEIM, A. 2006. Molecular identification of adenovirus sequences: a rapid scheme for early typing of human adenoviruses in diagnostic samples of immunocompetent and immunodeficient patients. *Journal of Medical Virology*, 78**,** 1210-1217.

MAGWALIVHA M, WOLFAARDT M, KIULIA NM, VAN ZYL WB, MWENDA JM, TAYLOR MB. 2010. High prevalence of species D human adenoviruses in fecal specimens from Urban Kenyan children with diarrhea. *Journal of medical virology*, 77-84.

MAHY, B. W. & VAN REGENMORTEL, M. H. 2010. *Desk Encyclopedia of Human and Medical Virology*, Academic press.

MANS J, NETSHIKWETA R, MAGWALIVHA M, VAN ZYL WB, TAYLOR MB. 2013. Diverse norovirus genotypes identified in sewage-polluted river water in *South Africa. Epidemiology & Infection,* 141, 03-13.

MARGULIES, M., EGHOLM, M., ALTMAN, W. E., ATTIYA, S., BADER, J. S., BEMBEN, L. A., BERKA, J., BRAVERMAN, M. S., CHEN, Y.-J. & CHEN, Z. 2005. Genome sequencing in microfabricated high-density picolitre reactors. *Nature,* 437, 376-380.

MARWAH A, SIDDIQUI N, MULLER M. 2020. Epidemic Keratoconjunctivitis Outbreak Investigation. UTJPH, 8, 1.

MATSUSHIMA, Y., SHIMIZU, H., KANO, A., NAKAJIMA, E., ISHIMARU, Y., DEY, S. K., WATANABE, Y., ADACHI, F., MITANI, K. & FUJIMOTO, T. 2013. Genome sequence of a novel virus of the species human adenovirus d associated with acute gastroenteritis. *Genome Announcement,* 1**,** e00068-12.

MCCONNELL, M. J. & IMPERIALE, M. J. 2004. Biology of adenovirus and its use as a vector for gene therapy. *Human Gene Therapy,* 15**,** 1022-1033.

METZGAR, D., OSUNA, M., KAJON, A. E., HAWKSWORTH, A. W., IRVINE, M. & RUSSELL, K. L. 2007. Abrupt emergence of diverse species B adenoviruses at US military recruit training centers. *The Journal of Infectious Diseases,* 196**,** 1465-1473.

MICKAN, L. & KOK, T.-W. 1994. Recognition of adenovirus types in faecal samples by southern hybridization in South Australia. *Epidemiology & Infection,* 112**,** 603-613.

MOORE, P., STEELE, A., LECATSAS, G. & ALEXANDER, J. 1998. Characterisation of gastroenteritis associated adenoviruses in South Africa. *South African Medical Journal,* 88**,** 1587-1592.

MINOR PD. Growth, assay and purification of picornaviruses. *Virology: A Practical Approach*. 1985:25-41.

MOYO, S. J., HANEVIK, K., BLOMBERG, B., KOMMEDAL, O., NORDBØ, S. A., MASELLE, S. & LANGELAND, N. 2014. Prevalence and molecular characterisation of human adenovirus in diarrhoeic children in Tanzania; a case control study. *BioMed Central Infectious Diseases,* 14**,** 666.

MUFSON, M. A. & BELSHE, R. B. 1976. A review of adenoviruses in the etiology of acute hemorrhagic cystitis. *The Journal of Urology,* 115**,** 191-194.

MUNOZ, F. M., FLOMENBERG, P., EDWARDS, M. S. & TORCHIA, M. M. Diagnosis, treatment, and prevention of adenovirus infection. *UpToDate (en línea)(consultado el 01/06/2015). Disponible en http://www. uptodate. com/contents/diagnosis-treatment-and-prevention-of-adenovirus-infection*.

MURPHY, H. 2017. Persistence of pathogens in sewage and other water types. *Global Water Pathogens Project. Part,* 4.

NANMOKU, K., ISHIKAWA, N., KUROSAWA, A., SHIMIZU, T., KIMURA, T., MIKI, A., SAKUMA, Y. & YAGISAWA, T. 2016. Clinical characteristics and outcomes of adenovirus infection of the urinary tract after renal transplantation. *Transplant Infectious Disease,* 18**,** 234-239.

NETSHIKWETA, R. 2019. Epidemiology of human adenovirus infections in hospitalised children with acute gastroenteritis in South Africa, 2009 to 2014. Masters Research, Department of Medical Virology, Faculty of Health Sciences. University of Pretoria.

NEWCOMB, W. W., BORING, J. W. & BROWN, J. 1984. Ion etching of human adenovirus 2: structure of the core. *Journal of Virology,* 51**,** 52-56.

O'MALLEY, R. P., MARIANO, T. M., SIEKIERKA, J., MATHEWS, M.B. 1986. A mechanism for the control of protein synthesis by adenovirus VA RNAI. Cell, 44, 391-400.

OYONG, K., KILLERBY, M., PAN, CY., HUYNH, T., GREEN, NM., WADFORD, DA., TERASHITA, D. 2018. Outbreak of epidemic keratoconjunctivitis caused by human

adenovirus type D53 in an eye care clinic—Los Angeles County, 2017. Morbidity and Mortality Weekly Report, 67, 1347.

OKADA, M., OGAWA, T., KUBONOYA, H., YOSHIZUMI, H., SHINOZAKI, K. 2007. Detection and sequence-based typing of human adenoviruses using sensitive universal primer sets for the hexon gene. Archives of virology, 152, 1-9.

OKOH, A. I., SIBANDA, T. & GUSHA, S. S. 2010. Inadequately treated wastewater as a source of human enteric viruses in the environment. *International Journal of Environmental Research and Public Health,* 7**,** 2620-2637.

OLIVE, M., EISENLOHR, L. C. & FLOMENBERG, P. 2001. Quantitative analysis of adenovirus-specific CD4+ T-cell responses from healthy adults. *Viral Immunology,* 14**,** 403-413.

ORENSTEIN, R. 2020. Gastroenteritis, Viral. *Encyclopedia of Gastroenterology***,** 652.

OSUOLALE, O. & OKOH, A. 2015. Incidence of human adenoviruses and Hepatitis A virus in the final effluent of selected wastewater treatment plants in Eastern Cape Province, South Africa. *Virology Journal,* 12**,** 98.

OUDE MUNNINK, B. B. & VAN DER HOEK, L. 2016. Viruses causing gastroenteritis: the known, the new and those beyond. *Viruses,* 8**,** 42.

PADUCH, D. A. 2007. Viral lower urinary tract infections. *Current Urology Reports,* 8**,** 324-335.

PANG, X., QIU, Y., GAO, T., ZURAWELL, R., NEUMANN, N. F., CRAIK, S. & LEE, B. E. 2019. Prevalence, levels and seasonal variations of human enteric viruses in six major rivers in Alberta, Canada. *Water Research,* 153**,** 349-356.

PERCIVAL, S. L. & WYN-JONES, P. 2014. Methods for the detection of waterborne viruses. *Microbiology of Waterborne Diseases.* Elsevier.

PEREIRA, H. 1956. Typing of adenoidal-pharyngeal-conjunctival (APC) viruses by complement-fixation. *Journal of Pathology and Bacteriology*, 72**,** 105-109.

PÉREZ-BERNÁ, A. J., MARION, S., CHICHÓN, F. J., FERNÁNDEZ, J. J., WINKLER, D. C., CARRASCOSA, J. L., STEVEN, A. C., ŠIBER, A. & SAN MARTÍN, C. 2015. Distribution of DNA-condensing protein complexes in the adenovirus core. *Nucleic acids Research,* 43**,** 4274-4283.

PIHOS, A. M. 2013. Epidemic keratoconjunctivitis: a review of current concepts in management. *Journal of Optometry,* 6**,** 69-74.

PINA, S., PUIG, M., LUCENA, F., JOFRE, J. & GIRONES, R. 1998. Viral pollution in the environment and in shellfish: human adenovirus detection by PCR as an index of human viruses. *Applied and Environmental Microbiology,* 64, 3376-3382.

PINTÓ RM, COSTAFREDA MI, BOSCH A. Risk assessment in shellfish-borne outbreaks of hepatitis A. 2009. Applied and Environmental Microbiology. 75(23):7350-7355.

PLATTS-MILLS, J. A., BABJI, S., BODHIDATTA, L., GRATZ, J., HAQUE, R., HAVT, A., MCCORMICK, B. J., MCGRATH, M., OLORTEGUI, M. P., SAMIE, A., SHAKOOR, S. 2015. Pathogen-specific burdens of community diarrhoea in developing countries: a multisite birth cohort study (MAL-ED). The Lancet Global Health, 3, 564-575.

PORTES, S.A., VOLOTÃO, E.D., ROCHA, M.S., REBELO, M.C., XAVIER, M.D., ASSIS, R.M., ROSE, T.L., MIAGOSTOVICH, M.P., LEITE, J.P., CARVALHO-COSTA, F.A. 2016. A non-enteric adenovirus A12 gastroenteritis outbreak in Rio de Janeiro, Brazil. Memórias do Instituto Oswaldo Cruz, 111,403-406.

PREVOST, B., GOULET, M., LUCAS, F., JOYEUX, M., MOULIN, L. & WURTZER, S. 2016. Viral persistence in surface and drinking water: Suitability of PCR pre-treatment with intercalating dyes. *Water Research,* 91**,** 68-76.

PRICE, R. H. M., GRAHAM, C. & RAMALINGAM, S. 2019. Association between viral seasonality and meteorological factors. *Scientific Reports,* 9**,** 1-11.

QIU, Y., LEE, B.E., NEUMANN, N., ASHBOLT, N., CRAIK, S., MAAL-BARED, R., PANG, X.L. 2015. Assessment of human virus removal during municipal wastewater treatment in Edmonton, Canada. Journal of Applied Microbiology, 119, 1729-1739.

RAMES, E., ROIKO, A., STRATTON, H. & MACDONALD, J. 2016. Technical aspects of using human adenovirus as a viral water quality indicator. *Water Research,* 96**,** 308-326.

RAMES, EK., MACDONALD, J. 2019. Rapid assessment of viral water quality using a novel recombinase polymerase amplification test for human adenovirus. Applied microbiology and biotechnology, 103, 8115-8125.

REIS, T. A. V., ASSIS, A. S. F., VALLE, D. A. D., BARLETTA, V. H., CARVALHO, I. P. D., ROSE, T. L., PORTES, S. A. R. & LEITE, J. P. G. 2016. The role of human adenoviruses type 41 in acute diarrheal disease in Minas Gerais after rotavirus vaccination. *Brazilian Journal of Microbiology,* 47**,** 243-250.

RIGOTTO C, VICTORIA M, MORESCO V, KOLESNIKOVAS CK, CORRÊA AA, SOUZA DS, MIAGOSTOVICH MP, SIMÕES CM, BARARDI CR. 2010. Assessment of adenovirus, hepatitis A virus and rotavirus presence in environmental samples in Florianopolis, South Brazil. Journal of applied microbiology, 109, 1979-1987.

ROBERTS, R. J., O'NEILL, K. E. & YEN, C. T. 1984. DNA sequences from the adenovirus 2 genome. *Journal of Biological Chemistry,* 259**,** 13968-13975.

ROBINSON, C. & ECHAVARRIA, M. 2011. Adenoviruses. *Manual of Clinical Microbiology, 10th Edition.* American Society of Microbiology.

ROBINSON, C. M., SINGH, G., LEE, J. Y., DEHGHAN, S., RAJAIYA, J., LIU, E. B., YOUSUF, M. A., BETENSKY, R. A., JONES, M. S. & DYER, D. W. 2013. Molecular evolution of human adenoviruses. *Scientific Reports,* 3**,** 1812.

RODRÍGUEZ, E., IP, W. H., KOLBE, V., HARTMANN, K., PILNITZ-STOLZE, G., TEKIN, N., GÓMEZ-MEDINA, S., MUÑOZ-FONTELA, C., KRASEMANN, S. & DOBNER, T. 2016. Humanized Mice Reproduce Acute and Persistent Infection of Human Adenovirus. *The Journal of Infectious Diseases***,** 499.

ROSEN, L. 1960. Hemagglutination-lnhibition Technique for Typing Adenoviruses. *American Journal of Hygiene,* 71**,** 120-28.

ROSSOUW, J. 2004. *Molecular Epidemiology and Characterization of Circulating Adenovirus Strains in Southern Africa.* Medunsa.

ROWE, W. P., HUEBNER, R. J., GILMORE, L. K., PARROTT, R. H. & WARD, T. G. 1953. Isolation of a cytopathogenic agent from human adenoids undergoing spontaneous degeneration in tissue culture. *Proceedings of the Society for Experimental Biology and Medicine,* 84**,** 570-573.

RUHANYA, V. 2013. Efficiency of glass wool adsorption-elution technique for the recovery of enteric viruses from water. Masters Research, Department of Medical Virology, Faculty of Health Sciences. University of Pretoria.

RUSINOL, M., GIRONES, R. 2017. Summary of excreted and waterborne viruses. Global Water Pathogen Project 2017.

RUSSELL, K. L., HAWKSWORTH, A. W., RYAN, M. A., STRICKLER, J., IRVINE, M., HANSEN, C. J., GRAY, G. C. & GAYDOS, J. C. 2006. Vaccine-preventable adenoviral respiratory illness in US military recruits, 1999–2004. *Vaccine,* 24**,** 2835-2842.

RUSSELL, W. 2009. Adenoviruses: update on structure and function. *Journal of General Virology,* 90**,** 1-20.

SAHA, B., WONG, C. M., PARKS, R. J. 2014. The adenovirus genome contributes to the structural stability of the virion. Viruses, 6, 3563-3583.

SAITOU N. AND NEI M. (1987). The neighbor-joining method: A new method for reconstructing phylogenetic trees. Molecular Biology and Evolution 4:406-425.

SAN MARTÍN, C. 2012. Latest insights on adenovirus structure and assembly. *Viruses,* 4**,** 847-877.

SANAEI DASHTI A, GHAHREMANI P, HASHEMPOOR T, KARIMI A. 2016. Molecular epidemiology of enteric adenovirus gastroenteritis in under-five-year-old children in Iran. Gastroenterology Research and Practice.

SARRETTE, B., DANGLOT, C. & VILAGINES, R. 1977. A new and simple method for recuperation of enteroviruses from water. *Water Research,* 11**,** 355-358.

SAUERBREI, A., SEHR, K., BRANDSTÄDT, A., HEIM, A., REIMER, K. & WUTZLER, P. 2004a. Sensitivity of human adenoviruses to different groups of chemical biocides. *Journal of Hospital Infection,* 57**,** 59-66.

SAUERBREI, A., SEHR, K., EICHHORN, U., REIMER, K. & WUTZLER, P. 2004b. Inactivation of human adenovirus genome by different groups of disinfectants. *Journal of Hospital Infection,* 57**,** 67-72.

SCOTT, M. K., CHOMMANARD, C., LU, X., APPELGATE, D., GRENZ, L., SCHNEIDER, E., GERBER, S. I., ERDMAN, D. D. & THOMAS, A. 2016. Human adenovirus associated with severe respiratory infection, Oregon, USA, 2013–2014. *Emerging Infectious Diseases,* 22**,** 1044.

SETH, P. Adenoviruses: basic biology to gene therapy. 1999. Landes Bioscience.

SHAYAKHMETOV, D. M., LI, Z.-Y., TERNOVOI, V., GAGGAR, A., GHARWAN, H. & LIEBER, A. 2003. The interaction between the fiber knob domain and the cellular attachment receptor determines the intracellular trafficking route of adenoviruses. *Journal of Virology,* 77**,** 3712-3723.

SIBANDA, T. & OKOH, A. I. 2012. Assessment of the incidence of enteric adenovirus species and serotypes in surface waters in the eastern cape province of South Africa: Tyume River as a case study. *The Scientific World Journal*.

SILVA, H. D., FONGARO, G., GARCÍAZAPATA, M. T., MELO, A. T., SILVEIRA-LACERDA, E. P., DE FARIA, K. M. & ANUNCIAÇÃO, C. E. 2015. High species C human adenovirus genome copy numbers in the treated water supply of a neotropical area of the central-west region of Brazil. *Food and Environmental Virology,* 7**,** 286-294.

SINCLAIR, R., JONES, E. & GERBA, C. P. 2009. Viruses in recreational water-borne disease outbreaks: A review. *Journal of Applied Microbiology,* 107**,** 1769-1780.

SINGH, G., ROBINSON, C. M., DEHGHAN, S., JONES, M. S., DYER, D. W., SETO, D. & CHODOSH, J. 2013. Homologous recombination in E3 genes of human adenovirus species D. *Journal of Virology,* 87, 12481-12488.

STASIAK, A. C., STEHLE, T. 2020. Human adenovirus binding to host cell receptors: a structural view. Medical microbiology and immunology. 325-333.

SWENSON, P. D., LOWENS, M. S., CELUM, C. L. & HIERHOLZER, J. C. 1995. Adenovirus types 2, 8, and 37 associated with genital infections in patients attending a sexually transmitted disease clinic. *Journal of Clinical Microbiology,* 33**,** 2728-2731.

TABAIN, I., LJUBIN-STERNAK, S., CEPIN-BOGOVIC, J., MARKOVINOVIC, L., KNEZOVIC, I. & MLINARIC-GALINOVIC, G. 2012. Adenovirus respiratory infections in hospitalized children: clinical findings in relation to species and serotypes. *The Pediatric Infectious Disease Journal,* 31**,** 680-684.

TAO, C.-W., HSU, B.-M., KAO, P.-M., HUANG, W.-C., HSU, T.-K., HO, Y.-N., LU, Y.-J. & FAN, C.-W. 2016. Seasonal difference of human adenoviruses in a subtropical river basin based on 1-year monthly survey. *Environmental Science and Pollution Research,* 23**,** 2928-2936.

TENG, C.-H. 1960. Adenovirus pneumonia epidemic among Peking infants and preschool children in 1958. *Chinese Medical Journal,* 80**,** 331-9.

THOMPSON, S. S., JACKSON, J. L., SUVA-CASTILLO, M., YANKO, W. A., EL JACK, Z., KUO, J., CHEN, C. L., WILLIAMS, F. P. & SCHNURR, D. P. 2003. Detection of infectious human adenoviruses in tertiary-treated and ultraviolet-disinfected wastewater. *Water Environment Research,* 75**,** 163-170.

THONGPRACHUM, A., FUJIMOTO, T., TAKANASHI, S., SAITO, H., OKITSU, S., SHIMIZU, H., KHAMRIN, P., MANEEKARN, N., HAYAKAWA, S., USHIJIMA, H. 2018. Detection of nineteen enteric viruses in raw sewage in Japan. Infection, Genetics and Evolution, 63:17-123

THURSTON-ENRIQUEZ, J. A., HAAS, C. N., JACANGELO, J. & GERBA, C. P. 2005. Inactivation of enteric adenovirus and feline calicivirus by chlorine dioxide. *Applied and Environmental Microbiology,* 71**,** 3100-3105.

TREI, J. S., JOHNS, N. M., GARNER, J. L., NOEL, L. B., ORTMAN, B. V., ENSZ, K. L., JOHNS, M. C., BUNNING, M. L. & GAYDOS, J. C. 2010. Spread of adenovirus to geographically dispersed military installations, May–October 2007. *Emerging Infectious Diseases,* 16**,** 769.

TROEGER, C., FOROUZANFAR, M., RAO, P. C., KHALIL, I., BROWN, A., REINER JR, R. C., FULLMAN, N., THOMPSON, R. L., ABAJOBIR, A. & AHMED, M. 2017. Estimates of global, regional, and national morbidity, mortality, and aetiologies of diarrhoeal diseases: a systematic analysis for the Global Burden of Disease Study 2015. *The Lancet Infectious Diseases,* 17**,** 909-948.

TSUKAHARA-KAWAMURA, T., HANAOKA, N., KONAGAYA, M., UCHIO, E., FUJIMOTO, T. 2020. Characteristic of slow growth in cell culture of adenovirus type 54 causing nationwide outbreak epidemic keratoconjunctivitis in Japan. *Japanese Journal of Ophthalmology,* 3,1-9.

UHNOO, I., WADELL, G., SVENSSON, L. & JOHANSSON, M. 1984. Importance of enteric adenoviruses 40 and 41 in acute gastroenteritis in infants and young children. *Journal of Clinical Microbiology,* 20**,** 365-372.

VAN DER AVOORT, H. G., A. G. WERMENBOL, T. P. ZOMERDIJK, J. A. KLEIJNE, J. A. VAN ASTEN, P. JENSMA, A. D. OSTERHAUS, A. H. KIDD, AND J. C. DE JONG. 1989. Characterization of fastidious adenovirus types 40 and 41 by DNA restriction enzyme analysis and by neutralizing monoclonal antibodies. *Virus Res.*12:139-157.

VAN DER VEEN, J., ABARBANEL, M. & OEI, K. G. 1968. Vaccination with live type 4 adenovirus: evaluation of antibody response and protective efficacy. *Epidemiology & Infection,* 66**,** 499-511.

VAN HEERDEN, J., EHLERS, M., HEIM, A. & GRABOW, W. 2005. Prevalence, quantification and typing of adenoviruses detected in river and treated drinking water in South Africa. *Journal of Applied Microbiology,* 99, 234-242.

VERGATAT, U. D. R. T. 2007. Prevalence of rotavirus, adenovirus and enteric parasites among pediatric patients attending Saint Camille Medical Centre in Ouagadougou. *Pakistan Journal of Biological Sciences,* 10**,** 4266-4270.

VERMA, H., CHITAMBAR, S. D. & VARANASI, G. 2009. Identification and characterization of enteric adenoviruses in infants and children hospitalized for acute gastroenteritis. *Journal of Medical Virology,* 81**,** 60-64.

VETTER, M. R., STAGGEMEIER, R., VECCHIA, A. D., HENZEL, A., RIGOTTO, C. & SPILKI, F. R. 2015. Seasonal variation on the presence of adenoviruses in stools from non-diarrheic patients. *Brazilian Journal of Microbiology,* 46**,** 749-752.

VILAGINÈS, P., SARRETTE, B., HUSSON, G. & VILAGINES, R. 1993. Glass wool for virus concentration at ambient water pH level. *Water Science and Technology,* 27**,** 299-306.

VOS, H. J. & KNOX, C. M. 2018. The recovery and molecular identification of HAdV-D17 in raw sewage and mussel samples collected in the Eastern Cape province of South Africa. *Southern African Journal of Infectious Diseases,* 33**,** 4-7.

WALKER, C. L. F., ARYEE, M. J., BOSCHI-PINTO, C. & BLACK, R. E. 2012. Estimating diarrhea mortality among young children in low and middle income countries. *PloS One,* 7, e29151.

WALLIS, C. & MELNICK, J. L. 1967. Concentration of viruses from sewage by adsorption on millipore membranes. *Bulletin of the World Health Organization,* 36**,** 219.

WEAVER, E. A., HILLESTAD, M. L., KHARE, R., PALMER, D., NG, P. & BARRY, M. A. 2011. Characterization of species C human adenovirus serotype 6 (Ad6). *Virology,* 412**,** 19-27.

WEITZMAN, M. D., ORNELLES, D. A. 2005. Inactivating intracellular antiviral responses during adenovirus infection. Oncogene, 24, 7686-7696

WESLEY, A., PATHER, M. & TAIT, D. 1993. Nosocomial adenovirus infection in a paediatric respiratory unit. *Journal of Hospital Infection,* 25**,** 183-190.

WILHELMI, I., ROMAN, E. & SANCHEZ-FAUQUIER, A. 2003. Viruses causing gastroenteritis. *Clinical Microbiology and Infection,* 9, 247-262.

WOLD, W. & HORWITZ, M. 2007. Fields Virology, In DM Knipe and PM Howley. Lippincott, Williams, & Wilkins, Philadelphia. PA.

WYN-JONES, A. P., CARDUCCI, A., COOK, N., D'AGOSTINO, M., DIVIZIA, M., FLEISCHER, J., GANTZER, C., GAWLER, A., GIRONES, R. & HÖLLER, C. 2011. Surveillance of adenoviruses and noroviruses in European recreational waters. *Water research,* 45**,** 1025-1038.

WYN-JONES, A. & SELLWOOD, J. 2001. Enteric viruses in the aquatic environment. *Journal of Applied Microbiology,* 91**,** 945-962.

ZAMPOLI, M. & MUKUDDEM-SABLAY, Z. 2017. Adenovirus-associated pneumonia in South African children: Presentation, clinical course and outcome. *SAMJ: South African Medical Journal,* 107**,** 123-126.

ZHANG, S., CHEN, T. H., WANG, J., DONG, C., PAN, J., MOE, C., CHEN, W., YANG, L., WANG, X. & TANG, H. 2011. Symptomatic and asymptomatic infections of rotavirus, norovirus, and adenovirus among hospitalized children in Xi'an, China. *Journal of Medical Virology,* 83, 1476-1484.

ZHANG, Q., JING, S., CHENG, Z., YU, Z., DEHGHAN, S., SHAMSADDINI, A., YAN, Y., LI, M., SETO, D. 2017. Comparative genomic analysis of two emergent human adenovirus type 14 respiratory pathogen isolates in China reveals similar yet divergent genomes. *Emerging microbes & infections,* 6, 1-2.

ZUBIETA, C., SCHOEHN, G., CHROBOCZEK, J., CUSACK, S. 2005. The structure of the human adenovirus 2 penton. Molecular cell, 17,121-135.

# APPENDIX A

## A1: Quantification Table

| Sample name | Month | WWTP (1 or 2) | Sample type (Raw/ Eff) | MV ct value | [MV] per reaction (5 µL) | Extraction efficiency (%) | HAdV ct value | [HAdV] per reaction (5µL) | Adjusted [HAdV] per reaction (5µL) | Number of copies per 1L |
|---|---|---|---|---|---|---|---|---|---|---|
| 17 | Aug '18 | 1 | R | 35.491 | 0.052 | 10.4 | 32.631 | $6.28x10^4$ | $6.03x10^7$ | $1.20x10^8$ |
| 18 | Aug '18 | 1 | E | 33.616 | 0.184 | 36.7 | 32.749 | $5.83x10^4$ | $1.58x10^5$ | $3.17x10^7$ |
| 19 | Aug '18 | 1 | R | 34.660 | 0.091 | 18.2 | 34.388 | $2.10x10^4$ | $1.15x10^5$ | $2.30x10^7$ |
| 20 | Aug '18 | 1 | E | 35.848 | 0.041 | 8.2 | 35.182 | $1.28x10^4$ | $1.56x10^5$ | $3.12x10^7$ |
| 21 | Aug '18 | 1 | R | 35.723 | 0.045 | 8.9 | 28.687 | $7.28x10^5$ | $8.17x10^6$ | $1.63x10^9$ |
| 22 | Aug '18 | 1 | E | 33.238 | 0.237 | 47.3 | 35.383 | $1.13x10^4$ | $2.38x10^4$ | $4.77x10^6$ |
| 23 | Aug '18 | 2 | R | 33.955 | 0.146 | 29.1 | 32.125 | $8.60x10^4$ | $2.95x10^5$ | $5.91x10^7$ |
| 24 | Aug '18 | 2 | E | 36.436 | 0.028 | 5.5 | 38.028 | $2.19x10^3$ | $3.98x10^4$ | $7.96x10^6$ |
| 25 | Aug '18 | 2 | R | 34.75 | 0.085 | 16.9 | 32.636 | $6.26x10^4$ | $3.70x10^5$ | $7.40x10^7$ |
| 26 | Aug '18 | 2 | E | 32.697 | 0.341 | 68.0 | 37.757 | $2.60x10^3$ | $3.82x10^3$ | $7.64x10^5$ |
| 27 | Aug '18 | 2 | R | 36.406 | 0.028 | 5.6 | 34.654 | $1.78x10^4$ | $3.17x10^5$ | $6.35x10^7$ |
| 28 | Aug '18 | 2 | E | 34.285 | 0.117 | 23.3 | 37.291 | $3.47x10^3$ | $1.48x10^4$ | $2.97x10^6$ |
| 29 | Sep'18 | 1 | R | 34.047 | 0.137 | 27.3 | 31.646 | $1.15x10^5$ | $4.21x10^5$ | $8.42x10^7$ |
| 30 | Sep'18 | 1 | E | 32.230 | 0.466 | 93.3 | 32.712 | $5.97x10^4$ | $6.39x10^4$ | $1.27x10^7$ |
| 31 | Sep'18 | 1 | R | 30.815 | 1.208 | 100 | 23.163 | $2.25x10^7$ | $2.25x10^7$ | $4.50x10^9$ |
| 32 | Sep'18 | 1 | E | 31.949 | 0.563 | 100 | 33.213 | $4.37x10^4$ | $4.37x10^4$ | $8.74x10^6$ |

| | | | | | | | | | | |
|---|---|---|---|---|---|---|---|---|---|---|
| 33 | Sep'18 | 2 | R | 34.057 | 0.137 | 27.3 | 26.823 | $2.31x10^{6}$ | $8.46x10^{6}$ | $1.69x10^{12}$ |
| 34 | Sep'18 | 2 | E | 33.688 | 0.175 | 34.9 | 37.110 | $3.89x10^{3}$ | $1.11x10^{4}$ | $2.22x10^{6}$ |
| 35 | Sep'18 | 2 | R | 35.7 | 0.043 | 8.5 | 32.487 | $6.87x10^{4}$ | $8.08x10^{6}$ | $1.61x10^{7}$ |
| 36 | Sep'18 | 2 | E | 34.208 | 0.123 | 24.5 | 34.817 | $1.61x10^{4}$ | $6.57x10^{4}$ | $1.31x10^{7}$ |
| 37 | Oct '18 | 1 | R | - | - | - | 27.025 | $1.08x10^{6}$ | - | - |
| 38 | Oct '18 | 1 | E | 33.20 | 0.242 | 48.3 | 28.888 | $3.03x10^{5}$ | $6.27x10^{5}$ | $1.25x10^{8}$ |
| 39 | Oct '18 | 1 | R | 33.90 | 0.152 | 30.3 | 27.600 | $7.31x10^{5}$ | $2.41x10^{6}$ | $4.82x10^{8}$ |
| 40 | Oct '18 | 1 | E | - | - | - | 32.478 | $2.62x10^{4}$ | - | - |
| 41 | Oct '18 | 2 | R | - | - | - | 28.552 | $3.82x10^{5}$ | - | - |
| 42 | Oct '18 | 2 | E | - | - | - | 34.750 | $5.57x10^{3}$ | - | - |
| 43 | Oct '18 | 2 | R | - | - | - | 32.338 | $2.88x10^{4}$ | - | - |
| 44 | Oct '18 | 2 | E | 35.26 | 0.060 | 11.9 | 37.830 | $6.81x10^{2}$ | $5.72x10^{3}$ | $1.14x10^{6}$ |
| 45 | Nov '18 | 1 | R | - | - | - | 25.973 | $2.21x10^{6}$ | - | - |
| 46 | Nov '18 | 1 | E | - | - | - | 31.144 | $6.52x10^{4}$ | - | - |
| 47 | Nov '18 | 1 | R | 33.46 | 0.203 | 40.5 | 27.912 | $5.91x10^{5}$ | $2.11x10^{6}$ | $4.23x10^{8}$ |
| 48 | Nov '18 | 1 | E | 32.382 | 0.421 | 84.0 | 31.703 | $4.45x10^{4}$ | $1.09x10^{5}$ | $2.19x10^{7}$ |
| 49 | Nov '18 | 2 | R | - | - | - | 28.710 | $3.43x10^{5}$ | - | - |
| 50 | Nov '18 | 2 | E | - | - | - | 33.507 | $1.30x10^{4}$ | - | - |
| 51 | Nov '18 | 2 | R | - | - | - | 26.854 | $1.21x10^{6}$ | - | - |

| | | | | | | | | | | |
|---|---|---|---|---|---|---|---|---|---|---|
| 52 | Nov ‘18 | 2 | E | 33.704 | 0.173 | 34.5 | 35.070 | 4.48x103 | $1.29x10^{4}$ | $2.59x10^{6}$ |
| 53 | Dec ‘18 | 1 | R | - | - | - | 27.013 | $1.09x10^{6}$ | - | - |
| 54 | Dec ‘18 | 1 | E | 33.444 | 0.206 | 41.1 | 31.556 | $4.92x10^{4}$ | $1.19x10^{5}$ | $2.39x10^{7}$ |
| 55 | Dec ‘18 | 1 | R | 36.69 | 4.5 | 100 | 25.784 | $2.52x10^{6}$ | $2.50x10^{6}$ | $5.04x10^{8}$ |
| 56 | Dec ‘18 | 1 | E | - | - | - | 30.915 | $7.62x10^{4}$ | - | - |
| 57 | Dec ‘18 | 2 | R | - | - | - | 29.055 | $2.71x10^{5}$ | - | - |
| 58 | Dec ‘18 | 2 | E | 33.061 | 0.267 | 53.2 | 35.719 | $2.87x10^{3}$ | $5.39x10^{3}$ | $1.07x10^{6}$ |
| 59 | Dec ‘18 | 2 | R | 35.59 | 0.049 | 9.7 | 36.064 | $2.27x10^{3}$ | $2.34x10^{4}$ | $4.68x10^{6}$ |
| 60 | Dec ‘18 | 2 | E | - | - | - | 35.512 | $3.31x10^{3}$ | - | - |
| 61 | Jan ‘19 | 1 | R | 36.74 | 0.022 | 4.4 | 30.445 | $1.05x10^{5}$ | $2.38x10^{6}$ | $4.77x10^{8}$ |
| 62 | Jan ‘19 | 1 | E | - | - | - | 32.394 | $2.77x10^{4}$ | - | - |
| 63 | Jan ‘19 | 1 | R | 35.97 | 0.038 | 7.5 | 29.805 | $1.62x10^{5}$ | $2.16x10^{6}$ | $4.32x10^{8}$ |
| 64 | Jan ‘19 | 1 | E | - | - | - | 29.886 | $1.53x10^{5}$ | - | - |
| 65 | Jan ‘19 | 2 | R | - | - | - | 41.298 | $6.40x10^{1}$ | - | - |
| 66 | Jan ‘19 | 2 | E | - | - | - | 35.767 | $2.78x10^{3}$ | - | - |
| 67 | Jan ‘19 | 2 | R | - | - | - | 27.904 | $5.94x10^{5}$ | - | - |
| 68 | Jan ‘19 | 2 | E | - | - | - | 34.492 | $6.64x10^{3}$ | - | - |
| 69 | Feb ‘19 | 1 | R | 36.246 | 0.031 | 6.1 | 30.375 | $1.10x10^{5}$ | $1.80x10^{6}$ | $3.60x10^{8}$ |
| 70 | Feb ‘19 | 1 | E | 33.168 | 0.248 | 49.5 | 31.910 | $3.86x10^{4}$ | $7.79x10^{4}$ | $1.55x10^{7}$ |

| | | | | | | | | | | |
|---|---|---|---|---|---|---|---|---|---|---|
| 71 | Feb ‘19 | 1 | R | 33.313 | 0.225 | 44.9 | 29.909 | $1.51x10^{5}$ | $3.36x10^{5}$ | $6.72x10^{7}$ |
| 72 | Feb ‘19 | 1 | E | 32.311 | 0.442 | 88.2 | 32.273 | $3.01x10^{4}$ | $3.41x10^{4}$ | $6.82x10^{6}$ |
| 73 | Feb ‘19 | 2 | R | 34.977 | 0.074 | 14.7 | 32.939 | $1.91x10^{4}$ | $1.29x10^{5}$ | $2.59x10^{7}$ |
| 74 | Feb ‘19 | 2 | E | 35.514 | 0.051 | 10.1 | 34.405 | $7.05x10^{3}$ | $6.98x10^{4}$ | $1.39x10^{7}$ |
| 75 | Feb ‘19 | 2 | R | 31.58 | 0.722 | 100 | 32.712 | $2.23x10^{4}$ | $2.23x10^{4}$ | $4.46x10^{6}$ |
| 76 | Feb ‘19 | 2 | E | 34.285 | 0.117 | 23.3 | 44.735 | 6.14 | $2.63x10^{1}$ | $5.27x10^{3}$ |
| 77 | Mar ‘19 | 1 | R | 33.804 | 0.421 | 84.1 | 25.170 | $3.83x10^{6}$ | $4.55x10^{6}$ | $9.10x10^{8}$ |
| 78 | Mar ‘19 | 1 | E | 32.707 | 0.173 | 34.5 | 33.934 | $9.72x10^{3}$ | $2.81x10^{4}$ | $5.63x10^{6}$ |
| 79 | Mar ‘19 | 1 | R | 34.676 | 0.206 | 41.1 | 34.151 | $8.38x10^{3}$ | $2.03x10^{4}$ | $4.07x10^{6}$ |
| 80 | Mar ‘19 | 1 | E | 34.415 | 0.267 | 53.2 | 33.447 | $1.35x10^{4}$ | $2.53x10^{4}$ | $5.07x10^{6}$ |
| 81 | Mar ‘19 | 2 | R | 33.578 | 0.162 | 32.3 | 33.015 | $1.81x10^{4}$ | $5.60x10^{4}$ | $1.12x10^{7}$ |
| 82 | Mar ‘19 | 2 | E | 33.775 | 0.339 | 67.1 | 29.087 | $2.65x10^{5}$ | $3.94x10^{5}$ | $7.89x10^{7}$ |
| 83 | Mar ‘19 | 2 | R | 34.381 | 0090 | 17.9 | 35.599 | $3.12x10^{4}$ | $1.74x10^{5}$ | $3.48x10^{7}$ |
| 84 | Mar ‘19 | 2 | E | 34.463 | 0.107 | 21.3 | 36.587 | $1.59x10^{3}$ | $7.46x10^{3}$ | $1.49x10^{6}$ |
| 85 | Apr ‘19 | 1 | R | 35.65 | 0.188 | 37.5 | 28.215 | $4.80x10^{5}$ | $1.28x10^{6}$ | $2.56x10^{8}$ |
| 86 | Apr ‘19 | 1 | E | 35.07 | 0.165 | 32.9 | 29.665 | $1.78x10^{5}$ | $5.41x10^{5}$ | $1.08x10^{8}$ |
| 87 | Apr ‘19 | 1 | R | 34.34 | 0.110 | 21.9 | 35.054 | $4.52x10^{3}$ | $2.06x10^{4}$ | $4.12x10^{6}$ |
| 88 | Apr ‘19 | 1 | E | 34.87 | 0.104 | 20.7 | 33.961 | $9.54x10^{3}$ | $4.60x10^{4}$ | $9.21x10^{6}$ |
| 89 | Apr ‘19 | 2 | R | 34.10 | 0.031 | 6.2 | 32.667 | $2.30x10^{4}$ | $3.70x10^{5}$ | $7.41x10^{7}$ |

| | | | | | | | | | | |
|---|---|---|---|---|---|---|---|---|---|---|
| 90 | Apr ‘19 | 2 | E | 34.73 | 0.079 | 15.7 | 32.221 | $3.12x10^{4}$ | $1.98x10^{5}$ | $3.97x10^{7}$ |
| 91 | Apr ‘19 | 2 | R | 34.09 | 0.133 | 26.5 | 37.077 | $1.13x10^{3}$ | $4.26x10^{3}$ | $8.52x10^{5}$ |
| 92 | May ‘19 | 2 | E | 33.64 | 0.180 | 35.9 | 35.476 | $3.39x10^{3}$ | $9.44x10^{3}$ | $1.88x10^{6}$ |
| 93 | May ‘19 | 1 | R | 34.90 | 0.077 | 15.3 | 31.867 | $3.98x10^{4}$ | $2.60x10^{5}$ | $5.20x10^{7}$ |
| 94 | May ‘19 | 1 | E | 35.47 | 0.053 | 10.5 | 29.319 | $2.26x10^{5}$ | $2.15x10^{6}$ | $4.30x10^{8}$ |
| 95 | May ‘19 | 1 | R | 34.49 | 0.102 | 20.3 | 30.578 | $9.59x10^{4}$ | $4.72x10^{5}$ | $9.44x10^{7}$ |
| 96 | May ‘19 | 1 | E | 35.65 | 0.047 | 9.3 | 32.765 | $2.15x10^{4}$ | $2.31x10^{5}$ | $4.62x10^{7}$ |
| 97 | May ‘19 | 1 | R | 34.48 | 0.103 | 20.5 | 31.534 | $4.99x10^{4}$ | $2.43x10^{5}$ | $4.86x10^{7}$ |
| 98 | May ‘19 | 1 | E | 33.79 | 0.163 | 32.5 | 33.353 | $1.44x10^{4}$ | $4.43x10^{4}$ | $8.86x10^{6}$ |
| 99 | May ‘19 | 2 | R | 35.20 | 0.053 | 10.5 | 33.451 | $1.35x10^{4}$ | $1.28x10^{5}$ | $2.57x10^{7}$ |
| 100 | May ‘19 | 2 | E | 35.30 | 0.059 | 11.7 | 31.078 | $6.81x10^{4}$ | $5.82x10^{5}$ | $1.16x10^{8}$ |
| 101 | May ‘19 | 2 | R | 34.99 | 0.073 | 14.5 | 33.495 | $1.31x10^{4}$ | $9.03x10^{4}$ | $1.80x10^{7}$ |
| 102 | May ‘19 | 2 | E | 33.59 | 0.187 | 37.3 | 36.371 | $1.84x10^{3}$ | $4.93x10^{3}$ | $9.86x10^{5}$ |
| 103 | May ‘19 | 2 | R | 33.32 | 0.223 | 44.5 | 31.451 | $5.28x10^{4}$ | $1.18x10^{5}$ | $2.37x10^{7}$ |
| 104 | May ‘19 | 2 | E | 34.30 | 0.116 | 23.1 | 34.859 | $5.17x10^{3}$ | $2.23x10^{4}$ | $4.47x10^{6}$ |
| 105 | Jun ‘19 | 1 | R | 36.41 | 0.034 | 6.7 | 35.572 | $3.18x10^{3}$ | $4.74x10^{4}$ | $9.49x10^{6}$ |
| 106 | Jun ‘19 | 1 | E | - | - | - | 41.872 | $4.32x10^{1}$ | - | - |
| 107 | Jun ‘19 | 1 | R | 37.58 | 0.013 | 2.5 | 40.206 | $1.34x10^{2}$ | $5.36x10^{3}$ | $1.07x10^{6}$ |
| 108 | Jun ‘19 | 1 | E | 36.68 | 0.023 | 4.5 | 42.948 | $2.07x10^{1}$ | $4.60x10^{2}$ | $9.20x10^{4}$ |

| | | | | | | | | | | |
|---|---|---|---|---|---|---|---|---|---|---|
| 109 | Jun ‘19 | 2 | R | 33.88 | 0.153 | 30.5 | 34.091 | $8.73x10^{3}$ | $2.86x10^{4}$ | $5.72x10^{6}$ |
| 110 | Jun ‘19 | 2 | E | 34.29 | 0.116 | 23.1 | 38.905 | $3.27x10^{2}$ | $1.41x10^{3}$ | $2.83x10^{5}$ |
| 111 | Jun ‘19 | 2 | R | 29.27 | 3.407 | 100 | 38.840 | $3.42x10^{2}$ | $3.42x10^{2}$ | $6.84x10^{4}$ |
| 112 | Jun ‘19 | 2 | E | 30.14 | 1.899 | 100 | - | - | - | - |
| 113 | Jul ‘19 | 1 | R | 29.11 | 3.779 | 100 | 37.812 | $6.90x10^{2}$ | $6.90x10^{2}$ | $1.38x10^{5}$ |
| 114 | Jul ‘19 | 1 | E | 10.43 | $4.38x10^{6}$ | 100 | 36.604 | $1.57x10^{3}$ | $1.57x10^{3}$ | $3.14x10^{5}$ |
| 115 | Jul ‘19 | 1 | R | 34.71 | 0.088 | 17.5 | 37.176 | $1.06x10^{3}$ | $6.05x10^{3}$ | $1.21x10^{6}$ |
| 116 | Jul ‘19 | 1 | E | 32.32 | 0.438 | 87.4 | 42.851 | $2.22x10^{1}$ | $2.54x10^{1}$ | $5.08x10^{3}$ |
| 117 | Jul ‘19 | 2 | R | 31.66 | 0.683 | 100 | 35.082 | $4.44x10^{3}$ | $4.44x10^{3}$ | $8.88x10^{5}$ |
| 118 | Jul ‘19 | 2 | E | 29.62 | 2.690 | 100 | 35.931 | $2.49x10^{3}$ | $2.49x10^{3}$ | $4.98x10^{5}$ |
| 119 | Jul ‘19 | 2 | R | 31.92 | 0.572 | 100 | - | - | - | - |
| 120 | Jul ‘19 | 2 | E | 30.45 | 1.543 | 100 | - | - | - | - |
| 121 | Aug ‘19 | 1 | R | 34.63 | 0.093 | 18.5 | 29.295 | $2.30x10^{5}$ | $1.24x10^{6}$ | $2.48x10^{8}$ |
| 122 | Aug ‘19 | 1 | E | 34.43 | 0.106 | 21.1 | 30.357 | $1.11x10^{5}$ | $5.26x10^{5}$ | $1.05x10^{8}$ |
| 123 | Aug ‘19 | 1 | R | 36.13 | 0.034 | 6.7 | 29.641 | $1.81x10^{5}$ | $2.70x10^{6}$ | $5.40x10^{8}$ |
| 124 | Aug ‘19 | 1 | E | 34.69 | 0.089 | 17.7 | 30.760 | $8.47x10^{4}$ | $4.78x10^{5}$ | $9.57x10^{7}$ |
| 125 | Aug ‘19 | 2 | R | 32.93 | 0.289 | 57.6 | 32.747 | $2.18x10^{4}$ | $3.78x10^{4}$ | $7.56x10^{6}$ |
| 126 | Aug ‘19 | 2 | E | 33.67 | 0.176 | 35.1 | 33.076 | $1.74x10^{4}$ | $4.95x10^{4}$ | $9.91x10^{6}$ |
| 127 | Aug ‘19 | 2 | R | 32.26 | 0.457 | 91.2 | 36.805 | $1.37x10^{3}$ | $1.50x10^{3}$ | $3.00x10^{5}$ |

| | | | | | | | | | | |
|---|---|---|---|---|---|---|---|---|---|---|
| 128 | Aug ‘19 | 2 | E | 32.66 | 0.347 | 69.2 | 36.125 | $2.18x10^3$ | $3.15x10^3$ | $6.30x10^5$ |
| 129 | Sep ‘19 | 1 | R | 34.05 | 0.137 | 27.3 | 36.301 | $1.93x10^3$ | $7.06x10^3$ | $1.41x10^6$ |
| 130 | Sep ‘19 | 1 | E | 34.49 | 0.102 | 20.3 | 35.520 | $3.29x10^3$ | $1.62x10^4$ | $3.24x10^6$ |
| 131 | Sep ‘19 | 1 | R | 34.20 | 0.124 | 24.7 | 32.622 | $2.37x10^4$ | $9.59x10^4$ | $1.91x10^7$ |
| 132 | Sep ‘19 | 1 | E | 10.41 | $1.09x10^5$ | 100 | 34.121 | $8.55x10^3$ | $8.55x10^3$ | $1.71x10^6$ |
| 133 | Sep ‘19 | 2 | R | 35.13 | 0.066 | 13.1 | 33.346 | $1.45x10^4$ | $1.10x10^5$ | $2.21x10^7$ |
| 134 | Sep ‘19 | 2 | E | 33.43 | 0.207 | 41.3 | - | - | - | - |
| 135 | Sep ‘19 | 2 | R | 32.80 | 0.318 | 63.4 | - | - | - | - |
| 136 | Sep ‘19 | 2 | E | 35.29 | 0.059 | 11.7 | - | - | | - |
| 137 | Oct ‘19 | 1 | R | - | - | - | 28.406 | $4.22x10^5$ | - | - |
| 138 | Oct ‘19 | 1 | E | 36.60 | 0.025 | 4.9 | 37.167 | $1.07x10^3$ | $2.18x10^4$ | $4.36x10^6$ |
| 139 | Oct ‘19 | 1 | R | 35.75 | 0.043 | 8.5 | - | - | - | - |
| 140 | Oct ‘19 | 1 | E | 36.47 | 0.027 | 5.3 | 36.994 | $1.20x10^3$ | $2.26x10^4$ | $4.52x10^6$ |
| 141 | Oct ‘19 | 2 | R | - | - | - | 33.678 | $1.15x10^4$ | - | - |
| 142 | Oct ‘19 | 2 | E | 34.94 | 0.075 | 14.9 | - | - | - | - |
| 143 | Oct ‘19 | 2 | R | 30.906 | 1.136 | 100 | 32.700 | $2.25x10^4$ | $2.25x10^4$ | $4.50x10^6$ |
| 144 | Oct ‘19 | 2 | E | 35.60 | 0.048 | 9.5 | 34.834 | $5.26x10^3$ | $5.53x10^4$ | $1.10x10^7$ |
| 145 | Nov ‘19 | 1 | R | 33.02 | 0.273 | 54.4 | 39.905 | $1.65x10^2$ | $3.03x10^2$ | $6.06x10^4$ |
| 146 | Nov ‘19 | 1 | E | 35.31 | 0.059 | 11.7 | 38.322 | $4.87x10^2$ | $4.16x10^3$ | $8.32x10^5$ |

| | | | | | | | | | | |
|---|---|---|---|---|---|---|---|---|---|---|
| 147 | Nov ‘19 | 1 | R | 34.34 | 0.112 | 22.3 | - | - | - | - |
| 148 | Nov ‘19 | 1 | E | 34.35 | 0.112 | 22.3 | 35.205 | $4.08x10^{3}$ | $1.82x10^{4}$ | $3.65x10^{6}$ |
| 149 | Nov ‘19 | 2 | R | 34.83 | 0.081 | 16.2 | 27.837 | $6.22x10^{5}$ | $3.83x10^{6}$ | $7.67x10^{8}$ |
| 150 | Nov ‘19 | 2 | E | 33.51 | 0.197 | 39.3 | 35.802 | $2.71x10^{3}$ | $6.89x10^{3}$ | $1.37x10^{6}$ |
| 151 | Nov ‘19 | 2 | R | 37.28 | 0.016 | 3.2 | 39.809 | $1.76x10^{2}$ | $5.50x10^{3}$ | $1.10x10^{6}$ |
| 152 | Nov ‘19 | 2 | E | 29.47 | 2.98 | 100 | - | - | - | - |
| 153 | Dec ‘19 | 1 | R | - | - | - | 37.382 | $9.25x10^{2}$ | - | - |
| 154 | Dec ‘19 | 1 | E | 35.86 | 0.040 | 7.9 | 34.329 | $7.42x10^{3}$ | $9.39x10^{4}$ | $1.87x10^{7}$ |
| 155 | Dec ‘19 | 1 | R | 32.49 | 0.391 | 78.0 | - | - | - | - |
| 156 | Dec ‘19 | 1 | E | 32.14 | 0.493 | 98.4 | 38.237 | $5.16x10^{2}$ | $5.24x10^{2}$ | $1.04x10^{5}$ |
| 157 | Dec ‘19 | 2 | R | 36.54 | 0.026 | 5.2 | 30.704 | $8.80x10^{4}$ | $1.69x10^{6}$ | $3.38x10^{8}$ |
| 158 | Dec ‘19 | 2 | E | 33.95 | 0.146 | 29.1 | 40.374 | $1.20x10^{2}$ | $4.12x10^{2}$ | $8.24x10^{4}$ |
| 159 | Dec ‘19 | 2 | R | 29.41 | 3.105 | 100 | - | - | - | - |
| 160 | Dec ‘19 | 2 | E | 5.73 | $2.5x10^{7}$ | 100 | - | - | - | - |
| 161 | Jan ‘19 | 1 | R | 39.70 | $5.9x10^{-3}$ | 1.17 | 32.621 | $2.81x10^{4}$ | $2.55x10^{6}$ | $5.10x10^{8}$ |
| 162 | Jan ‘19 | 1 | E | 32.39 | 0.418 | 83.4 | 37.213 | $1.03x10^{3}$ | $1.23x10^{3}$ | $2.47x10^{5}$ |
| 163 | Jan ‘19 | 1 | R | 35.12 | 0.067 | 13.3 | 33.752 | $1.10x10^{4}$ | $8.27x10^{4}$ | $1.65x10^{7}$ |
| 164 | Jan ‘19 | 1 | E | 35.65 | 0.047 | 9.3 | 32.216 | $3.13x10^{4}$ | $3.36x10^{5}$ | $6.73x10^{7}$ |
| 165 | Jan ‘19 | 2 | R | 37.17 | 0.017 | 3.3 | 33.442 | $1.35x10^{4}$ | $4.09x10^{5}$ | $8.18x10^{7}$ |

| | | | | | | | | | | |
|---|---|---|---|---|---|---|---|---|---|---|
| 166 | Jan ‘19 | 2 | E | 35.27 | 0.060 | 11.9 | 32.850 | $2.03x10^4$ | $1.70x10^5$ | $3.41x10^7$ |
| 167 | Jan ‘19 | 2 | R | 33.59 | 0.186 | 37.1 | 35.365 | $3.66x10^3$ | $9.86x10^3$ | $1.97x10^6$ |
| 168 | Jan ‘19 | 2 | E | 32.81 | 0.315 | 62.8 | 36.664 | $1.51x10^3$ | $2.40x10^3$ | $4.80x10^5$ |

## B1: BLAST sequencing results for Sanger sequencing

| Collection Date | Sample ID | Clone Number | WWTP 1 or 2 | Season | BLAST Genotype/Name | Identity % | Accession Number | Year | Country |
|---|---|---|---|---|---|---|---|---|---|
| October 2018 | 38 | 18 | 1 | Winter | HAdV D | 98.9 | KF268206.1 | 2013 | Germany |
| October 2018 | 38 | 20 | 1 | Winter | HAdV D53 | 97.7 | AB568098.1 | 2004 | Japan |
| October 2018 | 38 | 21 | 1 | Winter | HAdV D | 98.1 | KF268206.1 | 2013 | Germany |
| October 2018 | 38 | 22 | 1 | Winter | HAdV D | 98.2 | KF268206.1 | 2013 | Germany |
| October 2018 | 38 | 23 | 1 | Winter | HAdV D | 98.5 | KF268206.1 | 2013 | Germany |
| October 2018 | 38 | 26 | 1 | Winter | HAdV D9 | 98.4 | AB330090.1 | 2007 | Japan |
| October 2018 | 38 | 27 | 1 | Winter | HAdV D | 98.9 | KF268206.1 | 2013 | Germany |
| October 2018 | 38 | 28 | 1 | Winter | HAdV D | 98.7 | KF268206.1 | 2013 | Germany |
| October 2018 | 38 | 29 | 1 | Winter | HAdV D | 97.8 | KF268206.1 | 2013 | Germany |
| October 2018 | 38 | 30 | 1 | Winter | HAdV D | 98.6 | KF268206.1 | 2013 | Germany |
| January 2019 | 62 | 31 | 1 | Summer | HAdV D | 98.7 | MF476842.1 | 2017 | USA |
| January 2019 | 62 | 33 | 1 | Summer | HAdV F41 | 99.1 | FR849547.1 | 2009 | Italy |
| January 2019 | 62 | 34 | 1 | Summer | HAdV F41 | 99.1 | FR849547.1 | 2009 | Italy |
| January 2019 | 62 | 36 | 1 | Summer | HAdV D | 98.1 | MF476842.1 | 2017 | USA |
| January 2019 | 62 | 37 | 1 | Summer | HAdV D | 98.7 | MF476842.1 | 2017 | USA |
| January 2019 | 62 | 39 | 1 | Summer | HAdV D | 98.1 | MF476842.1 | 2017 | USA |
| January 2019 | 62 | 41 | 1 | Summer | HAdV D | 98.5 | MF476842.1 | 2017 | USA |
| January 2019 | 62 | 45 | 1 | Summer | HAdV D | 98.3 | MF476842.1 | 2017 | USA |
| January 2019 | 64 | 46 | 1 | Summer | HAdV 16 | 97.2 | AB330097.1 | 2007 | Japan |
| January 2019 | 64 | 47 | 1 | Summer | HAdV 16 | 97.6 | AB330097.1 | 2007 | Japan |
| January 2019 | 64 | 49 | 1 | Summer | HAdV 16 | 97.7 | AB330097.1 | 2007 | Japan |
| January 2019 | 64 | 50 | 1 | Summer | HAdV 16 | 98.3 | AB330097.1 | 2007 | Japan |
| January 2019 | 64 | 52 | 1 | Summer | HAdV 16 | 97.5 | AB330097.1 | 2007 | Japan |
| January 2019 | 64 | 53 | 1 | Summer | HAdV 16 | 97.9 | AB330097.1 | 2007 | Japan |
| January 2019 | 64 | 54 | 1 | Summer | HAdV 16 | 98.6 | AB330097.1 | 2007 | Japan |
| January 2019 | 64 | 55 | 1 | Summer | HAdV 16 | 97.7 | AB330097.1 | 2007 | Japan |
| January 2019 | 64 | 59 | 1 | Summer | HAdV 16 | 98.7 | AB330097.1 | 2007 | Japan |
| January 2019 | 64 | 60 | 1 | Summer | HAdV 16 | 98.1 | AB330097.1 | 2007 | Japan |

| | | | | | | | | | |
|---|---|---|---|---|---|---|---|---|---|
| February 2019 | 70 | 47 | 1 | Summer | HAdV D | 97.7 | KF976531.1 | 2011 | DRC |
| February 2019 | 70 | 49 | 1 | Summer | HAdV D | 98.1 | KF976531.1 | 2011 | DRC |
| February 2019 | 70 | 51 | 1 | Summer | HAdV D | 97.8 | KF976531.1 | 2011 | DRC |
| February 2019 | 70 | 52 | 1 | Summer | HAdV D | 98.0 | KF976531.1 | 2011 | DRC |
| February 2019 | 70 | 54 | 1 | Summer | HAdV 16 | 97.7 | AB330097.1 | 2007 | Japan |
| February 2019 | 70 | 56 | 1 | Summer | HAdV D | 97.2 | KF976531.1 | 2011 | DRC |
| February 2019 | 70 | 58 | 1 | Summer | HAdV D | 97.6 | KF976531.1 | 2011 | DRC |
| April 2019 | 87 | 31 | 1 | Autumn | HAdV D | 90 | KF976531.1 | 2011 | DRC |
| April 2019 | 87 | 33 | 1 | Autumn | HAdV 12 | 97.7 | AB330093.1 | 2007 | Japan |
| April 2019 | 87 | 34 | 1 | Autumn | HAdV D | 97.7 | KF976531.1 | 2011 | DRC |
| April 2019 | 87 | 35 | 1 | Autumn | HAdV D | 89.9 | KF976531.1 | 2011 | DRC |
| April 2019 | 87 | 36 | 1 | Autumn | HAdV D | 97.7 | KF976531.1 | 2011 | DRC |
| April 2019 | 87 | 38 | 1 | Autumn | HAdV D | 89.4 | KF976531.1 | 2011 | DRC |
| April 2019 | 87 | 39 | 1 | Autumn | HAdV D | 89.9 | KF976531.1 | 2011 | DRC |
| May 2019 | 98 | 81 | 1 | Autumn | HAdV D | 97.2 | KF976531.1 | 2011 | DRC |
| May 2019 | 98 | 85 | 1 | Autumn | HAdV B66 | 99.2 | MG000708.1 | 2002 | Argentina |
| May 2019 | 98 | 86 | 1 | Autumn | HAdV B66 | 98.7 | MG000708.1 | 2002 | Argentina |
| May 2019 | 98 | 87 | 1 | Autumn | HAdV D26 | 96.9 | AB330107.1 | 2007 | Japan |
| May 2019 | 98 | 88 | 1 | Autumn | HAdV D | 96.9 | KF976531.1 | 2011 | DRC |
| May 2019 | 98 | 89 | 1 | Autumn | HAdV D | 97.3 | KF976531.1 | 2011 | DRC |
| June 2019 | 110 | 01 | 2 | Winter | HAdV D33 | 98.2 | JN226758.1 | 2013 | USA |
| June 2019 | 110 | 02 | 2 | Winter | HAdV D33 | 98.1 | JN226758.1 | 2013 | USA |
| June 2019 | 110 | 03 | 2 | Winter | HAdV D33 | 98.8 | JN226758.1 | 2013 | USA |
| June 2019 | 110 | 04 | 2 | Winter | HAdV 21a | 98.6 | MN686206.1 | 2019 | China |
| June 2019 | 110 | 05 | 2 | Winter | HAdV D33 | 98 | JN226758.1 | 2013 | USA |
| June 2019 | 110 | 06 | 2 | Winter | HAdV D33 | 98.9 | JN226758.1 | 2013 | USA |
| June 2019 | 110 | 07 | 2 | Winter | HAdV 21a | 99 | MN686206.1 | 2019 | China |
| June 2019 | 110 | 08 | 2 | Winter | HAdV D33 | 98.7 | JN226758.1 | 2013 | USA |
| June 2019 | 110 | 09 | 2 | Winter | HAdV 33 | 98.9 | JN226758.1 | 2013 | USA |
| June 2019 | 110 | 10 | 2 | Winter | HAdV 33 | 98.2 | JN226758.1 | 2013 | USA |
| July 2019 | 113 | 40 | 1 | Winter | HAdV D | 89.8 | KF976523.1 | 2011 | DRC |
| July 2019 | 113 | 41 | 1 | Winter | HAdV D | 89.9 | KF976523.1 | 2011 | DRC |
| July 2019 | 113 | 42 | 1 | Winter | HAdV D | 89.4 | KF976523.1 | 2011 | DRC |
| July 2019 | 113 | 44 | 1 | Winter | HAdV D | 89.1 | KF976523.1 | 2011 | DRC |

| | | | | | | | | | |
|---|---|---|---|---|---|---|---|---|---|
| July 2019 | 113 | 48 | 1 | Winter | HAdV D | 89.2 | KF976523.1 | 2011 | DRC |
| August 2019 | 125 | 13 | 2 | Winter | HAdV F41 | 98.8 | MK955319.1 | 2009 | South Africa |
| August 2019 | 125 | 15 | 2 | Winter | HAdV F41 | 98.8 | MK883610.1 | 2015 | China |
| August 2019 | 125 | 17 | 2 | Winter | HAdV F41 | 98 | MK883610.1 | 2015 | China |
| August 2019 | 125 | 18 | 2 | Winter | HAdV F41 | 98.6 | MK883610.1 | 2015 | China |
| August 2019 | 125 | 19 | 2 | Winter | HAdV F41 | 98.9 | FR849550.1 | 2009 | Italy |
| August 2019 | 125 | 20 | 2 | Winter | HAdV F41 | 98.3 | AB103343.1 | 2003 | Japan |
| August 2019 | 125 | 22 | 2 | Winter | HAdV B66 | 99 | MG000708.1 | 2002 | Argentina |
| December 2019 | 160 | 25 | 1 | Summer | HAdV B7 | 98.5 | KP729820.1 | 2013 | Germany |
| December 2019 | 160 | 26 | 1 | Summer | HAdV B66 | 98.8 | MG000708.1 | 2002 | Argentina |
| December 2019 | 160 | 27 | 1 | Summer | HAdV B66 | 97.1 | MG000708.1 | 2002 | Argentina |
| December 2019 | 160 | 28 | 1 | Summer | HAdV D | 89.2 | KF976523.1 | 2011 | DRC |
| December 2019 | 160 | 30 | 1 | Summer | HAdV D | 89.3 | KF976523.1 | 2011 | DRC |

## B2: BLAST sequencing results for next generation sequencing

| Collection Date | Sample ID | Contig ID | WWTP 1 or 2 | Season | Top HIT on BLAST /Genotype Name | Identity % | Accession Number | Year | Country |
|---|---|---|---|---|---|---|---|---|---|
| August 2018 | 25 | 104 | 2 | Winter | HAdV B | 100 | MK847517.1 | 2011 | China |
| August 2018 | 25 | 105 | 2 | Winter | HAdV B | 99.1 | MK847517.1 | 2011 | China |
| August 2018 | 26 | 206 | 2 | Winter | HAdV F41 | 100 | MK883610.1 | 2015 | China |
| August 2018 | 26 | 446 | 2 | Winter | HAdV F41 | 100 | AB103345.1 | 2003 | Japan |
| September 2018 | 29 | 09 | 1 | Spring | HAdV B7 | 100 | MN507870.1 | 2019 | China |
| September 2018 | 29 | 10 | 1 | Spring | HAdV D | 99.26 | KP274043.1 | 2012 | China |
| September 2018 | 30 | 5 | 1 | Spring | HAdV D87 | 99.5 | MF476842.1 | 1963 | USA |
| September 2018 | 38 | 2 | 1 | Spring | HAdV D9 | 99.1 | KP274043.1 | 2012 | Cote d' Ivoire |
| November 2018 | 47 | 1 | 1 | Spring | HAdV D9 | 99.4 | AB330090.1 | 2007 | Japan |
| December 2018 | 60 | 819 | 1 | Summer | HAdV F41 | 99.6 | MK883610.1 | 2015 | China |
| December 2018 | 60 | 850 | 1 | Summer | HAdV F41 | 100 | MK883610.1 | 2015 | China |
| January 2019 | 62 | 54 | 1 | Summer | HAdV D87 | 99.2 | MF476844.1 | 1963 | USA |
| January 2019 | 62 | 90 | 1 | Summer | HAdV D87 | 99.6 | MF476844.1 | 1963 | USA |
| January 2019 | 62 | 197 | 1 | Summer | HAdV D87 | 99.1 | MF476844.1 | 1963 | USA |
| January 2019 | 64 | 3 | 1 | Summer | HAdV B7 | 96.7 | MTO19911.1 | 2012 | China |
| February 2019 | 70 | 125 | 1 | Summer | HAdV D23 | 100 | KF976531.1 | 2012 | Cote d' Ivoire |
| February 2019 | 70 | 224 | 1 | Summer | HAdV D23 | 98.3 | KF976531.1 | 2012 | Cote d' Ivoire |
| February 2019 | 70 | 475 | 1 | Summer | HAdV D23 | 99.5 | KF976531.1 | 2012 | Cote d' Ivoire |
| February 2019 | 70 | 477 | 1 | Summer | HAdV D23 | 98.8 | KF976531.1 | 2012 | Cote d' Ivoire |
| April 2019 | 86 | 4 | 1 | Autumn | HAdV D24 | 92.5 | JN2226751.1 | 2016 | China |
| April 2019 | 87 | 142 | 1 | Autumn | HAdV D | 91.3 | KF976523.1 | 2010 | Uganda |
| April 2019 | 87 | 582 | 1 | Autumn | HAdV D | 91.6 | KF976523.1 | 2010 | Uganda |
| April 2019 | 88 | 3 | 1 | Autumn | HAdV D | 91.1 | KF976523.1 | 2011 | DRC |
| April 2019 | 89 | 1 | 2 | Autumn | HAdV F41 | 99.5 | FR849550.1 | 2009 | Italy |
| April 2019 | 89 | 4 | 2 | Autumn | HAdV D9 | 98.5 | KP274043.1 | 2012 | Cote d' Ivoire |
| April 2019 | 89 | 7 | 2 | Autumn | HAdV D67 | 99.6 | KP274043.1 | 2012 | Cote d' Ivoire |
| April 2019 | 89 | 22 | 2 | Autumn | HAdV D67 | 99.6 | KP274043.1 | 2012 | Cote d' Ivoire |

| | | | | | | | | | |
|---|---|---|---|---|---|---|---|---|---|
| May 2019 | 94 | 4 | 1 | Autumn | HAdV B7 | 100 | MK847517.1 | 2011 | China |
| May 2019 | 98 | 4 | 1 | Autumn | HAdV D23 | 100 | KF976531.1 | 2012 | Cote d' Ivoire |
| May 2019 | 98 | 10 | 1 | Autumn | HAdV D23 | 99.6 | KF976531.1 | 2012 | Cote d' Ivoire |
| June 2019 | 110 | 2 | 2 | Winter | HAdV B3 | 99.1 | KU145043.1 | 2011 | Malaysia |
| June 2019 | 110 | 3 | 2 | Winter | HAdV D24 | 98.5 | KF976521.1 | 2011 | DRC |
| June 2019 | 110 | 6 | 2 | Winter | HAdV D33 | 99.6 | JN226758.1 | 1965 | USA |
| June 2019 | 110 | 19 | 2 | Winter | HAdV D33 | 100 | JN226758.1 | 1965 | USA |
| July 2019 | 113 | 6 | 2 | Winter | HAdV D | 92.1 | KF976533.1 | 2010 | Uganda |
| July 2019 | 113 | 8 | 2 | Winter | HAdV D | 91.7 | KF976533.1 | 2010 | Uganda |
| July 2019 | 113 | 17 | 2 | Winter | HAdV D27 | 97.9 | JN226753.1 | 1958 | USA |
| July 2019 | 113 | 19 | 2 | Winter | HAdV D36 | 93.1 | KP274049.1 | 2012 | Cote d' Ivoire |
| July 2019 | 117 | 2 | 2 | Winter | HAdV F41 | 100 | MK883610.1 | 2015 | China |
| July 2019 | 117 | 3 | 2 | Winter | HAdV F41 | 99.2 | MK955319.1 | 2009/2011 | South Africa |
| July 2019 | 117 | 7 | 2 | Winter | HAdV D87 | 100 | MF476844.1 | 2017 | USA |
| July 2019 | 117 | 8 | 2 | Winter | HAdV D87 | 99.3 | MF476844.1 | 2017 | USA |
| July 2019 | 117 | 10 | 2 | Winter | HAdV D87 | 98.8 | MF476844.1 | 2017 | USA |
| July 2019 | 117 | 40 | 2 | Winter | HAdV B7 | 95.5 | MN507870.1 | 2019 | China |
| July 2019 | 118 | 1416 | 2 | Winter | HAdV F40 | 94.9 | MK955319.1 | 2009/2014 | South Africa |
| July 2019 | 118 | 1597 | 2 | Winter | HAdV F40 | 94.7 | MK955319.1 | 2009/2014 | South Africa |
| July 2019 | 118 | 1848 | 2 | Winter | HAdV F41 | 99.2 | MK88361.1 | 2015 | China |
| July 2019 | 118 | 2298 | 2 | Winter | HAdV F41 | 99.5 | MK88361.1 | 2015 | China |
| July 2019 | 118 | 3397 | 2 | Winter | HAdV F41 | 97.4 | MK88361.1 | 2015 | China |
| July 2019 | 118 | 3440 | 2 | Winter | HAdV F40 | 100 | MK955319.1 | 2009/2014 | South Africa |
| August 2019 | 126 | 1 | 2 | Winter | HAdV D | 97.9 | MK1774992.1 | 2010 | Canada |
| August 2019 | 126 | 3 | 2 | Winter | HAdV D26 | 95.7 | AB330107.1 | 2007 | Japan |
| August 2019 | 126 | 6 | 2 | Winter | HAdV D36 | 91.6 | KF976523.1 | 2011 | DRC |
| August 2019 | 126 | 7 | 2 | Winter | HAdV D25 | 93.9 | JN226752.1 | 1956 | USA |
| August 2019 | 126 | 9 | 2 | Winter | HAdV D19 | 94.6 | JQ326209.1 | 1995 | USA |
| August 2019 | 126 | 10 | 2 | Winter | HAdV B7 | 99.6 | MN507870.1 | 2019 | China |
| August 2019 | 126 | 26 | 2 | Winter | HAdV D | 92.2 | KP274049.1 | 2012 | Cote d'Ivoire |
| August 2019 | 126 | 29 | 2 | Winter | HAdV D | 92.2 | KP274049.1 | 2012 | Cote d'Ivoire |
| August 2019 | 126 | 30 | 2 | Winter | HAdV D86 | 90.7 | MK174992.1 | 2010 | Canada |
| August 2019 | 126 | 50 | 2 | Winter | HAdV D44 | 92.5 | JN226763.1 | 2007 | USA |
| August 2019 | 126 | 103 | 2 | Winter | HAdV D64 | 88.4 | JF799911.1 | 2007 | USA |

| | | | | | | | | | |
|---|---|---|---|---|---|---|---|---|---|
| August 2019 | 126 | 245 | 2 | Winter | HAdV D64 | 97.8 | MK174992.1 | 2010 | Canada |
| August 2019 | 126 | 227 | 2 | Winter | HAdV D67 | 96.5 | KP274043.1 | 2012 | Cote d'Ivoire |
| August 2019 | 126 | 253 | 2 | Winter | HAdV D67 | 99.5 | KP274043.1 | 2012 | Cote d'Ivoire |
| August 2019 | 126 | 273 | 2 | Winter | HAdV B7 | 95.7 | KP729820.1 | 2013 | Singapore |
| August 2019 | 126 | 313 | 2 | Winter | HAdV B7 | 97.7 | MN507870.1 | 2019 | China |
| August 2019 | 126 | 350 | 2 | Winter | HAdV B66 | 100 | MG000708.1 | 2002 | Argentina |
| August 2019 | 126 | 496 | 2 | Winter | HAdV D19 | 87.2 | JQ326209.1 | 1995 | USA |
| August 2019 | 127 | 2 | 2 | Winter | HAdV F40 | 98.2 | MK955319.1 | 2009/2014 | South Africa |
| August 2019 | 127 | 7 | 2 | Winter | HAdV F41 | 100 | MK883610.1 | 2019 | China |
| September 2019 | 132 | 8 | 1 | Spring | HAdV D | 97.2 | MF476842.1 | 1963 | USA |
| September 2019 | 132 | 34 | 1 | Spring | HAdV D | 97.1 | MF476842.1 | 1963 | USA |
| January 2020 | 167 | 2 | 1 | Summer | HAdV D | 100 | KF268206.1 | 1984 | USA |
| January 2020 | 167 | 15 | 1 | Summer | HAdV D | 99.6 | KP274043.1 | 2012 | Cote d' Ivoire |
| January 2020 | 167 | 61 | 1 | Summer | HAdV D | 99.6 | KP274043.1 | 2012 | Cote d' Ivoire |
| January 2020 | 167 | 404 | 1 | Summer | HAdV D | 99.1 | KF976531.1 | 2012 | Cote d' Ivoire |
| January 2020 | 170 | 9 | 2 | Summer | HAdV D33 | 99.6 | KF268322.1 | 1986 | Germany |
| January 2020 | 170 | 53 | 2 | Summer | HAdV D33 | 98.7 | KF268322.1 | 1986 | Germany |
| January 2020 | 170 | 71 | 2 | Summer | HAdV A12 | 99.5 | KX868300.1 | 1978/2010 | Sweden |
| January 2020 | 170 | 99 | 2 | Summer | HAdV B7 | 100 | MN507870.1 | 2019 | China |
| January 2020 | 170 | 102 | 2 | Summer | HAdV B7 | 100 | MN507870.1 | 2019 | China |
| January 2020 | 170 | 106 | 2 | Summer | HAdV D33 | 94.4 | KF268322.1 | 1986 | Germany |
| January 2020 | 170 | 128 | 2 | Summer | HAdV A12 | 100 | KX868300.1 | 1978/2010 | Sweden |

## B3: BLAST sequencing results for reference strains

| Reference strain | BLAST Genotype/Name | Accession Number | Identity Percentage (%) | Year | Country |
|---|---|---|---|---|---|
| HAdV A MK955319.1 | HAdV-A12 | X73487.1 | 100 | 1993 | Germany |
| HAdV B MG000721.1 | HAdV-B3 | DQ086466.1 | 100 | 2005 | Switzerland |
| HAdV D KF268206.1 | HAdV-D9 | AJ854486.1 | 100 | 2004 | Germany |
| HAdV F KX868300.1 | HAdV F | L19443.1 | 100 | 1993 | UK |
| Simian adenovirus 44 FJ025899.1 | Simian adenovirus 44 | FJ025899.1 | 100 | 2008 | USA |

# C1: Ethical Approval forms-Umbrella Study Ethics 2018

The Research Ethics Committee, Faculty Health Sciences, University of Pretoria complies with ICH-GCP guidelines and has US Federal wide Assurance.
- FWA 00002567, Approved dd 22 May 2002 and Expires 03/20/2022.
- IRB 0000 2235 IORG0001762 Approved dd 22/04/2014 and Expires 03/14/2020.

UNIVERSITEIT VAN PRETORIA
UNIVERSITY OF PRETORIA
YUNIBESITHI YA PRETORIA

Faculty of Health Sciences Research Ethics Committee

1/03/2018

**Approval Certificate**
**New Application**

**Ethics Reference No: 75/2018**

**Title:** Molecular detection and genotyping of human adenoviruses from clinical and environmental samples

Dear Walda van Zyl

The **New Application** as supported by documents specified in your cover letter dated 2/02/2018 for your research received on the 2/02/2018, was approved by the Faculty of Health Sciences Research Ethics Committee on its quorate meeting of 28/02/2018.

Please note the following about your ethics approval:
- Ethics Approval is valid for 3 years
- Please remember to use your protocol number (**75/2018**) on any documents or correspondence with the Research Ethics Committee regarding your research.
- Please note that the Research Ethics Committee may ask further questions, seek additional information, require further modification, or monitor the conduct of your research.

**Ethics approval is subject to the following:**
- The ethics approval is conditional on the receipt of **6 monthly written Progress Reports**, and
- The ethics approval is conditional on the research being conducted as stipulated by the details of all documents submitted to the Committee. In the event that a further need arises to change who the investigators are, the methods or any other aspect, such changes must be submitted as an Amendment for approval by the Committee.

We wish you the best with your research.

**Yours sincerely**

**Dr R Sommers,** MBChB; MMed (Int); MPharMed,PhD
**Deputy Chairperson** of the Faculty of Health Sciences Research Ethics Committee, University of Pretoria

*The Faculty of Health Sciences Research Ethics Committee complies with the SA National Act 61 of 2003 as it pertains to health research and the United States Code of Federal Regulations Title 45 and 46. This committee abides by the ethical norms and principles for research, established by the Declaration of Helsinki, the South African Medical Research Council Guidelines as well as the Guidelines for Ethical Research: Principles Structures and Processes, Second Edition 2015 (Department of Health).*

012 356 3084 deepeka.behari@up.ac.za / fhsethics@up.ac.za http://www.up.ac.za/healthethics
Private Bag X323, Arcadia, 0007 - Tswelopele Building, Level 4, Room 60 / 61, 31 Bophelo Road, Gezina, Pretoria

# C2: Ethical Approval forms- Umbrella Study Ethics Renewal 2020

UNIVERSITEIT VAN PRETORIA
UNIVERSITY OF PRETORIA
YUNIBESITHI YA PRETORIA

Faculty of Health Sciences

**Institution:** The Research Ethics Committee, Faculty Health Sciences, University of Pretoria complies with ICH-GCP guidelines and has US Federal wide Assurance.

- FWA 00002567, Approved dd 22 May 2002 and Expires 03/20/2022.
- IORG #: IORG0001762 OMB No. 0990-0279 Approved for use through February 28, 2022 and Expires: 03/04/2023.

14 May 2020

**Approval Certificate**
**Annual Renewal**

**Ethics Reference No.: 75/2018**
**Title: Molecular detection and characterisation of human adenoviruses from clinical and environmental samples**

Dear Dr WB van Zyl

The **Annual Renewal** as supported by documents received between 2020-04-15 and 2020-05-13 for your research, was approved by the Faculty of Health Sciences Research Ethics Committee on its quorate meeting of 2020-05-13.

Please note the following about your ethics approval:

- Renewal of ethics approval is valid for 1 year, subsequent annual renewal will become due on 2021-05-14.
- Please remember to use your protocol number (75/2018) on any documents or correspondence with the Research Ethics Committee regarding your research.
- Please note that the Research Ethics Committee may ask further questions, seek additional information, require further modification, monitor the conduct of your research, or suspend or withdraw ethics approval.

**Ethics approval is subject to the following:**

- The ethics approval is conditional on the research being conducted as stipulated by the details of all documents submitted to the Committee. In the event that a further need arises to change who the investigators are, the methods or any other aspect, such changes must be submitted as an Amendment for approval by the Committee.

We wish you the best with your research.

**Yours sincerely**

**Dr R Sommers**
MBChB MMed (Int) MPharmMed PhD
**Deputy Chairperson** of the Faculty of Health Sciences Research Ethics Committee, University of Pretoria

*The Faculty of Health Sciences Research Ethics Committee complies with the SA National Act 61 of 2003 as it pertains to health research and the United States Code of Federal Regulations Title 45 and 46. This committee abides by the ethical norms and principles for research, established by the Declaration of Helsinki, the South African Medical Research Council Guidelines as well as the Guidelines for Ethical Research: Principles Structures and Processes, Second Edition 2015 (Department of Health)*

Research Ethics Committee
Room 4-60, Level 4, Tswelopele Building
University of Pretoria, Private Bag x323
Gezina 0031, South Africa
Tel +27 (0)12 356 3084
Email: deepeka.behari@up.ac.za
www.up.ac.za

Fakulteit Gesondheidswetenskappe
Lefapha la Ditsense tša Maphelo

# C3: Ethical Approval forms- Masters Study Ethics 2019

UNIVERSITEIT VAN PRETORIA
UNIVERSITY OF PRETORIA
YUNIBESITHI YA PRETORIA

Faculty of Health Sciences

The Research Ethics Committee, Faculty Health Sciences, University of Pretoria complies with ICH-GCP guidelines and has US Federal wide Assurance.

- FWA 00002567, Approved dd 22 May 2002 and Expires 03/20/2022.
- IRB 0000 2235 IORG0001762 Approved dd 22/04/2014 and Expires 03/14/2020.

17 May 2019

**Approval Certificate**
**New Application**

**Ethics Reference No.: 249/2019**
**Title: Molecular characterisation of human adenoviruses from environmental samples in Tshwane, Gauteng**

Dear Miss M Davids

The **New Application** as supported by documents received between 2019-05-03 and 2019-05-15 for your research, was approved by the Faculty of Health Sciences Research Ethics Committee on its quorate meeting of 2019-05-15.

Please note the following about your ethics approval:

- Ethics Approval is valid for 1 year and needs to be renewed annually by 2020-05-17.
- Please remember to use your protocol number (249/2019 ) on any documents or correspondence with the Research Ethics Committee regarding your research.
- Please note that the Research Ethics Committee may ask further questions, seek additional information, require further modification, monitor the conduct of your research, or suspend or withdraw ethics approval.

**Ethics approval is subject to the following:**

- The ethics approval is conditional on the research being conducted as stipulated by the details of all documents submitted to the Committee. In the event that a further need arises to change who the investigators are, the methods or any other aspect, such changes must be submitted as an Amendment for approval by the Committee.

We wish you the best with your research.

**Yours sincerely**

**Dr R Sommers**
MBChB MMed (Int) MPharmMed PhD
**Deputy Chairperson** of the Faculty of Health Sciences Research Ethics Committee, University of Pretoria

*The Faculty of Health Sciences Research Ethics Committee complies with the SA National Act 61 of 2003 as it pertains to health research and the United States Code of Federal Regulations Title 45 and 46. This committee abides by the ethical norms and principles for research, established by the Declaration of Helsinki, the South African Medical Research Council Guidelines as well as the Guidelines for Ethical Research: Principles Structures and Processes, Second Edition 2015 (Department of Health)*

Research Ethics Committee
Room 4-60, Level 4, Tswelopele Building
University of Pretoria, Private Bag X323
Arcadia 0007, South Africa
Tel +27 (0)12 356 3084
Email deegeka.behari@up.ac.za
www.up.ac.za

Fakulteit Gesondheidswetenskappe
Lefapha la Disaense tša Maphelo

# C4: Ethical Approval forms- Masters Study Ethics Renewal 2020

UNIVERSITEIT VAN PRETORIA
UNIVERSITY OF PRETORIA
YUNIBESITHI YA PRETORIA

Faculty of Health Sciences

**Institution:** The Research Ethics Committee, Faculty Health Sciences, University of Pretoria complies with ICH-GCP guidelines and has US Federal wide Assurance.
- FWA 00002567, Approved dd 22 May 2002 and Expires 03/20/2022.
- IORG #: IORG0001762 OMB No. 0990-0279 Approved for use through February 28, 2022 and Expires: 03/04/2023.

21 April 2020

**Approval Certificate**
**Annual Renewal**

**Ethics Reference No.: 249/2019**
**Title: Molecular characterisation of human adenoviruses from environmental samples in Tshwane, Gauteng**

Dear Miss M Davids

The **Annual Renewal** as supported by documents received between 2020-03-19 and 2020-04-08 for your research, was approved by the Faculty of Health Sciences Research Ethics Committee on its quorate meeting of 2020-04-08.

Please note the following about your ethics approval:
- Renewal of ethics approval is valid for 1 year, subsequent annual renewal will become due on 2021-04-21.
- Please remember to use your protocol number (249/2019 ) on any documents or correspondence with the Research Ethics Committee regarding your research.
- Please note that the Research Ethics Committee may ask further questions, seek additional information, require further modification, monitor the conduct of your research, or suspend or withdraw ethics approval.

**Ethics approval is subject to the following:**
- The ethics approval is conditional on the research being conducted as stipulated by the details of all documents submitted to the Committee. In the event that a further need arises to change who the investigators are, the methods or any other aspect, such changes must be submitted as an Amendment for approval by the Committee.

We wish you the best with your research.

**Yours sincerely**

**Dr R Sommers**
MBChB MMed (Int) MPharmMed PhD
**Deputy Chairperson** of the Faculty of Health Sciences Research Ethics Committee, University of Pretoria

*The Faculty of Health Sciences Research Ethics Committee complies with the SA National Act 61 of 2003 as it pertains to health research and the United States Code of Federal Regulations Title 45 and 46. This committee abides by the ethical norms and principles for research, established by the Declaration of Helsinki, the South African Medical Research Council Guidelines as well as the Guidelines for Ethical Research: Principles Structures and Processes, Second Edition 2015 (Department of Health)*

Research Ethics Committee
Room 4-60, Level 4, Tswelopele Building
University of Pretoria, Private Bag x323
Gezina 0031, South Africa
Tel +27 (0)12 356 3084
Email: deepeka.behari@up.ac.za
www.up.ac.za

Fakulteit Gesondheidswetenskappe
Lefapha la Ditsebeng tša Maphelo

## C5: Wastewater treatment plant Permission Letter

CITY OF TSHWANE
IGNITING EXCELLENCE

Utility Services Department

Water and Sanitation & Energy and Electricity

Room 601 I 6th Floor I Bothongo Plaza East Building I 285 Francis Baard Street I Pretoria I 0002
PO Box 1022 I Pretoria I 0001
Tel: 012 358 4101 I Fax: 012 358 4684
Email: steven@tshwane.gov.za I www.tshwane.gov.za I www.facebook.com/CityOfTshwane

My ref: W9/2/1/1
Your ref:
Contact person: CM Esterhuyse
Section/Unit: Waste Water Treatment

Tel: 012 358 0702
Fax: -
Email: kerneelse@tshwane.gov.za

TO: Dr Janet Mans
Senior Lecturer/Medical Scientist: Department of Medical Virology
University of Pretoria

By Email: janet.mans@up.ac.za

26 July 2018

**REQUEST FOR SAMPLING OF A RAW AND TREATED EFFLUENT SAMPLES: BAVIAANSPOORT, DASPOORT, ROOIWAL AND ZEEKOEGAT WWTWS UP TILL JULY 2020**

Your email dated 25 July 2018 regarding the above subject matter refers.

Your request to get permission access to the Baviaanspoort, Daspoort, Rooiwal and Zeekoegat Waste Water Treatment Works for raw and final effluent sampling have been approved by the Utility Services Department. The information gained must be solely used for the purpose stated in your request letter and not for any other puposes.

The following contactable official will assist in providing the requested information:

- Mr David Ntsowe – Director: Waste Water Treatment Section
  012 358 0693 / davidn@tshwane.gov.za

Trust you will find the above in order.

Yours faithfully

Stephens Notoane
GROUP HEAD: UTILITY SERVICES

# D1: MSc Committee Letter

UNIVERSITEIT VAN PRETORIA
UNIVERSITY OF PRETORIA
YUNIBESITHI YA PRETORIA

MSc Committee
School of Medicine
Faculty of Health Sciences

MSc Committee
25 April 2019

Dr WB van Zyl
Department of Medical Virology
Faculty of Health Sciences

Dear Dr,

**Ms M Davids, Student no 14105447**

Please receive the following comments with reference to the MSc Committee submission of the abovementioned student:

| | | | |
|---|---|---|---|
| **Student name** | Ms Michaela Davids | **Student number** | 14105447 |
| **Name of study leader** | Dr WB van Zyl | | |
| **Department** | Medical Virology | | |
| **Title of MSc** | Molecular characterisation of human adenoviruses from environmental samples in Tshwane, Gauteng | | |
| **Date of first submission** | **April 2019** | | |
| **Comments to study leader April 2019** | • Please remove 'Epidemiology and' from the title.<br>• Please put bacterial names in italics.<br>• Please correct the wording of "golden standard technique" to "gold standard technique".<br>• The number of samples should be clearer.<br>• Please correct all typographical errors.<br>• Please provide the details of all instruments used in the study.<br>• Please correct Mr Ismail's title to Dr A Ismail. | | |
| | • Thank you for submitting a revised protocol and new MSc form. | | |
| **Decision** | This protocol has been provisionally approved.<br>Please submit the revised protocol to ethics, and supply the MSc committee with proof of acceptance.<br>The internal and external examiners can be nominated and submitted to the MSc Committee six months prior to submission of the dissertation. Please ensure that the CV of the examiners includes: supervision, examination and publication records. | | |

Yours sincerely

Prof Marleen Kock
Chair: MSc Committee

MSc Committee, School of Medicine
Faculty of Health Sciences
University of Pretoria,
Private Bag X323
Pretoria 0001, South Africa
Tel +27 (0) 12 319 2325
Fax +27 (0) 12 323 0732

Fakulteit Gesondheidswetenskappe
Lefapha la Disaense tša Maphelo